MODELING OF FERRO-SILICON AND FERRO-MANGANESE SMELTING IN ELECTRIC ARC FURNACE

by

PRADIP SAHANA

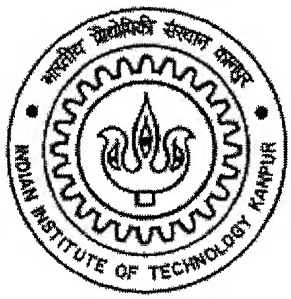

to the

DEPARTMENT OF MATERIALS AND METALLURICAL ENGINEERING

INDIAN INSTITUTE OF TECHNOLOGY, KANPUR

December, 2003

MODELING OF FERRO-SILICON AND FERRO-MANGANESE SMELTING IN ELECTRIC ARC FURNACE

A Thesis Submitted

In Partial Fulfillment of the Requirements

for the Degree of

MASTER OF TECHNOLOGY

by

PRADIP SAHANA

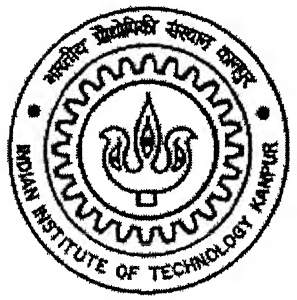

to the

DEPARTMENT OF MATERIALS AND METALLURICAL ENGINEERING

INDIAN INSTITUTE OF TECHNOLOGY, KANPUR

December, 2003

CERTIFICATE

It is certified that the work contained in the thesis entitled ***"Modeling of Ferrosilicon and Ferromanganese smelting in Electric Arc Furnace"***, by Pradip Sahana has been carried out under my supervision and that this work has not been submitted elsewhere for a degree.

for **(Late Dr.N.K.Batra)**

December, 2003

Department of Materials & Metallurgical Engineering
I.I.T. Kanpur.

ACKNOWLEDGEMENT

Foremost, I would like to express my sincere gratitude to my respected guide late Dr.N.K.Batra for his kind guidance and invaluable suggestions that have helped this thesis work to assume a meaningful shape. I am grateful to him for providing me with useful references, materials and books that enriched my knowledge and understanding about the problem in hand. I also thank him for giving me full freedom to think and approach in my own way.

I would like to special thanks to Dr. S. C. Koria, for carefully editing this thesis report. Without his active cooperation, it would not have been possible for me to complete this thesis.

I am deeply indebted to the faculty members who have taught me different subjects and clarified my doubts regarding the basics. I am also thankful to the departmental stuff-members for their generous help during my stay over here.

I also extend my thanks and gratitude to Mr. K. S. Tripathi and Mr. Surendra Agnihotri, for extending their kind cooperation at every stage of my work. A number of other persons too stretched their helpful hands during my thesis work. Gopi Kishor, M.Sankar (M.Tech student in Materials & Metallurgical Engineering Department) helped me with various documents and tools related to my work. My heartfelt thanks go to all of them. I am also thankful to all my batch-mates for their cooperation during my entire M.Tech period.

Last but not the least, I owe to my parents whose blessing and inspiration has made me successful removing all the obstacles I found in my journey of studentship.

Pradip Sahana

(*Pradip Sahana*)

CONTENTS

List of Figures

List of Tables

NOMENCLATURE

a_{Si}	Activity of silicon in the liquid Ferrosilicon alloy
a_{Mn}	Activity of manganese in the liquid Ferromanganese alloy
a_{SiO2}	Activity of silica in the slag phase
a_C	Activity of Carbon in the liquid Ferromanganese alloy
[%C]	Weight percent carbon in liquid iron
ΔC_P	Heat capacity (Cal/deg/mole)
E	Electrical energy consumption rate (KWh/ton alloy)
f_{Si}	Weight fraction of silicon in the Ferrosilicon alloy
f_{Mn}	Weight fraction of Mn in the Ferromanganese alloy
H_{Fe}	Heat content of Fe at smelting temperature of alloy (KCal)
H_{Si}	Heat content of Si at smelting temperature of alloy (KCal)
H_f^{Si}	Heat of fusion of Si (Cal/mole)
H_{Mn}	Heat content of Mn at smelting temperature of alloy (KCal)
$H_{Mn(v)}$	Heat content of Mn vapor at smelting temperature of alloy (Kcal)
$H_{p\,t(Mn)}$	Heat required to phase transformation of Mn
H_{FeSi}	Sensible heat of Ferrosilicon alloy in (Kcal)
H_{alloy}	Sensible heat of alloy in (Kcal)
$\Delta H^0_{FeSi,}$	Standard heat content of Ferrosilicon alloy (Cal/mole) at 298^0K
ΔH^0_{CO}	Standard heat content of CO (Cal/mole) at 298^0K
H_{CO}	Total heat content of carbon monoxide at t_g temperature in (Kcal)

$\Delta H^0_{CO_2}$	Standard heat content of CO_2 (Cal/mole) at 298^0K
H_{CO2}	Total heat content of CO_2 at t_g temperature in (Kcal)
$\Delta H^0_{SiO_2}$	Standard heat content of SiO_2 (Cal/mole) at 298^0K
H_{SiO_2}	Heat of dissociation of Silica (Kcal)
ΔH^0_{SiO}	Standard heat content of SiO (Cal/mole) at 298^0K
H_{SiO}	Total heat content of SiO (Kcal)
$\Delta H^0_{Fe_2O_3}$	Standard heat content of Fe_2O_3 (Cal/mole) at 298^0K
$H_{Fe_2O_3}$	Heat of dissociation of Fe_2O_3 (Kcal)
$\Delta H^0_{Mn_3O_4}$	Standard heat content of Mn_3O_4 (Cal/mole) at 298^0K
$H_{Mn_3O_4}$	Heat of dissociation of Mn_3O_4 (Kcal)
ΔH^0_{Mn}	Standard heat content of Mn at 298K
H_{Mn}	Total heat content of Mn at smelting temperature of alloy (Kcal)
H_{Slag}	Sensible heat of slag (MJ)
H_{C_alloy}	Heat content of C in Ferromanganese alloy (Kcal)
hr	Heat required to produce one ton alloy (MJ)
N_{Si}	Mole fraction of Si in Ferrosilicon alloy
n_{Si}	Mole of Si in Ferrosilicon alloy (Kmole)
n_{CO}	Mole of CO (Kmole)
n_{CO_2}	Mole of CO_2 (Kmole)
n_{SiO}	Mole of SiO (Kmole)
n_{SiO_2}	Mole fraction of SiO_2 (Kmole)

n_{FeSi}	Moles of FeSi (Kmoles)
n_{Mn}	Moles of Mn in Mn_3O_4 (Kmole)
$n_{Mn(v)}$	Moles of Mn vapor (Kmole)
n_{Mn_alloy}	Moles of Mn in Ferromanganese alloy (Kmole)
$n_{Mn_3O_4}$	Moles of Mn_3O_4 (Kmole)
η	Thermal efficiency of the furnace
P_0	Applied pressure (atm.)
P_{CO}	Partial pressure of CO (atm.)
P_{SiO}	Partial pressure of SiO (atm.)
P_{Mn}	Partial pressure of Mn vapors (atm.)
r_{Si}	Instantaneous recovery of Si
r_{Mn}	Instantaneous recovery of Mn
R_{Si}	Overall recovery of Si
R_{Mn}	Overall recovery of Mn
T,t	Smelting temperature of alloy (K)
t_g	Flue gas temperature (^{0}K)
α	Degree of direct reduction of $Fe_{0.95}O$
β	SiO to CO molar ratio in the gas phase
W_C	Weight of C per ton of alloy
w_{SiO_2}	Weight of Silica (Kg) per kg alloy
W_{SiO_2}	Weight of Silica (Kg) per ton alloy

W_{slag} Weight of Slag (Kg)

ABSTRACT

Ferrosilicon and Ferromanganese alloys are used for deoxidation, desulphurization and also used in particular grades of steels to change its physical and chemical properties. Ferromanganese modifies the structure of graphite and retard the grain growth, produces the fine grains steel. Silicon on the other hand tends to favour increase in grain size. The solubility of Carbon in liquid iron decreases decreases with an increase in Silicon content in Ferrosilicon alloy. Above 20 wt. pct Si in Ferrosilicon alloy, solubility of Carbon ignored. But in case of Ferromanganese, solubility of Carbon increases with Mn content in alloy.

The main objective of this study is to compute the smelting temperature to which charge materials must be heated and Carbon, electrical energy, Silica and Mn_3O_4 consumption to produce certain grades of alloy for different conditions. When Fe is used in the burden for the production of certain grades of Ferrosilicon with or without recirculation of SiO gas, Carbon, Silica and electrical energy consumption is same up to 35 pct Si in alloy but all are increases above 35 pct Si in alloy when no recirculation of SiO gas. Calculation shows that the recycling of SiO could be saving of more than 2510 KWh/t electrical energy and 100kg/ton Carbon for Fe-80%Si. When Fe_2O_3 used in the burden Carbon and electrical energy consumption is highest when Fe_2O_3 is directly reduced by Carbon. Here much loss of Calorific value of CO. Computed results shows that the around 47 pct input energy consumed to obtain elemental Si for Ferrosilicon alloy and around 39 pct input energy consumed to obtained elemental Mn for Ferromanganese alloy. Around 30 pct input energy is wasted as calorific value of CO to produce Ferrosilicon and Ferromanganese. Only 8 pct input energy for Ferrosilicon and 22 pct input energy for Ferromanganese being consumed by the sensible heat of alloy.

Effects of other parameters such as Slag rate, flue gas or gases temperature and efficiency of the furnace on electrical energy consumption has computed for different conditions. There could be a decrease of 50 to 65 KWh/ton for 50pct Si, 70 to 80 KWh/ton for 80 pct Si in Ferrosilicon alloy and 13 to 28 KWh/ ton, 14 to 50KWh/ton for 50 and 70 pct Mn in Ferromanganese alloy for every 100^0C decrease in the temperature of out going gas or gases for different conditions. Every one kg of slag produced would consume of additional 2000KJ energy and it could increase the energy demand by about

11 KWh for 20 Kg slag. Heat losses contribute as high as 1790-2102 KWh/t of Fe-50 Si alloy, 2864-3617 KWh/t of Fe-80 Si alloy and 542-955 KWh/t of Fe-50 Mn alloy, 624-1006 KWh/t of Fe-70 Mn alloy at assumed furnace efficiency of 70 percent.

Chapter 1
INTRODUCTION

INTRODUCTION

Steel making is carried out under oxidizing conditions. A certain fraction is inevitably left over as dissolved oxygen in the liquid steel at end of the refining. The solid solubility of oxygen in pure iron is only 0.003 pct, at 16000C is 0.23 pct and rises to 0.48 pct at 1800^0C. The oxygen content in the iron varies inversely with the impurity contents. As refining progresses the oxygen content in the melt, therefore, increases and at the end of refining a considerable amount of oxygen is left in liquid steel. If such steel is cast, the excess oxygen is evolved in the form of gases, leading to an unsound casting. Ferrosilicon and Ferromanganese are commonly used for de-oxidation of steel. Virgin elements like Silicon and Manganese may not dissolved in steel readily because of the adherent oxide layer on their surfaces. But if these are used in the form of the Ferro-alloys dissolution poses no problem since iron acts as the carrier.

Ferro-silicon and Ferro-manganese alloys are commonly manufactured in submerged electric arc furnaces with little slag. In presence of iron, silica and Manganese ore will be reduced by carbon to give maximum of around 22 wt. pct Silicon in Ferrosilicon alloy and around 15.5 wt. pct Mn for Ferromanganese alloys. Rest of carbon will be consumed to transform silica to silicon carbide at around 1810^0K and MnO to Mn_7C_3 at around 1546^0K. Higher grades of Ferro-silicon and Ferro-manganese alloys may be produced due to the reactions occurring between silicon carbide and silica at temperatures above 1810^0K, Manganese Carbide (Mn_7C_3) and MnO at the temperature above 1546^0K. Thermodynamic data on standard free energy of formation of species are used in the study to calculate the required smelting temperature at different silicon and Manganese content of the alloys. Sum of partial pressures of gases must equal the applied pressure of 1 atmosphere at the smelting temperature. It is important to know the activity coefficient of silicon or manganese in the alloy as a function of temperature and silicon or Manganese content of the alloy using the date in the literature. Mass and enthalpy balances are used to determine the carbon and electricity requirements of the process. Recycling of silicon monoxide is promoted by maintaining a bed of certain height so that evolved gases are cooled due to heat exchange between the gas and solid phases. It might be resulting in saving of more than 3000 KWh per ton of Fe-80Si alloy. Reduction of

silica is found to account for just 47.6% of the total energy that is added via the calorific value of carbon and the electricity in producing the alloy. Further improvement in the performance is visualized by reducing electrical losses and recovering as much as possible the calorific value of outgoing carbon monoxide.

Different modeling work has been done to investigate the followings. 1. To calculate the smelting temperature to which the charge materials must be heated to obtain a certain grade of Ferrosilicon and Ferromanganese alloys. 2. To see the Carbon, Silica and electrical energy consumption with or without recirculation of SiO gas, when pure Fe is used. 3. To calculate the Carbon and electrical energy consumption rate for different grades of Ferrosilicon and Ferromanganese alloy for different conditions. 4. To see the effect of other parameters, such as flue gas temperature, Slag rate and efficiency of the furnace.

CHAPTER 2
LITERATURE SUEVEY

2. PRODUCTION OF FERROALLOYS

2.1 General

Ferroalloys are alloys of iron that contain one or more other chemical elements. These alloys are used to add these other elements into molten metal, usually in steelmaking, deoxidation, desulphurization. Ferro Alloys is a very important additive material used in the production of several grades of carbon and alloy steel also used in particular grades of steel to change its physical and chemical properties, such as, hardness, corrosion resistance, change in tensile strength, ductility, abrasion resistance etc. Various kind of Ferro alloys are Ferro Silicon, Ferro Manganese, Ferro Chrome, Silico Manganese etc. The top five-ferroalloy producers in the world in 2000, in decreasing order, were China, South Africa, Norway, Russia, and Ukraine. Ferroalloys impart distinctive qualities to steel or cast iron or serve important functions during the production cycle. The ferroalloy industry is closely associated with the iron and steel industry, its largest customer. World production in 2000 of the bulk ferroalloys chromium, manganese, and silicon, was estimated at 16.6 million metric tons (Mt).

The principal ferroalloys are those of silicon, manganese and chromium. Manganese is essential to the production of virtually all steels and is important to the production of cast iron. Manganese is used to neutralize the harmful effect of 'S' and as an alloying element. Silicon is used primarily for deoxidation in steel and as an alloying element in cast iron. Boron, chromium, cobalt, columbium, copper, molybdenum, nickel, phosphorus, titanium, tungsten, vanadium, zirconium, and the rare-earth elements are among the other elements contributing to the character of the various alloy steels and cast irons.

In the major ferroalloys and probably some specialty ferroalloys, alternative materials to ferroalloys use, principally alloy scrap and oxide; overall have gained moderately on ferroálloys use per ton of steel production over the past 20 years. A combination of factors, including technology availability, and price, is responsible for this general decline in unit consumption of the ferroalloy form, and ferroalloy metal from all sources, for the major ferroalloys in steelmaking. The steel industry continues to improve processing technology to reduce raw materials needs, and metallurgists develop steel grades with lower alloying metal content and equal or better performance to lower costs. For many stainless steel applications there are no acceptable substitutes, and its key constituents, chromium and nickel, are essential. As technology and industry practices result in greater efficiency of use of ferroalloys, the strong demand for metals in construction, the chemical industry, transportation, and household appliances is expected to more than offset any basic reduction

in unit consumption in the future. Competition from other materials, such as plastics and nonferrous metals in the transportation sector, will be strong, but the use of lightweight, high-strength grades is expected to make steel competitive for many years.

On a country basis, China was by far the largest producer of manganese ferroalloys, with an output greater than that of South Africa and Ukraine combined the countries with the next largest production. Table 2.1 contains information of top ten Ferro-alloy producing countries in different years [1]. Demand for silicon ferroalloys is driven principally by the production of steel and cast iron. China was estimated to be the world's largest producer of ferrosilicon, with production more than twice that of either Norway or Russia, the countries with the next largest production.

2.2 Process Descriptions:

A typical ferroalloy production process is illustrated in Figure 2.1. A variety of furnace types, including submerged electric arc furnaces, exothermic (metallothermic) reaction furnaces can be used to produce ferroalloys. Furnace descriptions and their ferroalloy products are given in Table 2.2

2.2.1 Submerged Electric Arc Process:

In most cases, the submerged electric arc furnace produces the desired product directly. It may produce an intermediate product that is subsequently used in additional processing methods. The submerged arc process is a reduction smelting operation. The reactants consist of metallic ores (ferrous oxides, silicon oxides, manganese oxides, chrome oxides, etc.) and a carbon-source reducing agent, usually in the form of coke, charcoal, high and low-volatility coal, or wood chips. Limestone may also be added as a flux material. Raw materials are crushed, sized, and, in some cases, dried, and then conveyed to a mix house for weighing and blending. Conveyors, buckets, skip hoists, or cars transport the processed material to hoppers above the furnace. The mix is then gravity-fed through a feed chute either continuously or intermittently, as needed. At high temperatures in the reaction zone, the carbon source reacts with metal oxides to form carbon monoxide and to reduce the ores to base metal. A typical reaction producing ferrosilicon is shown below:

$$Fe_2O_3 + 2SiO_2 + 7C \rightarrow 2FeSi + 7\,CO$$

Smelting in an electric arc furnace is accomplished by conversion of electrical energy to heat. An alternating current applied to the electrodes causes' current to flow through the charge between the electrode tips. This provides a reaction zone at temperatures up to 2000°C (3632°F). The tip of each electrode changes polarity continuously as the alternating current

flows between the tips. To maintain a uniform electric load, electrode depth is continuously varied automatically by mechanical or hydraulic means.

The lower part of the submerged electric arc furnace is composed of a cylindrical steel shell with a flat bottom or hearth. The interior of the shell is lined with 2 or more layers of carbon blocks. The furnace shell may be water cooled to protect it from the heat of the process. A water-cooled cover and fume collection hood are mounted over the furnace shell.

Normally, 3 carbon electrodes arranged in a triangular formation extend through the cover and into the furnace shell opening. Prebaked or selfbaking (Soderberg) electrodes ranging from 76 to over 100 cm (30 to over 40 inches) in diameter are typically used. Raw materials are sometimes charged to the furnace through feed chutes from above the furnace. The surface of the furnace charge, which contains both molten material and unconverted charge during operation, is typically maintained near the top of the furnace shell. The lower ends of the electrodes are maintained at about 0.9 to 1.5 meters (3 to 5 feet) below the charge surface. Three phase electric current arcs from electrode to electrode, passing through the charge material. The charge material melts and reacts to form the desired product as the electric energy is converted into heat. The carbonaceous material in the furnace charge reacts with oxygen in the metal oxides of the charge and reduces them to base metals. The reactions produce large quantities of carbon monoxide (CO) that passes upward through the furnace charge. The molten metal and slag are removed (tapped) through 1 or more tap holes extending through the furnace shell at the hearth level. Feed materials may be charged continuously or intermittently. Power is applied continuously. Tapping can be intermittent or continuous based on production rate of the furnace.

Submerged electric arc furnaces are of two basic types, open and covered. Open furnaces have a fume collection hood at least 1 meter (3.3 feet) above the top of the furnace shell. Moveable panels or screens are sometimes used to reduce the open area between the furnace and hood, and to improve emissions capture efficiency. Carbon monoxide rising through the furnace charge burns in the area between the charge surface and the capture hood. This substantially increases the volume of gas the containment system must handle. Additionally, the vigorous open combustion process entrains finer material in the charge. Fabric filters are typically used to control emissions from open furnaces. Covered furnaces may have a water-cooled steel cover that fits closely to the furnace shell. The objective of covered furnaces is to reduce air infiltration into the furnace gases, which reduces combustion of that gas. This reduces the volume of gas requiring collection and treatment. The cover has holes for the charge and electrodes to pass through. Covered furnaces that partially close

these hood openings with charge material are referred to as "mix-sealed" or "semi-enclosed furnaces". Although these covered furnaces significantly reduce air infiltration, some combustion still occurs under the furnace cover. Covered furnaces that have mechanical seals around the electrodes and sealing compounds around the outer edges are referred to as "sealed" or "totally closed". These furnaces have little, if any, air infiltration and undercover combustion. Water leaks from the cover into the furnace must be minimized as this leads to excessive gas production and unstable furnace operation. Products prone to highly variable releases of process gases are typically not made in covered furnaces for safety reasons. As the degree of enclosure increases, less gas is produced for capture by the hood system and the concentration of carbon monoxide in the furnace gas increases. Wet scrubbers are used to control emissions from covered furnaces. The scrubbed, high carbon monoxide content gas may be used within the plant.

The molten alloy and slag that accumulate on the furnace hearth are removed at 1 to 5 hour intervals through the tap hole. Tapping typically lasts 10 to 15 minutes. Tap holes are opened with pellet shot from a gun, by drilling, or by oxygen lancing. The molten metal and slag flow from the tap hole into a carbon-lined through, then into a carbon-lined runner that directs the metal and slag into a reaction ladle, ingot molds, or chills. (Chills are low, flat iron or steel pans that provide rapid cooling of the molten metal.) After tapping is completed, the furnace is resealed by inserting a carbon paste plug into the tap hole.

Chemistry adjustments may be necessary after furnace smelting to achieve a specified product. Ladle treatment reactions are batch processes and may include metal and alloy additions. During tapping, and/or in the reaction ladle, slag is skimmed from the surface of the molten metal. It can be disposed of in landfills, sold as road ballast, or used as a raw material in a furnace or reaction ladle to produce a chemically related ferroalloy product. After cooling and solidifying, the large ferroalloy castings may be broken with drop weights or hammers. The broken ferroalloy pieces are then crushed, screened (sized), and stored in bins until shipment. In some instances, the alloys are stored in lump form in inventories prior to sizing for shipping.

2.2.2 Exothermic (Metallothermic) Process:

The exothermic process is generally used to produce high-grade alloys with low-carbon content. The intermediate molten alloy used in the process may come directly from a submerged electric arc furnace or from another type of heating device. Silicon or aluminum combines with oxygen in the molten alloy, resulting in a sharp temperature rise and strong

agitation of the molten bath. Low and medium-carbon content Ferrochromium (FeCr) and Ferromanganese (FeMn) are produced by silicon reduction. Aluminum reduction is used to produce chromium metal, ferrotitanium, ferrovanadium, and Ferrocolumbium. Mixed alumino/silico thermal processing is used for producing ferromolybdenum and ferrotungsten. Although aluminum is more expensive than carbon or silicon, the products are purer. Low-carbon (LC) ferrochromium is typically produced by fusing chromium ore and lime in a furnace. A specified amount is then placed in a ladle. A known amount of an intermediate grade ferrochromesilicon is then added to the ladle. The reaction is extremely exothermic and liberates chromium from its ore, producing LC ferrochromium and a calcium silicate slag. This slag, which still contains recoverable chromium oxide, is reacted in a second ladle with molten high-carbon ferrochromesilicon to produce the intermediate grade ferrochromesilicon. Exothermic processes are generally carried out in open vessels and may have emissions similar to the submerged arc process for short periods while the reduction is occurring.

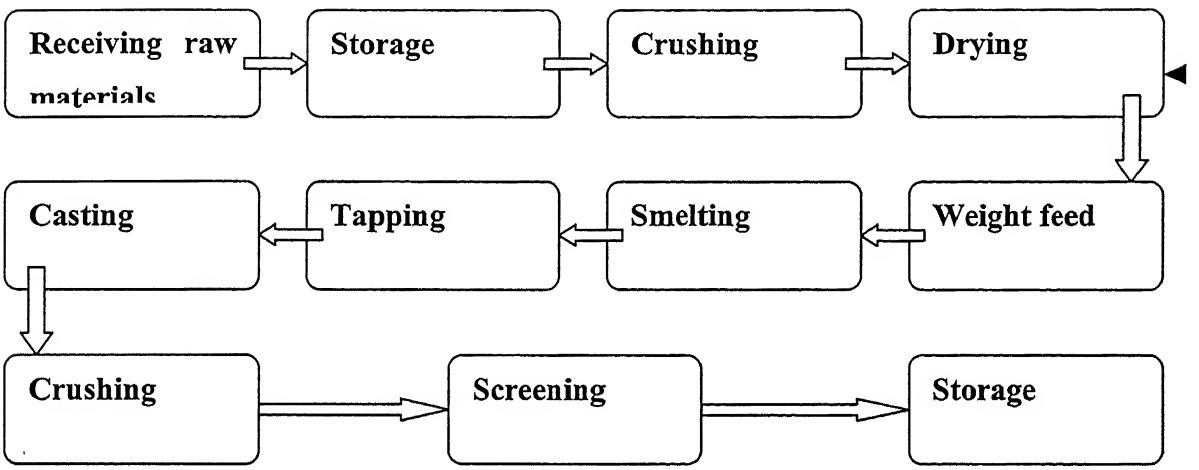

Fig 2.1: Typical Ferroalloy production process

Table 2.1: Top ten Ferroalloy producing Countries in different years (in MT):

Year / Countries	1996	1997	1998	1999	2000
China	4180,000	4040,000	3560,000	3800,000	4030,000
South Africa	2400,000	2910,000	2990,000	3120,000	3160,000
Ukraine	1160,000	1170,000	993,000	1030,000	1380,000
Norway	1120,000	1210,000	1230,000	1200,000	1210,000
Russia	831,000	940,000	889,000	1070,000	1130,000
Kazakhstan	551,000	845,000	725,550	861,946 r	939,000
Japan	951,431	1004,446 r	903,299	847,278 r	917,985 7
Brazil	1022,183	864,567 r	718,918 r	762,696 r	816,000
India	717,000	744,000	777,000 r	774,000	776,000
France	695,000	695,000	691,000	700,000 r	705,000
Total	13627614	14423013	13477767	14165920	15063985

e: Estimated

r: Revised

7: Reported figure

Table 2.2: Ferroalloy processes and respective product groups

Process	Product
Submerged arc furnace [a]	Silvery iron (15-22% Si) Ferrosilicon High carbon (HC)ferromanganese Silicomanganese High carbon ferromanganese High carbon ferrochrome
Exothermic [b] Silicon reduction	Low carbon (LC) ferrochrome, Low carbon ferromanganese, Medium carbon (MC) ferromanganese.
Aluminum reduction	Ferrotitanium, Ferrovanadium, Ferrocolumbium
Mixed aluminothermal / silicothermal	Ferromolybdenun, Ferrotungsten

a. Process by which metal is smelted in a refractory-lined cup-shaped steel shell by submerged graphite electrodes.

b. Process by which molten charge material is reduced, in exothermic reaction, by addition of silicon, aluminum, or a combination of the 2.

2.3: RAW MATERIALS FOR PRODUCTION OF Fe-Si AND Fe-Mn [2]

Raw Materials for Ferrosilicon

The Ore component of the charge for making Ferro-silicon are mineral having a high content of Silica, such as Quartz, Quartzite and Chalcedony, Good grades of quartzite contain 96-97 percent SiO_2, around 1 percent Al_2O_3, roughly 1 percent CaO + MgO, and not more than 0.02 % P_2O_5. Aluminium and Phosphorous oxides are detrimental impurities in the charge; the lower the content of alumina in the quartzite, the smaller will be the bulk of slag, and therefore the lower the loss of electric energy.

Quartz with high content of alumina should be washed after grinding. Quartzite must not crack being heated, otherwise the charge can become poorly permeable for evolving gases; the optimum size of the quartzite lumps is 20 to 80 mm. Fines formed during grinding of quartzite contain much alumina and should be screened off.

The main requirements to meet by a reducer are low ash content, a high electric resistance, a low content of volatiles, and a high strength of lump on heating. The best reducers are charcoal and pitch and petroleum coke; they contain little ash, but are rather expensive. For that reason, charcoal is only used for making crystalline silicon. Certain grades of anthracite and coke may be applicable for the purpose, but mainly in combination with other reducers, because they are liable to cracking on being heating. The material that is used most commonly for the manufacture of Ferro-silicon is coke breeze, i.e. fines remained from screening of blast furnace coke. A large disadvantage of coke breeze is a high moisture content, which may vary within wide limits, depending on the conditions of transportation and storage, and sometimes reaches 25%. A high and unstable moisture content of coke breeze can often cause an unstable run of the furnace. The ash of coke breeze is the main source of aluminium in alloys. Therefore, low-ash materials are needed as reducers in order to make 75% Ferro-silicon with a low content in aluminium, as required, for instance, in the manufacture of transformer steels.

For the manufacture of Ferro-silicon petroleum coke is sometimes used, in a mixture with coke breeze. It may contain up to 4% S, 2% Ash and up to 0.025 % P. Petroleum coke is less expensive than coke, contains little ash, and has a relatively low electrical conductivity.

In recent years, semi coke has found with application along with coke. It is product of coke coking at temperatures up to 700^0C. Use of a mixture of common coke breeze and semi coke allows a deeper position of electrodes and improves furnace operation. Another material

employed in the manufacture of Ferro-silicon is turning of Carbon steels having a low content of Phosphorus and no addition of alloying or non-ferrous metals. Fine turning are the best choice. Long curled turning can involve difficulties in charging and servicing of furnaces and cannot be distributed evenly in the charge.

Raw Materials for Fe-Mn

The main Mn minerals are Pyrolusite (MnO_2), Braunite (Mn_2O_3), Manganite ($Mn_2O_9.H_2O$) and Hausmannite (Mn_3O_4). Manganese ores used to be used for smelting of ferro-manganese should meet the following process conditions: (a) The content of Manganese in ore should be at least 45 percent; a higher content of Manganese ensures a higher productivity of furnaces and a lower use of electrical energy per ton of alloy; (b) The content of Silica in the ore should be as low as possible; silica increase the slag ratio and cause a larger loss of manganese to slag and a higher use of electrical energy. The reductant process is usually coke breeze with not more than 12 percent ash, 11percent (on average) moisture, 2 percent volatiles, and less than 0.02 percent Phosphorus; its grain size should be from 3 to 15 mm. Ground slightly oxidized steel turnings are also used in the process.

2.4: Use of Ferro-Silicon and Ferro-Manganese grades [2]:

Ferro-Silicon grade:

1. It is a necessary deoxidizer for steel smelting. In steel smelting, the product is used to sedimentary accretion and expanding deoxidizing, and also an alloy addition in steel smelting and to change physical and chemical properties, such as hardness, tensile strength, ductility and abrasion resistance;
2. In alloy industry, the high-silicon content ferrosilicon or silicon alloy are used to be the reducer in the production of low-carbon alloy. Putting ferrosilicon into iron casting, it can be an inoculant of nodular cast iron, and can prevent the formation of carbide, improve the separating out and balling of graphite, and improve the property of casting iron.

Ferro-Manganese grade:

1. Alloying: Used in alloying, especially in aluminum base alloys, to which it imparts hardness, strength and corrosion resistance. It is also used to improve mechanical properties of lead base alloy containing Calcium, Tin, In.
2. Deoxidation: Added to the molten iron bath to deoxidized, refine or 'settle' the steel bath to produce ingot of desired quality and texture. In this process Mn reduces iron oxide to produce inactive Manganese oxide.
3. Desulphuriser: To improve the rolling properties of the steel by reduction of its 'S'content. Manganese combines with sulphur and the sulphides formed are taken up in the slag. Although other elements, such as Silicon and Aluminium, perform the function of deoxidation adequately. They do not exercise the dual function of deoxidation and desulphurization which is exercise by Mn.
4. Modifying structure of graphite in cast irons: Ferro-manganese can effectively nodulize graphite particles in cast iron producing spherodial graphite, which is strong tougher and more ductile than ordinary cast iron
5. Manganese by retarding the rate of grain growth, produces a fine grained steel. This reduces the steel less intensive to the process of hot rolling and is also said to improve

the cold rolling and also said to improve cold rolling adequately. Si on the other hand tend to favors increase in grain size.

2.5 Activity of Silicon in Fe-Si and Fe-C-Si alloys:

Chipman, Fulton, Gokcen and Caskey [3] tries to evaluate the relevant data on these systems and deduced the desired relationship between the activity, composition and the temperature. The binary solution of Fe-C and Fe-Si exhibit strong negative deviation from ideality, indicating strong attractive forces between unlike atoms. The author published data on the solubility of graphite in molten Fe-C-Si alloy at different temperatures in the range 1200-1600^{0}C and the distribution of Silicon between the liquid iron and liquid Silver.

The solubility of graphite in molten iron and in Fe-C-Si alloys containing up to about 23 percent Silicon has also been reported by Chipman, Alferd, Gott and Small[4]. In the binary system the result in the temperature range of 1153^{0}C (eutectic) to about 1950^{0}C are adequately represented by the following expression

$$\%C = 1.34 + 2.54 \times 10^{-3} t\ (^0C) \quad \text{.....(2.4.1)}$$

In the ternary solution the graphite solubility could not be determined above 23 percent Silicon because the precipitation of a second solid phase (β-SiC). This is cubic form, which is stable below 2200^{0}C. It differes in structure in structure from the α-SiC, but the thermodynamic properties of these two form are the same.

In the distribution experiments of Chipman et al[4] and also Chou[5], a silver bed was equilibrated with Fe-Si or Fe-C-Si alloys. The experiments were carried out in a simple high frequency induction furnace. The charge, consisting of 10-11 grams of silver and 9-10 grams of alloy was placed in a 10 mm diameter silica crucible.

After considerable time, the crucible was quenched and specimens were prepared for analysis. From the analysis of iron and silver phase the atom fraction of silicon in both the phases were determined. In the case of Fe-C-Si alloy, atom fraction of carbon in the alloy was also determined. There was no need to do so with silver phase as carbon is insoluble in silver. As the two phases are in equilibrium, the following can be written:

$$a_{Si}^{Ag} = a_{Si}^{Fe}$$

$$\text{or, } N_{Si}^{Ag}\, \gamma_{Si}^{Ag} = N_{Si}^{Fe}\, \gamma_{Si}^{Fe}$$

$$\text{or, } \gamma_{Si}^{Fe} = [N_{Si}^{Ag} / N_{Si}^{Fe}]\, \gamma_{Si}^{Ag}$$

$$\therefore \log(\gamma_{Si}^{Fe}) = \log[N_{Si}^{Ag} / N_{Si}^{Fe}] + \log \gamma_{Si}^{Ag} \quad .. \quad (2.4.2)$$

There remains uncertainty and scatter in the determination of $\gamma^0_{Si}{}^{Ag}$ values from the binary phase diagram. The value given by some workers are:

(i) Chipman et al [3] : $\log \gamma^0_{Si}{}^{Ag} = 0.3 \pm 0.1$.....(2.4.3)

(ii) Chou [5] : $\log \gamma^0_{Si}{}^{Ag} = 0.301$.....(2.4.4)

(iii) Turkdogan [6] : $\log \gamma^0_{Si}{}^{Ag} = 0.245$.....(2.4.5)

The value of $\gamma^0_{Si}{}^{Ag}$ may also been obtained by another method. Rewriting equation (2.4.2) for very finite dilute solutions in iron phase:

$\log \gamma^0_{Si}{}^{Ag} = \log \gamma^0_{Si}{}^{Fe} - \log [N_{Si}{}^{Ag} / N_{Si}{}^{Fe}]$.....(2.4.6)

If terms on the right hand side are known, $\gamma^0_{Si}{}^{Fe}$ can be found out. The ratios $N_{Si}{}^{Ag} / N_{Si}{}^{Fe}$ in very dilute solutions were found out by extrapolation of the $\log N_{Si}{}^{Ag} / N_{Si}{}^{Fe}$ Vs N_{Si} plots to $N_{Si} = 0$ for the Fe-Si alloys. Activity coefficient of silicon in dilute solutions, $\gamma^0_{Si}{}^{Fe}$ was obtained from the free energy of formation and other thermodynamic data as discussed below.

Chipman and Baschwitz[7] used the data by Gokcen and Chipman[8] and Matoba[9] to derived the following expression for the free energy change, i.e.,

$Si(l) = Si(wt\%)$.....(2.4.7)

$\Delta G^0_{(2\,4\,7)} = -28{,}500 - 5.8T$.....(2.4.8)

Raoultion activity coefficient, $\gamma^0_{Si}{}^{Fe}$ may be calculated using the well known relationship given below :

$\Delta G^0_{(2\,4\,7)} = 4.575T \log[\{55.85\gamma^0_{Si}{}^{Fe}\} / \{28.98 \times 100\}]$..... (2.4.9)

Which yields, $\log \gamma^0_{Si}{}^{Fe} = -(6236 / T) + 0.434$.....(2.4.10)

The activity coefficient of silicon at infinite dilution, $\gamma^0_{Si}{}^{Fe}$, was also derived from the work of Matoba, Gunji and Kuwana[10] who equilibrated Fe-Si melts with solid silica and hydrogen plus water vapor mixtures over the temperature range 1570^0 to 1680^0C and the composition range 0.04 to 2-9 percent silicon. Their equation for obtaining the activity coefficient of silicon in dilute solution of iron was as follows:

$\log \gamma^0_{Si}{}^{Fe} = -(7594 / T) + 1.156$.....(2.4.11)

There does not exit any notable difference in the value of $\gamma^0_{Si}{}^{Fe}$ calculated by using equations (2.4.10) and (2.4.11) in the temperature range 1400 to 1600^{0}C.

These studies were extended by Chipman et al [7] to Fe-C-Si systems (graphite saturated). The results showed that the $\log[N_{Si}{}^{Ag} / N_{Si}{}^{Fe}]$ (Fe-C-Si) or $\log \gamma_{Si}{}^{Fe\text{-}C\text{-}Si}$ vs $(N_{Si} + N_C)$ plots were very identical to the $\log[N_{Si}{}^{Ag} / N_{Si}{}^{Fe}]$ or $\log \gamma_{Si}{}^{Fe}$ vs N_{Si} plots obtained by the same authors earlier. The Henrian activity coefficients $f_{Si}{}^{Fe\text{-}C\text{-}Si}$ on the weight percent standard state scale may be defined as follows:

$$f_{Si}{}^{Fe\text{-}C\text{-}Si} = (\gamma_{Si}{}^{Fe\text{-}C\text{-}Si}) / (\gamma^0_{Si}{}^{Fe}) \text{.....(2.4.12)}$$

The use of Henerian activity coefficients permits us to write the concentration of silicon in weight percentage rather than in mole fraction and greatly simplifies the calculations of both carbon and silicon in iron tends to approach zero. With reference to the new weight percentage standard state, the free energy change for reaction may be written as follows:

$$SiO_2 + 2C = Si + 2CO\ (g) \text{ .....(2.4.13)}$$

$$\Delta G^0_{(wt\%)} = \Delta G^0_{Th} + \Delta G^0_{(2.4.7)}$$

$\Delta G^0_{Th}\rightarrow$ Free energy for the reaction (2.4.13) with reference to Raoultian standard state,

$$\Delta G^0_{Th} = 2\,\Delta G^0_{CO} - \Delta G^0_{SiO2}.$$

$$\Delta G^0_{Th} = -RT\ln K = -RT\ln\left(\frac{a_{Si}\,p^2_{CO}}{a_{SiO_2}.a^2_C}\right) \text{ .....(2.4.13a)}$$

$\Delta G^0_{(2.4.7)}\rightarrow$ Heat of formation for reaction (2.4.7). $\Delta G^0_{(wt\%)}\rightarrow$Standard free energy change for the reaction (2.4.13) when the standard state of silicon is taken to be 1 wt%.

Combining (2.4.13a) and (2.4.8)

$$\Delta G^0_{(wt\%)} = 138670 - 92.03T \text{.....(2.4.14)}$$

May be written for reaction (2.4.15)

$$(SiO_2) + 2C = Si\ (wt\%) + 2CO\ (g) \text{.....(2.4.15)}$$

The new equilibrium constant K′ may be expressed as the following equation:

$$\Delta G^0_{(wt\%)} = -RT\ln K = -RT\ln\{f_{Si}\,[\%Si]\,P^2_{CO} / (\gamma_{SiO2}.N_{SiO_2})\}$$

$$\log\{f_{Si}\,[\%Si]\,P^2_{CO} / (\gamma_{SiO2}.NSiO_2)\} = 30343/T + 20.13 \ldots\ldots\ldots\ldots (2.4.16)$$

The above review of the works of many investigators reveals that enough care should be taken while using the reported data to find the activity coefficient of silicon in iron due to the large scatter and uncertainty in the data. This error may be attributed to the factors such as error in the estimation of $\gamma^0_{Si}{}^{Fe}$ value, extrapolation of the data to very dilute solutions of silicon and carbon in iron etc.

In some other method of determining γ_{Si}, Fe-Si alloy was equilibrated by Turkdogan, Grieveson and Bisler [6] with Si_3N_4 phase at one atm. pressure of purified nitrogen at 1400,1500, and 1600^0C for 24 hours. At the end of the experiment, the sample was quenched and analysed. Using the free energy of formation of silicon nitride, the activity coefficient of silicon was evaluated from the experimental solubility data. Only a limited number of experiments were conducted in this case.

2.6. Production of Silicon Carbide [11]:

The most common forms of SiC include powders, fibers, whiskers, coatings and single crystals. There are several methods to produce SiC depending on the product form desired and its application. Purity of the product imposes certain restrictions on the selection of the method of production.

SiC powders are produced predominantly via the traditional Acheson method where a reaction mixture of green petroleum coke and sand is heated to 2500°C using two large graphite electrodes. Due to the high temperatures, the Acheson process yields the alpha form of SiC, i.e. hexagonal or rhombohedra (α-SiC). The SiC product, usually in the form of a large chunk, is broken, sorted, crushed, milled, and classified into different sizes to yield the commercial grades of SiC powder. To produce ultra fine SiC powder, the finest grade of the Acheson product is further milled, typically for days, and then acid-treated to remove metallic impurities. Fine SiC powder can also be produced using a mixture of fine powders of silica and carbon reacted at lower temperatures for short periods of time followed by quenching to prevent grain growth. The product, however, is agglomcrates of SiC and needs to be attrition milled to break up the agglomerates and reduce the particle size to submicron range. SiO_2 powder can be replaced with SiO(silicon monoxide) powder which, when mixed with nano-scale carbon and heated to moderate temperatures, produces nanocrystalline SiC powder with particle size in the range 20-100 nm. The SiC particle characteristics, such as size, shape and surface chemistry, are very important for the subsequent densification processes of the SiC powder. For this reason, some post processes may be needed, such as the addition of certain elements as sintering aids, to achieve high density during hot pressing or pressure less sintering.

SiC whiskers, which are nearly single crystals, are produced (grown) using different methods, including the heating of coked rice hulls, reaction of silanes, reaction of silica and carbon, and the sublimation of SiC powder. In some cases a third element used as a catalyst, such as iron, is added to the reacting materials to facilitate the precipitation of the SiC crystals. In this arrangement, the mechanism for the SiC whisker growth is called the vapor liquid- solid (VLS) mechanism. SiC whiskers are in the order of microns in diameter and grow several hundred microns in length. The VLS process, developed by the Los Alamos National Laboratory to produce longer SiC whiskers with larger diameters, did not show promise for production due to the extremely low yield. Currently, commercially available SiC whiskers are produced using the

rice-hull process with the whisker growth being largely of VS mechanism due to the absence of a catalyst. Because of their excellent mechanical properties, SiC whiskers are very desirable as reinforcements of metal and ceramic matrix composites for structural applications where fracture toughness and strength are significantly improved.

2.6.1: POCO's Process for SiC production:

POCO's process starts with graphite that has already been processed, pre-machined into the desired part, and purified, followed by the chemical conversion to SiC, without altering the shape or purity of the part. This approach yields a SiC product that has superior chemical properties and very high purity as compared to traditionally produced SiC products. The conversion of the graphite parts to SiC takes place when they are exposed to silicon-carrying species, such as silicon monoxide (SiO) gas, at high temperatures. Figure 2.6.1 is a flowchart showing, in sequence, all the steps involved in POCO's SiC conversion process. The SiO gas is generated in-situ using a proprietary mixture of high-purity silica and carbon powders in inert atmosphere. The following is a typical reaction for the generation of SiO gas:

$$SiO_2 + C \Leftrightarrow SiO + CO$$

It is essential that the graphite material have a reasonable open porosity for the SiO gas diffusion. POCO's specially developed graphite grade, with the tailored porosity and particle size distribution properties, meets the requirements of the conversion process. The generated SiO is transported from the generation zone to the conversion zone, which contains the graphite parts to be converted to SiC. POCO has engineered the process so that SiO gas is transported efficiently from the generation zone to the conversion zone and distributed evenly to ensure uniform conversion. In the conversion zone, the reaction between the SiO and graphite takes place according to the following reaction:

$$SiO + 2\,C \Leftrightarrow SiC + C$$

This reaction is a typical gas-solid reaction in which the rate-limiting step is the pore-diffusion resistance. Accordingly, it is essential to ensure a large SiO concentration gradient between the bulk gas phase and the SiC/C interface, or the reaction front. At this interface, the reaction rate is controlled by surface kinetics, which is spontaneous due to the high temperatures. In other words, the conversion rate is controlled by the inward diffusion of the SiO and outward

diffusion of the CO gasses through the SiC shell. Following the chemical conversion of the net-shape graphite part to SiC, the parts are usually grit blasted using high purity SiC to remove any surface debris, followed by ultrasonic cleaning to remove any dust and loose particles.

2.6.2: Properties of SiC:

Low density

High strength

Low thermal expansion

High thermal conductivity

High hardness

High elastic modulus

Excellent thermal shock resistance

Superior chemical inertness

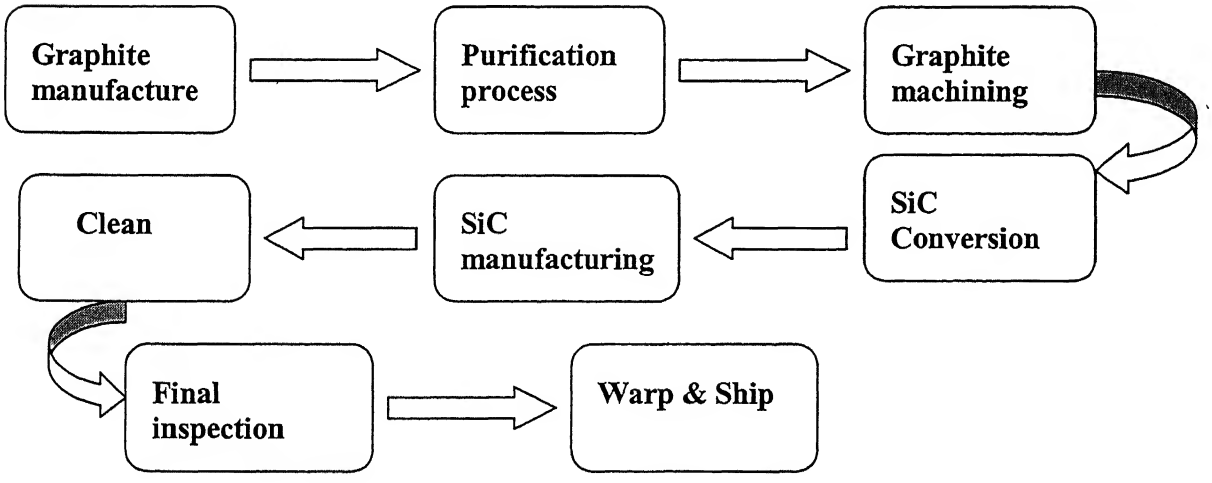

Fig. 2.6.1: Flowchart of POCO's SiC manufacturing process

Chapter: 3

Thermodynamic models for smelting of Ferrosilicon and Ferromanganese alloys for different conditions

3.1: Thermodynamic models of manufacture of Ferrosilicon

First Stage of Reduction

Standard free energies of formation of species of interest in the present study are taken from the literature [12] and are summarized in Table 3.1. Standard heat of formation at 298°K, heat of fusion and heat capacity of the species are summarized in Tables 3.2. Both carbon and silicon combine with iron to form Fe_3C and Fe-Si respectively. Chipman et al [3] reported that solubility of carbon in liquid iron decreased with an increase in silicon content of the metal. Mathematical expression to describe the solubility data of carbon in the iron-carbon-silicon system may be described as follows:

$$[\%C] = 0.65 + 0.00254\ T - 0.34\ [\%Si] \qquad (1)$$

T is temperature in degree Kelvin. For all practical purposes, solubility of carbon in Ferro silicon alloys containing more than 20 wt. pct silicon may be ignored. Reduction of silica will be favoured at high temperature and by lowering the activity of silicon in presence of iron as shown below:

$$SiO_2 + 2\ [C] = Si + 2\ CO\ (g) \qquad a_{Si}\left(P_{CO}^2/a_{SiO_2}\right) = \exp\left(45.6 - \frac{87720.2}{T}\right) \qquad (2\ \&\ 2a)$$

Reaction (2) has been widely studied in the last five decades or so by a number of investigators [13-19] as it was considered to be important in controlling the silicon content of the blast furnace iron to low levels. There has been general consensus so far that transfer of silicon via the above written slag metal reaction is sluggish in nature. It was attributed to simultaneous involvement of liquid metal, liquid slag and gas phases in the overall transfer of silicon from slag to metal phase. Batra and Bhaduri [20] reported that reduction of quartz alone could be occurring at high rate in presence of liquid iron carbon. Chipman and Baschwitz[7] determined the activity of silicon in the liquid alloy by equilibrating it with liquid silver and determining silicon content of both phases. Results reported by the investigators may be described by the following mathematical expressions with minimal of error:

$$a_{Si} = \exp\left(0.2274 \times \{f_{Si} \times 100\} - 8.4906\right) \qquad 0 < f_{Si} \le 0.30 \qquad (3)$$

$$= \exp\left(0.0556 \times \{f_{Si} \times 100\} - 3.145\right) \qquad 0.30 < f_{Si} \le 0.42 \qquad (4)$$

$$= \exp\left(0.0158 \times \{f_{Si} \times 100\} - 1.3832\right) \qquad 0.42 < f_{Si} \qquad (5)$$

Mole fraction of silicon in Fe-Si alloys is related to its weight fraction as shown below:

$$N_{Si} = \frac{\left(\frac{f_{Si}}{28}\right)}{\left(\frac{f_{Si}}{28} + \frac{1-f_{Si}}{56}\right)} = \left(\frac{2f_{Si}}{1+f_{Si}}\right) \quad (6)$$

Computed mole fraction and activity of silicon are plotted against weight fraction of silicon in the alloy in Fig. 3.1. Calculations using equation (2a) show that at unit activity of silica and carbon, silicon content of metal could reach 22 pct. at around 1810°K at unit partial pressure of carbon monoxide. In presence of free carbon, any silicon in excess of 22 wt. pct transforms to silicon carbide:

$$[Si] + C = SiC \qquad a_{Si} = \exp(3.98 - 12632.11/T) \quad (7)$$

It follows that it will not be possible to manufacture Fe-Si alloys of silicon content greater than 22 in presence of excess of carbon. This agrees with findings of Rein and Chipman [14]. Overall reaction may be written as follows:

$$SiO_2 + 3\ C = SiC + 2\ CO\ (g) \quad P_{CO} = \exp(41.615 - 75088.1/T) \quad (8)$$

There could be simultaneous evolution of silicon monoxide gas as a result of the following reaction:

$$SiO_2 + C = SiO\ (g) + CO\ (g) \quad P_{CO}P_{SiO} = \exp(40.485 - 82964.27/T) \quad (9)$$

Partial pressure of silicon monoxide is computed to be at 0.0045 atm at 1810°K. For practical purposes, evolution of silicon monoxide is ignored during the first stage of reduction. In presence of excess silica, phases present after first stage of reduction will be silica, silicon carbide and Fe-22 wt. pct Si alloy.

Second Stage of Reduction

If condensed phases containing silica, silicon carbide and Fe-22 wt. pct Si alloy are heated beyond 1810°K, silicon content of the alloy could increase as a result of the following reaction:

$$SiO_2 + 2\ SiC = 3\ [Si] + 2\ CO\ (g) \quad (10)$$

$$a_{Si}^3 P_{CO}^2 = \exp(53.56 - 112984.4/T) \quad (11)$$

$$P_{CO} = \sqrt{\frac{\exp(53.56 - 112984.4/T)}{a_{Si}^{3}}} \qquad (11a)$$

Simultaneous evolution of silicon monoxide due to the following reaction may no longer be ignored:

$$SiO_2 + Si = 2\ SiO\ (g) \qquad (12)$$

$$a_{si} P_{SiO}^2 = \exp(36.1 - 78208.3/T) \qquad (13)$$

$$P_{SiO} = \sqrt{[\exp(36.1 - 78208.3T) \times a_{Si}]} \qquad (13a)$$

For the reactions to proceed, sum of partial pressures of evolved silicon monoxide and carbon monoxide must exceed the applied pressure of one atmosphere. At any temperature, let "p" moles of silica and "q" moles of silicon carbide combine to produce n_{CO}, n_{Si} and n_{SiO} moles of carbon monoxide, silicon and silicon monoxide. Carbon, oxygen and silicon atom balances yield the following:

$$n_{CO} = q \qquad (14)$$

$$n_{CO} + n_{SiO} = 2p \qquad (15)$$

$$n_{Si} + n_{SiO} = p + q \qquad (16)$$

Instantaneous silicon recovery at any temperature may be defined as follows:

$$r_{Si} = \left(\frac{n_{Si}}{n_{Si} + n_{SiO}}\right) \qquad (17)$$

Assuming ideal gases, molar ratio of carbon monoxide and silicon monoxide phase will be proportional to their partial pressure in the gas at any temperature and it can be determined using the thermodynamic data. Solving at unit pressure,

$$r_{Si} = \left(\frac{3 - \beta}{3 + \beta}\right) \qquad (18)$$

where

$$\beta = P_{SiO} / P_{CO} = P_{SiO} / (1 - P_{SiO}) \qquad (19)$$

r_{Si} gives ratio of silicon atoms going into the metal to that being added as silica in the burden at a particular level of silicon in the alloy. Rest of silica is being transformed to silicon monoxide. Silicon recovery is assumed to be unity till silicon concentration of 22 wt. pct. is reached in the alloy as losses, as evolution of silicon monoxide are ignored in the first stage

of reduction. Overall silicon recovery may be calculated by considering the amount of silicon present per unit amount of iron in the alloy, as amount of iron remains unchanged as silicon content increases.

$$W_{Si} = \left(\frac{f_{Si}}{1 - f_{Si}} \right) \quad (20)$$

$$\delta W_{Si} = \delta f_{Si} / (1 - f_{Si})^2 \quad (21)$$

Expression for the overall silicon recovery in the alloy of certain grade can be obtained as follows:

$$R_{Si} = \frac{W_{Si}}{\int_0^{f_{Si}} \frac{1}{r_{Si}} \delta W_{Si}} \quad (22)$$

The equation is solved numerically using a computer programme. Computed values of instantaneous and overall silicon recoveries are plotted against weight fraction silicon in the Ferrosilicon alloy in Fig. 3.2. In general, as silicon content increases silicon recovery decreases.

The modeling of Ferrosilicon alloys of various grades and for different conditions are reported in this chapter

MODEL 1: Production of Fe-Si alloy by using a mixture of pure Fe, SiO_2 and Carbon, without recirculation of SiO

MODEL 2: Production of Fe-Si alloy by using a mixture of pure Fe, SiO_2 and Carbon, with recirculation of SiO

Recycling of Silicon Monoxide

In practice, electrodes are immersed 1 to 1.5m deep inside the burden. Hot gases such as carbon monoxide and silicon monoxide that are evolved beneath the arc are allowed to come in contact with descending burden materials such as silica, carbon and iron chips. Gases are cooled due to the heat exchange between the solid and gas phases. Silicon monoxide is not stable at lower temperature and could transform to silicon carbide and silica. Assuming that no silicon monoxide vapors escape to the atmosphere and some sensible heat of flue gas or gases is or are recovered in the shaft.

MODEL 3: Production of Fe-Si alloy by using a mixture of Fe_2O_3, Silica and Carbon. It is assumed that complete reduction of Fe_2O_3 to Fe occurs at the lower part of the furnace, the flue gas will consist of Carbon monoxide.

$Fe_2O_3 + 3C = 2Fe + 3CO\ (g)$

MODEL 4: Production of Fe-Si alloy by using a mixture of Fe_2O_3, Silica and Carbon. If Fe_2O_3 is pre-reduced completely in the shaft region. The flue will consist of Carbon monoxide and Carbon dioxide.

$Fe_2O_3 + CO = 2FeO + CO_2$

$FeO + C = Fe + CO$

MODEL 5: Production of Fe-Si by using a mixture of Fe_2O_3, Silica and Carbon. Pre-reduction of Fe_2O_3 is completed in the shaft region, a part of FeO phase might be reduced by CO gas at around 900^0C if solid particles pickup heat ahead of the arc by radiation, assuming gas solid equilibrium.

$Fe_2O_3 + CO = 2FeO + CO_2$

$FeO + C = Fe + CO$

$FeO + CO = Fe + CO_2$

RT ln(K)=62050-14.95T.

If "α" is the degree of direct reduction of $Fe_{0.95}O$ in the arc region. Thermodynamics condition gives the following.

$$\frac{(1-\alpha)\times(1-f_{Si})}{0.95\times 56}=2\times K\times\left(\frac{f_{Si}}{28}\right)+\frac{\alpha\times(1-f_{Si})}{0.95\times 56}-\frac{(1-\alpha)\times(1-f_{Si})}{0.95\times 56}$$

$$\alpha=\frac{1}{2.K+1}\left(\{1+K\}-\frac{3.8.K.f_{Si}}{1-f_{Si}}\right)$$

Where, K is the equilibrium constant of the following reaction.

$Fe_{0.95}O + CO = 0.95\ Fe + CO_2$

At higher level of Si in the alloy, there may be little unreduced iron oxide in the arc region. Value of α could be taken zero for such cases

Silica required to produce per Kg Ferrosilicon alloy

$$w_{SiO_2} = \frac{28}{60}\int_0^{f_{Si}} \frac{\partial f_{Si}}{r_{Si}(1-f_{Si})^2} \qquad \text{For model 1}$$

$$= \frac{28}{60} \times f_{Si} \qquad \text{For other models}$$

$$n_{SiO_2} = \frac{w_{SiO_2}}{60}$$

$$W_{SiO_2} = w_{SiO_2} \times 1000.$$

Oxygen atom balance would the following,

Oxygen atoms in $SiO_2 = 2 \times n_{SiO_2}$

$$n_{SiO} = n_{SiO_2}(1 - R_{Si})$$

$$n_{CO} = n_{SiO_2}(1 + R_{Si}) \qquad \text{For model 1}$$

$$n_{CO} = 2 \times n_{SiO_2} \qquad \text{For model 2}$$

$$= 2 \times n_{SiO_2} + 3 \times n_{Fe_2O_3} \qquad \text{For model 3}$$

$$= 2 \times n_{SiO_2} + n_{Fe_2O_3} \qquad \text{For model 4}$$

$$n_{CO_2} = n_{Fe_2O_3} \qquad \text{For model 4}$$

For case 5,

$$n_C = 2 \times n_{SiO_2} + \left(\frac{1 - f_{Si}}{0.95 \times 56}\right)\alpha$$

$$n_{CO_2} = \frac{(1-\alpha) \times (1 - f_{Si})}{0.95 \times 56} + \frac{(1 - f_{Si})}{2 \times 56}$$

$$n_{CO} = n_C - n_{CO_2} \qquad \text{For model 5}$$

Heat and Mass Balance:

Overall heat and mass balances have been carried out in the present work in order to determine the carbon and electrical energy requirements of the process. Assuming that chemical and sensible heat of outgoing gases such as Carbon monoxide, Carbon dioxide and silicon monoxide are not recovered; oxygen and carbon atom balances give the following expression for carbon rate in kg per 1000 kg of the liquid alloy:

$$W_C = 12 \times n_{CO} \times (1 - f_{Si}) \times 1000 \qquad \text{For model 1}$$

$$= 12 \times n_{CO} \times 1000 \qquad \text{For model 2, 3, 4}$$

$$= 12 \times n_{C} \times 1000 \qquad \text{For model 5} \qquad (23)$$

It has been assumed for simplicity that Sensible heat of the liquid slag is produced in the process is 2000KJ/ Kg Slag. Sensible heat of the liquid alloy is determined from the heat capacity date of elements such as silicon and iron and heat of formation of Fe-Si as follows:

$$H_{Si} = n_{Si} \times \left(\int_{298}^{1685} \Delta C_{P,Si(298-1685K)}.dt + \int_{1685}^{t} \Delta C_{P,Si(1685-tK)}.dt + H_f^{Si} \right)$$

$$H_{Fe} = n_{Fe} \times \left(\int_{298}^{1042} \Delta C_{P,Fe(298-1042K)}.dt + \int_{1042}^{1182} \Delta C_{P,Fe(1042-1182K)}.dt + \int_{1182}^{1665} \Delta C_{P,Fe(1182-1665K)}.dt + \right.$$

$$\left. \int_{1665}^{1810} \Delta C_{P,Fe(1665K-1810)}.dt + \int_{1810}^{t} \Delta C_{P,Fe(1810-tK)}.dt \right)$$

Heat of Formation of Fe-Si

$$H_{FeSi} = \Delta H^{0}_{FeSi,298K} \times (n_{FeSi})$$

$$H_{alloy} = H_{Si} + H_{Fe} + H_{FeSi}$$

Sensible heat of Slag $(H_{Slag} \text{in} MJ)$

H_{Slag} = Weight of slag (*Kg*) × Sensible heat of Slag (*KJ/Kg slag*)/10^6

$$= 2 \times W_{Slag}.$$

Sensible heat of Slag = 2000 KJ/Kg Slag (*assumption*) for simplicity

$$H_{CO} = n_{CO} \times \left(\Delta H^{0}_{CO,298K} + \int_{298}^{tg} \Delta C_{P,CO}.dt \right)$$

$$H_{CO_2} = n_{CO_2} \times \left(\Delta H^{0}_{CO_2,298K} + \int_{298}^{tg} \Delta C_{P,CO_2}.dt \right)$$

$$H_{SiO} = n_{SiO} \times \left(\Delta H^{\circ}_{SiO,at298K} + \int_{298}^{tg} \Delta C_{P,SiO}.dt \right)$$

$$H_{SiO_2} = n_{SiO_2} \times \Delta H^{0}_{SiO_2,298^{\circ}K}$$

$$= \left(\frac{1 - f_{Si}}{56 \times 2} \right) \times \Delta H^{0}_{Fe_2O_3,298^{\circ}K}$$

Taking overall thermal efficiency of the furnace as "η", heat balance gives the following expression for heat required in MJ/1000Kg Fe-Si alloy and electrical energy consumption in KWh per 1000 kg of Fe-Si alloy:

$$hr = \left(\frac{\{H_{alloy} + (H_{CO} + H_{SiO} - H_{SiO_2})\} \times 4.184 + H_{Slag}}{\eta} \right) \quad \text{For model 1}$$

$$= \left(\frac{\{H_{alloy} + (H_{CO} - H_{SiO_2})\} \times 4.184 + H_{Slag}}{\eta} \right) \quad \text{For model 2}$$

$$= \left(\frac{\{H_{alloy} + (H_{CO} - H_{SiO_2} - H_{Fe_2O_3})\} \times 4.184 + H_{Slag}}{\eta} \right) \quad \text{For model 3}$$

$$= \left(\frac{\{H_{alloy} + (H_{CO} + H_{CO_2} - H_{SiO_2} - H_{Fe_2O_3})\} \times 4.184 + H_{Slag}}{\eta} \right) \quad \text{For model 4 and 5}$$

Electrical energy required (E) = $\left(\frac{hr}{3.6} \right)$ KWh/ton alloy

Heat demand, heat supply and heat utilization in KWh/ 1000Kg Fe-Si alloy to produce in submerged arc furnace

Heat supply:

Electrical energy (E) = $\left(\frac{hr}{3.6} \right)$

Calorific value of Carbon = $\left(\frac{W_C}{12} \right) \times \Delta H^0_{CO_2} \times \left(\frac{4.184}{3.6} \right)$

Chemical heat of Fe in liquid Fe-Si alloy = $n_{Fe_2O_3} \times \Delta H^0_{Fe_2O_3} \times \left(\frac{4.184}{3.6} \right)$

Heat demand:

Dissociation of SiO_2 = $n_{SiO_2} \times \Delta H^0_{SiO_2,298K} \times (4.184/3.6)$

Dissociation of Fe_2O_3 = $n_{Fe_2O_3} \times \Delta H^0_{Fe_2O_3,298K} \times (4.184/3.6)$

Heat of formation of CO = $n_{CO} \times \Delta H^0_{CO,298K} \times (4.184/3.6)$

Heat of formation of CO_2 = $n_{CO_2} \times \Delta H^0_{CO2,298K} \times (4.184/3.6)$

Heat of formation of SiO = $n_{SiO_2} \times \left(2 \times \Delta H^0_{SiO,298K} - \Delta H^0_{SiO_2,298K}\right) \times (4.184/3.6)$

Heat Utilization:

Sensible heat of liquid Fe-Si alloy $= \left(\frac{H_{alloy} \times 4.184}{3.6} \right)$

Sensible heat of Slag $= \left(\frac{H_{slag}}{3.6} \right)$

Sensible heat of gases $= \left(\frac{H_{CO} + H_{CO_2} + H_{SiO}}{3.6} \right) \times 4.184$

Calorific value of CO $= \left(\frac{n_{CO} \times (\Delta H^0_{CO_2,298K} - \Delta H^0_{CO,298K}) \times 4.184}{3.6} \right)$

Chemical heat of Si in Fe-Si alloy $= \left(\frac{f_{Si}}{28} \right) \times \Delta H^0_{SiO_2,298K} \times (4.184/3.6)$

Chemical heat of Fe in liquid Fe-Si alloy $= \left(\frac{1 - f_{Si}}{2 \times 56} \right) \times \Delta H_{Fe_2O_3,298K} \times (4.184/3.6)$

Circuit loss $= E \times (1 - \eta)$

TABLE: 3.1

Standard free energy and enthalpy of formation of Species of interest in the present study.

Species	$\Delta G^0(Cal/mole), T(^0K)$	$\Delta H^0_{298}(Cal/mole)$	*Temperature range* (^0C)
CO (g)	-26700-20.95T	-26420	25-2000
CO_2 (g)	-94200-0.20T	-94050	25-2000
SiO_2(s)	-227700+48.71T	-217000	1410-1700
SiO (g)	-36150-11.51T	-23200	1410-1700
SiC (s)	-25100+7.91T	-15000	1410-1700
Fe_2O_3 (s)	-19870+11.2T	-196800	25-1400
FeO(s)	-62050+14.95T	-63800	25-1371
FeO (l)	-55620+10.83T	-	1537-1700
FeSi	-	-19200	-
Mn_3O_4	-15800-13.91T	-331400	25-1100
MnO	-91950+17.4T	-92000	25-1500
Mn (g)	53857.1-23.05T	-	1530-1750
Mn_7C_3	-15800-13.91T	-15800	1240-1730

TABLE: 3.2 Heat Capacity, Heat of fusion, Heat of transformation of Species of interest in the present study

Species	*Heat Capacity (Cal/deg/mole)*	*Heat of fusion and Heat of transformation*$^+$	*Temperature range* (^0K)
CO (g)	$6.97+0.98\times10^{-3}T-0.11\times10^{5}T^{-2}$	-	25-2000
CO_2 (g)	$10.57+2.1\times10^{-3}T-2.06\times10^{5}T^{-2}$	-	25-2000
SiO_2(s)	--	290$^+$	1410-1700
SiO (g)	$7.7+0.74\times10^{-3}T-0.7\times10^{5}T^{-2}$	-	1410-1700
SiC (s)	$9.97+1.82\times10^{-3}T-3.64\times10^{5}T^{-2}$	-	1410-1700
Si	$5.7+0.7\times10^{-3}T-1.04\times10^{5}T^{-2}$ 6.1	12100	298-1685 1685-1973
Fe	$3.04+7.58\times10^{-3}T-0.6\times10^{5}T^{-2}$ 11.13 $5.8+1.98\times10^{-3}T$ $6.74+1.6\times10^{-3}T$ $9.77+0.4\times10^{-3}T$	3670 326$^+$ 215$^+$ 165$^+$	298-1042 1042-1182 1182-1665 1665-1810 1810-2973
FeSi	-	-	-
Mn	$5.7+3.38\times10^{-3}T-.37\times10^{5}T-2$ $8.33+.66\times10^{-3}T$ 10.7 11.3	3500 535$^+$ 545$^+$ 4306$^+$	298-1000 1000-1374 1374-1410 1410-1513 1513-2273

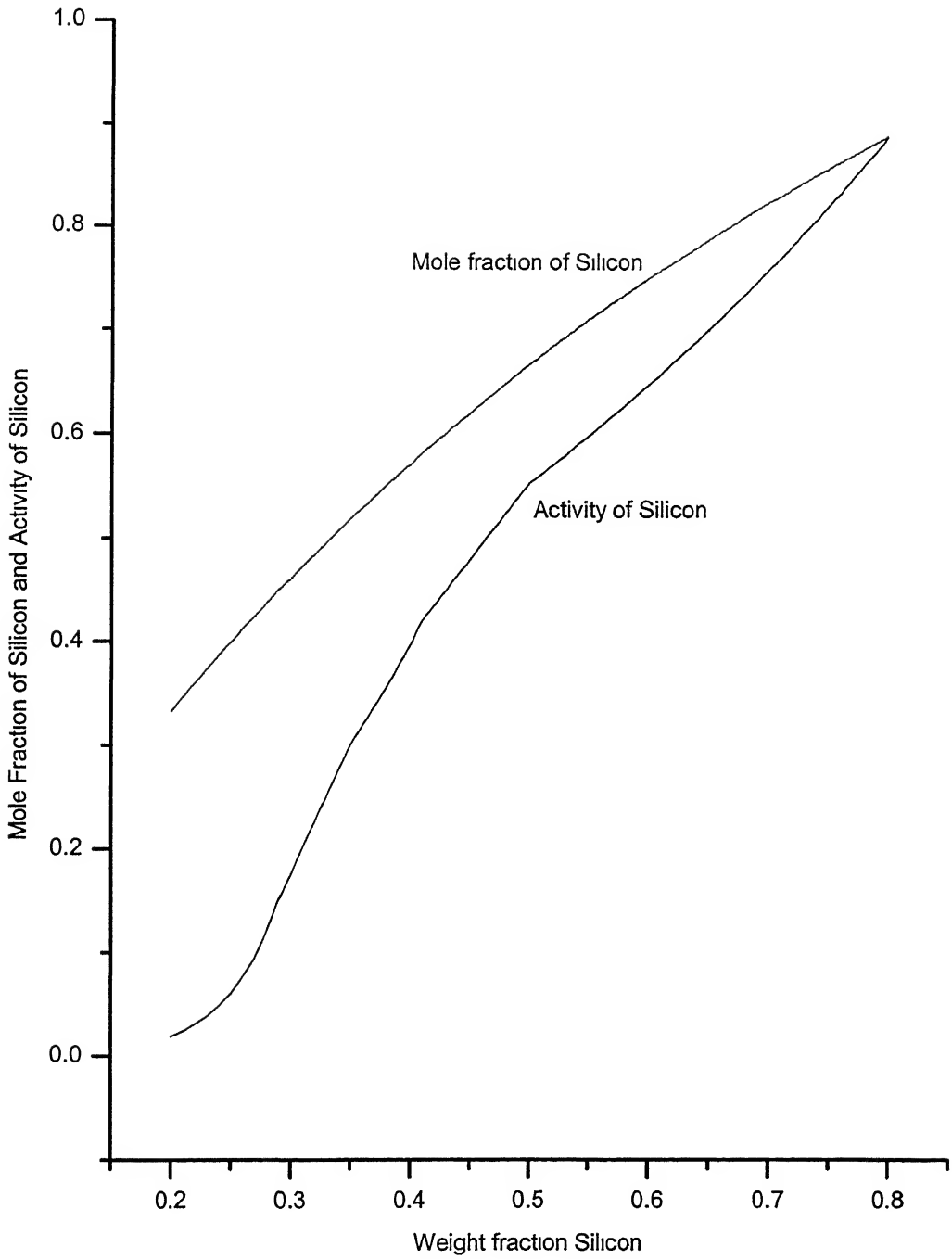

Fig.3.1 Mole fraction and activity of Silicon Vs. weight fraction Si in Ferrosilicon in alloy

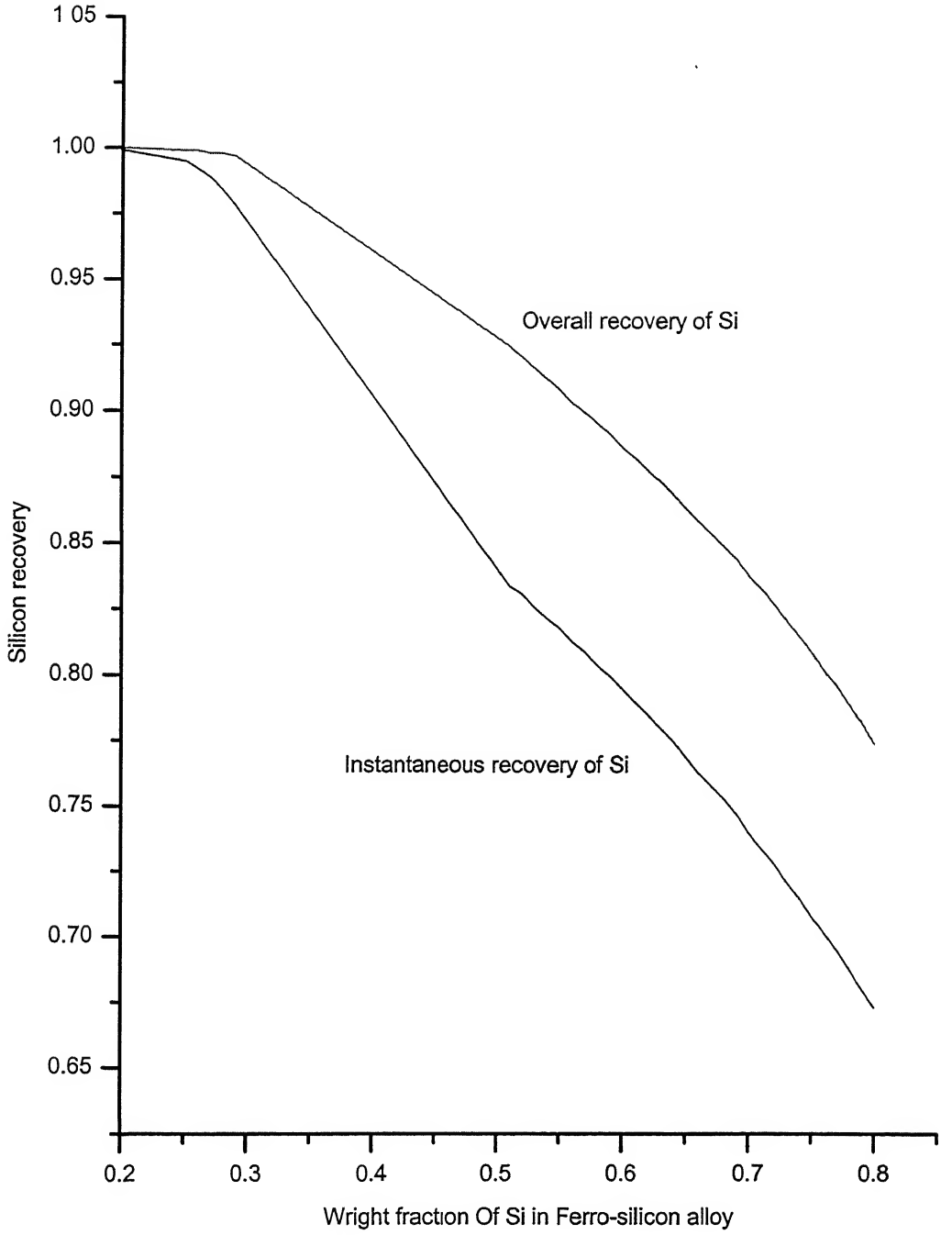

Fig.3.2: Instantaneous and overall recovery of Silicon verses Silicon content in Fe-Si alloy.

3.2: Thermodynamic models of manufacture of Ferromanganese

First stage of reduction:

The standard free energies of formation of the species of interest for the present study taken from literature [12] and are summarized in table 3.1. The standard heat of formation at 298^0K, heat of fusion, heat of phase transformation and heat capacity of the species are summarized in table 3.2. Initially manganese ore (Mn_3O_4) in the burden reduced by CO and form MnO. Relative stability of oxide phases in presence of reducing agents such as carbon and Mn_7C_3 could be evaluated by determining the partial pressure of oxygen due to dissociation of different oxides. The reactions by which oxygen can be evolved are summarized in table3. Computed values of $RT\ln P_{O_2}$ are plotted against temperature in Fig.1. Results show that at applied pressure of one atmosphere, carbon and MnO phases remain intact till temperature of 1546^0K is reached. At this temperature, partial pressure of evolved oxygen due to dissociation of manganese oxide is greater than that required to oxidize carbon to carbon monoxide at unit atmosphere. The condensed phases will consist of carbon and Mn_7C_3 with excess of carbon, but MnO and Mn_7C_3 with excess of MnO at temperature above 1546K. The last two phases can remain intact till higher temperature of about 2015K is reached. At this temperature one or both phases could disappear via reaction (2). Phases present at different temperatures on heating of different proportion of MnO and Carbon together are summarized in Table 3.4. Overall chemical reactions occurring in reduction of MnO during the two stages are described below:

$$7MnO+10C= Mn_7C_3+ 7CO\ (g) \quad (1)$$

$$-RT\ln P_{CO}^7 = 440950-282.6\,T \quad (1a)$$

$$3MnO+ Mn_7C_3=10Mn+3CO\ (g) \quad (2)$$

$$-RT\ln P_{CO}^3 = 937100-461.4\,T \quad (2a)$$

At temperature of less than 1546K, manganese vapors could be simultaneously produced due to the following reaction:

$$MnO + C = Mn\ (v) + CO\ (g) \quad (3)$$

$$-RT\ln(P_{CO}P_{Mn}) = 516500 - 269.4\,T \quad (3a)$$

Solubility of carbon in the metal at equilibrium with Mn_7C_3 phase may be determined from the following consideration:

$$Mn_7C_3 = 7\,Mn + 3[C] \quad (4)$$

$$-RT\ \ln a_C^3 = 6200 + 58.3\,T \quad (4a)$$

Activity of manganese has been taken as unity in deriving equation (4). Carbon content of metal at equilibrium with excess of MnO will be governed by the following:

$$MnO + [C] = Mn + CO\ (g) \quad (5)$$

$$-RT\ \ln\left(P_{CO}/a_{Si}\right) = 290300 - 172.3\,T \quad (5a)$$

Second stage of reduction:

However, for practical purposes, manganese vapors may be ignored as partial pressure of manganese vapor is less than 0.001 at P_{CO} of 1 atm. At temperature above 1546K, manganese vapors in the gas phase will be formed due to the following:

$$3MnO + Mn_7C_3 = 10Mn\ (g) + 3CO\ (g) \quad (6)$$

$$-RT\ \ln\left(P_{CO}^3 P_{Mn(g)}^{10}\right) = 319910 - 1423.4\,T \quad (6a)$$

Combining equations (2) and (6), vapors pressure of manganese might be determined at equilibrium with manganese metal as described below:

$$Mn\ (l) = Mn\ (v) \quad (7)$$

$$-RT\ \ln\ P_{Mn(v)} = (53857.14 - 23.047T) \quad (7a)$$

Let Δn_{CO} moles of carbon monoxide be produced by reaction (2) at any temperature. Moles of manganese produced by the same reaction are given below from stoichiometry:

$$\Delta n_{Mn} = (1/3) \times \Delta n_{CO} \quad (8)$$

Simultaneously, a part of manganese will be lost as vapors i.e. equation (7). Assuming that manganese vapors and carbon monoxide behave as ideal gases, one may determine the amount of manganese vapors formed by computing the partial pressure of two species i.e.

$$\Delta n_{Mn(v)} = (P_{Mn}/P_{CO}) \times \Delta n_{CO} \quad (9)$$

At 2015K, vapour pressure of manganese is computed to be 0.15 atm. and that of carbon monoxide as 0.85 atm. Instantaneous manganese recovery can be determined as follows:

$$r_{Mn} = \left(\frac{\Delta n_{Mn} - \Delta n_{Mn(v)}}{\Delta n_{Mn}}\right) = 1 - 0.3 \times \left(\frac{P_{Mn}}{P_0 - P_{Mn}}\right) \quad (10)$$

Where Po is the applied pressure and must equal the sum of partial pressures of carbon monoxide and manganese vapours.

Iron-Manganese-Carbon-Oxygen System

Activity of manganese in the liquid alloy is lowered due to presence of iron and carbon at temperature above 1423K. For simplicity, activity of manganese is taken same as the mole fraction of manganese in the alloy as iron and manganese are known to behave ideally. Mole fraction in turn will around 1.2 times the weight fraction of manganese in carbon saturated metal. Solubility of carbon in the alloy tends to increase with an increase in temperature as well as increase in the manganese content of the metal. Carbon and MnO phases can react in presence of liquid iron carbon alloy via reaction (5) to give manganese in metal, as to satisfy the following:.

$$MnO + C = [Mn] + CO\ (g) \qquad (11)$$

$$-RT \ln (P_{CO}\, a_{Mn}) = 290300 - 172.3\ T \qquad (11a)$$

Activity of manganese in the binary Fe--Mn system may be taken as its weight fraction as molecular weights of manganese and iron being 55 and 56 respectively are very close to each other and these elements are reported to form an ideal solution. For carbon saturated alloy, activity of manganese is taken to be 1.2 times the weight fraction of manganese in the alloy to simplify the calculations. At unit activity of carbon and unit partial pressure of CO gas, manganese content of metal must increase with an increase in temperature. At 1546K, manganese content in the alloy reaches around 15.5 weight percent manganese. Rest of carbon in presence of excess of MnO should be transformed to Mn_7C_3 phase at this temperature as mentioned in the previous section. Further increase in manganese content of metal with simultaneous formation of manganese vapors will be governed via reaction (2) and (5). Overall recovery of manganese in any grade of the alloy may be determined by integrating as shown below;

$$R_{Mn} = \frac{\dfrac{f_{Mn}}{1-f_{Mn}}}{\displaystyle\int_0^{f_{Mn}} \frac{\delta f_{Mn}}{r_{Mn}(1-f_{Mn})^2}}$$

Computed values of partial pressure of manganese vapors and manganese recovery at applied pressure of unit atmosphere are plotted against manganese content of the alloys in Figures 3.4 to 3.5. Solubility of carbon in the alloy at temperature above 1546K will be governed by equation (7) or (8) after taking due care of reduced activity of manganese in the alloy. Mn ore contains 44 pct Mn (max.), SiO_2 and Al_2O_3 12 pct (max.), Fe 14 pct (max.) and Phosphorous 0.10 pct (max.)(Specification of Mn Ore produced by Orissa Mining Corporation [42-44 pct grade Ore]).

The modeling of Ferromanganese alloys of various grades and for different conditions are reported in this chapter. No loss of Mn vapors (assumption).

Model: 1

Production of Ferromanganese by using mixture of iron ore (Fe_2O_3) and manganese ore (Mn_3O_4) and Carbon. If pre reductions of manganese and iron ores are completed in the shaft region, a part of FeO phase might be reduced by CO gas at around 900°C if the solid particles pick up heat ahead of the arc by radiation and rest FeO reduced by Carbon. Assuming gas solid equilibrium, modified equations are derived as follows:

$Fe_2O_3 + CO = 2FeO + CO_2$

$FeO + CO = Fe + CO_2$

$-RT\ln K = (-62050+14.95T)$

Where, K is the equilibrium constant of the above reaction. If "α" is the degree of direct reduction of FeO in the arc region

$FeO + C = Fe + CO\ (g)$

$Mn_3O_4 + CO = 3\ MnO + CO_2$

$MnO + C = Mn + CO$

Carbon and oxygen atom balances would yield the following

$$n_C = (n_{Mn}) + \alpha \times n_{Fe\_Fe_2O_3}$$

$$n_{CO} = (n_{Mn}) + (2\alpha - 1) \times n_{Fe\_Fe_2O_3}$$

$$n_{CO_2} = (1-\alpha) \times n_{Fe\_Fe_2O_3}$$

$$W_C = 12 \times (n_C + C_{alloy}) \times 1000.$$

Thermodynamic condition gives the following:

$$K = \left(\frac{n_{CO_2}}{n_{CO}}\right) = \left[\frac{(1-\alpha)\times(w_{Fe\_Fe_2O_3})}{56\times n_{Mn\_alloy} + (2\alpha-1)\times(w_{Fe\_Fe_2O_3})}\right]$$

$$\alpha = \left[\frac{(K+1)\times(W_{Fe\_Fe_2O_3}) - 56\times n_{Mn}\times K}{(2K+1)\times(W_{Fe\_Fe_2O_3})}\right]$$

At high levels of manganese in the alloy, there may be little unreduced iron oxide in the arc region. Value of α could be taken as zero for such cases. Thus equations (24) to (27) are valid at manganese levels less than the limiting value given below;

Model: 2

Production of Ferromanganese by using mixture of iron ore (Fe_2O_3) and manganese ore (Mn_3O_4) and Carbon. If pre reductions of manganese and iron ores are completed in the shaft region. MnO and FeO directly reduced by Carbon

$Fe_2O_3 + CO = 2FeO + CO_2$

$FeO + CO = Fe + CO_2$

$FeO + C = Fe + CO$

$Mn_3O_4 + CO = 3\ MnO + CO_2$

$MnO + C = Mn + CO$

Model: 3

Production of Ferromanganese by using mixture of iron ore (Fe_2O_3) and manganese ore (Mn_3O_4) and Carbon. In absence of any pre reduction of higher oxides of manganese (Mn_3O_4) and iron (Fe_2O_3) occurring in the shaft region, the outgoing gas will consist of carbon monoxide.

$Fe_2O_3 + 3C = 2Fe + 3CO$

$Mn_3O_4 + 4C = 3Mn + 4CO$

Model: 4

Production of Ferromanganese by using mixture of pure iron and manganese ore (Mn_3O_4) and Carbon. If pre reduction of higher oxide of manganese (Mn_3O_4) occurring in the shaft region. MnO will reduced by CO and the outgoing gas will consist of carbon monoxide and carbon dioxide.

$Mn_3O_4 + CO = 3\ MnO + CO_2$

$MnO + C = Mn + CO$

Model: 5

Production of Ferromanganese by using mixture of pure iron and manganese ore (Mn_3O_4) and Carbon. In absence of any pre reduction of higher oxide of manganese (Mn_3O_4) occurring in the shaft region and the outgoing gas will consist of carbon monoxide.

$Mn_3O_4 + 4\,C = 3\,Mn + 4\,CO$

Heat and Mass Balance:

Overall heat and mass balances have been carried out in the present work in order to determine the carbon and electrical energy requirements of the process. Assuming that chemical and sensible heat of outgoing gases such as Carbon monoxide, Carbon dioxide and silicon monoxide are not recovered. Oxygen and carbon atom balances give the following expression for carbon rate in kg per 1000 kg of the liquid alloy:

$n_C = (n_{Mn}) + n_{Fe\_Fe_2O_3}$ for model 2

$= 3\times(n_{Fe_2O_3}) + 4\times(n_{Mn_3O_4})$ for model 3

$= (n_{Mn})$ for model 4

$= (4/3)\times(n_{Mn})$ for model 5

$n_{CO_2} = (n_{Mn_3O_4}) + (n_{Fe_2O_3})$ for model 2

$= (n_{Mn_3O_4})$ for model 4

$n_{CO} = n_C - n_{CO_2}$ for model 2 and model 4

$= n_C$ for model 3 and model 5

$W_C = 12\times(n_C + C_{alloy})\times 1000.$

1. Total heat content of Fe, $(H_{Fe}\text{inKcal})$

H_{Fe} = Moles of Fe× Heat energy stored in Fe up to reaction temperature

$= n_{Fe}\times\Delta H^0_{Fe(298\rightarrow t)}$

$$= \int_{298}^{1042}\Delta C_{P,Fe(298-1042K)}.dt + \int_{1042}^{1182}\Delta C_{P,Fe(1042-1182K)}.dt + \int_{1182}^{1665}\Delta C_{P,Fe(1182-1665K)}.dt + \int_{1665}^{1810}\Delta C_{P,Fe(1665K-1810)}.dt$$

$$+ \int_{1810}^{t}\Delta C_{P,Fe(1810-tK)}.dt$$

2. Total heat content of Mn in alloy, $(H_{Mn}\text{inKcal})$

$$H_{Mn} = n_{Mn}\left(\Delta H^{0}_{Mn(298\rightarrow tK)} + h_{p\,t\,(Mn)}\right)$$

$$= \int_{298}^{1000} \Delta C_{P,Mn(298\rightarrow 1000)}\,dt + \int_{1000}^{1374} \Delta C_{P,Mn(1000\rightarrow 1374)}\,dt + \int_{1374}^{1410} \Delta C_{P,Mn(1374\rightarrow 1410)}\,dt \int_{1410}^{1517} \Delta C_{P,Mn(1410\rightarrow 1517)}\,dt$$

$$+ \int_{1517}^{t} \Delta C_{P,Mn(1517\rightarrow tK)}\,dt + h_{p\,t(Mn)}$$

3. Heat content by Carbon in alloy, $\left(H_{C\_alloy}\text{inKcal}\right)$

$$H_{C\_alloy} = n_{C\_alloy} \times \int_{298}^{t} \Delta C_{P.Carbon(298\rightarrow tK)}.dt$$

4. Sensible heat of alloy, $\left(H_{alloy}\right) = H_{Fe} + H_{Mn} + H_{C\_alloy}$

5. Total heat content by Mn vapor, $\left(H_{Mn(v)}\text{inKcal}\right)$

$$H_{Mn(v)} = n_{Mn(v)} \times \left(H^{0}_{Mn,(298\rightarrow t)} + H_{p\,t(Mn)}\right)$$

Weight of Slag, $\left(W_{Slag}\text{inKg}\right)$

$$W_{slag} = \left(\frac{[\%Al_2O_3 + \%SiO_2]_{\text{inMn\_Ore}}}{100}\right) \times W_{Mn_3O_4}$$

6. Heat content of Slag, $\left(H_{Slag}\text{inMJ}\right)$

$$H_{Slag} = W_{slag} \times 1000 \times 2000/10^{6}$$

7. Sensible heat of Slag = 2000 KJ/Kg (assumption)

8. Total heat content of CO at temperature t_g, $\left(\text{inKcal}, H_{CO}\right)$

$$H_{CO} = n_{CO} \times \left(\Delta H^{0}{}_{CO,298K} + \int_{298}^{tg} \Delta C_{P,CO}.dt\right)$$

9. Total heat content of CO_2 at temperature t_g $\left(\text{inKcal}, H_{CO_2}\right)$

$$H_{CO_2\_1} = n_{CO_2} \times \left(\Delta H^{0}{}_{CO_2,298K} + \int_{298}^{tg} \Delta C_{P,CO_2}.dt\right).$$

10. Heat of dissociation Mn_3O_4 $\left(\text{inKcal}, H_{Mn_3O_4}\right)$

$$H_{Mn_3O_4} = n_{Mn_3O_4} \times \Delta H^{0}{}_{Mn_3O_4,298K}$$

11. Heat of dissociation Fe_2O_3, $\left(H_{Fe_2O_3} \text{ inKcal}\right)$

$$H_{Fe_2O_3} = n_{Fe_2O_3} \times \Delta H^0{}_{Fe_2O_3,298K}$$

Taking overall thermal efficiency "η", heat balance give the following the following expression for heat required (MJ) and electricity consumption (KWh) per 1000 Kg Ferromanganese alloy.

$$hr = \left(\frac{[H_{alloy} + (H_{CO} + H_{CO_2} - H_{Mn_3O_4} - H_{Fe_2O_3})] \times 4.184 + H_{Slag}}{\eta}\right) \quad \text{(for model 1)}$$

$$= \left(\frac{[H_{alloy} + (H_{CO} + H_{CO_2} - H_{Mn_3O_4} - H_{Fe_2O_3})] \times 4.184 + H_{Slag}}{\eta}\right) \quad \text{(for model 2)}$$

$$= \left(\frac{[H_{alloy} + (H_{CO\_3} - H_{Mn_3O_4} - H_{Fe_2O_3} - H_{Mn(v)})] \times 4.184 + H_{Slag}}{\eta}\right) \quad \text{(for model 3)}$$

$$= \left(\frac{[H_{alloy} + (H_{CO} + H_{CO_2} - H_{Mn_3O_4})] \times 4.184 + H_{Slag}}{\eta}\right) \quad \text{(for model 4)}$$

$$= \left(\frac{[H_{alloy} + (H_{CO} - H_{Mn_3O_4})] \times 4.184 + H_{Slag}}{\eta}\right) \quad \text{(for model 5)}$$

$$\text{Electrical energy required} = \left(\frac{hr}{3.6}\right). \text{KWh/ton alloy}$$

Heat demand (KWh/ 1000Kg alloy) of the unit to produce molten Ferro manganese alloy in a submerged arc furnace could arises due to the following:

1. Heat of dissociation of Manganese oxide (Mn_3O_4) $= n_{Mn_3O_4} \times \Delta H^0_{Mn_3O_4(298K)} \times \left(\frac{4.184}{3.6}\right)$

2. Heat of dissociation of Iron oxide (Fe_2O_3) $= n_{Fe_2O_3} \times \Delta H^0_{Fe_2O_3(298K)} \times \left(\frac{4.184}{3.6}\right)$

3. Sensible heat of Ferrosilicon alloy $= \left(H_{Fe} + H_{Mn} + H_C\right) \times \left(\frac{4.184}{3.6}\right)$

4. Sensible heat of Slag $= W_{slag} \times \left(\frac{2}{3.6}\right)$

5. Sensible heat of CO $= \left(H^0_{CO} - n_{CO} \times \Delta H^0_{CO(298K)}\right) \times \left(\frac{4.184}{3.6}\right)$

6. Sensible heat of $CO_2 = \left(H^0_{CO_2} - n_{CO_2} \times \Delta H^0_{CO_2(298K)}\right) \times \left(\frac{4.184}{3.6}\right)$

7. Sensible heat of Mn vapor $= H^0_{Mn(v)} \times \left(\frac{4.184}{3.6}\right)$

8. Heat losses by CO and Mn vapor

Calorific value of CO gas $= n_{CO} \times \left(\Delta H^0_{CO_2(298K)} - \Delta H^0_{CO(298K)}\right) \times \left(\frac{4.184}{3.6}\right)$

9. Calorific value of Carbon in alloy $= n_{C(alloy)} \times \Delta H^0_{CO_2(298K)} \times \left(\frac{4.184}{3.6}\right)$

10. Electrical energy required (E) $= \left(\frac{hr}{3.6}\right)$

Heat supply:

Electrical energy $= \left(\frac{hr}{3.6}\right)$

Calorific value of Carbon $= \left(\frac{W_C}{12}\right) \times \Delta H^0_{CO_2} \times \left(\frac{4.184}{3.6}\right)$

Chemical heat of Fe in liquid Fe-Si alloy $= n_{Fe_2O_3} \times \Delta H^0_{Fe_2O_3} \times \left(\frac{4.184}{3.6}\right)$

Heat Utilization:

1. Calorific value of CO $= n_{CO} \times \left(\Delta H^0_{CO_2(298K)} - \Delta H^0_{CO(298K)}\right) \times \left(\frac{4.184}{3.6}\right)$
2. Calorific value of Mn vapor $= n_{Mn(v)} \times \left(\Delta H^0_{Mn_3O_4} - \Delta H^o_{Mn(v)}\right) \times \left(\frac{4.184}{3.6}\right)$
3. Calorific value of Mn in alloy $= n_{Mn} \times \left(\Delta H^0_{Mn_3O_4} - \Delta H^o_{Mn(v)}\right) \times \left(\frac{4.184}{3.6}\right)$
4. Sensible heat of Ferromanganese alloy $= \left(H_{Fe} + H_{Mn} + H_C\right) \times \left(\frac{4.184}{3.6}\right)$
5. Sensible heat of CO, CO_2 and Mn vapor
6. Heat losses $= E \times (1 - \eta)$

Table 3.3: The reactions by which oxygen can be evolved are summarized.

Symbols	Reaction	$-RT \ln P_{CO_2}$ (MJ)
A	$2CO = 2C + O_2$	$236.89+.01693T-0.0167\ln P_{CO}$
B	$2MnO + (6/7)C = (2/7)Mn_7C_3 + O_2$	800.04 -0.1949T
C	$2MnO = 2Mn + O_2$	$819.0 - 0.1782T$
D	$0.6CO + 1.4MnO = 0.2Mn_7C_3 + O_2$	$631.090 - 0.0856T - 0.005T \ln P_{CO}$
E	$2CO + (14/3)Mn = (2/3)Mn_7C_3 + O_2$	$192.7 + 0.37264T - 0.0167T \ln P_{CO}$
F	$2MnO = 2Mn(v) + O_2$	$1272.85 - 0.37264T + 0.0167T \ln P_{Mn}$

Table 3.4

Phase present on heating of MnO and Carbon Mixture at Unit Pressure

Carbon to MnO weight ratio	$T < 1540^0K$	$1540<T<2015^0K$	$T>2015^0K$
Less than 0.17	MnO, C	MnO, Mn7C3	MnO, Mn
0.17-0.24	MnO, C	MnO, Mn7C3	Mn7C3, Mn
More than 0.24	MnO, C	Mn7C3, C	Mn7C3, C

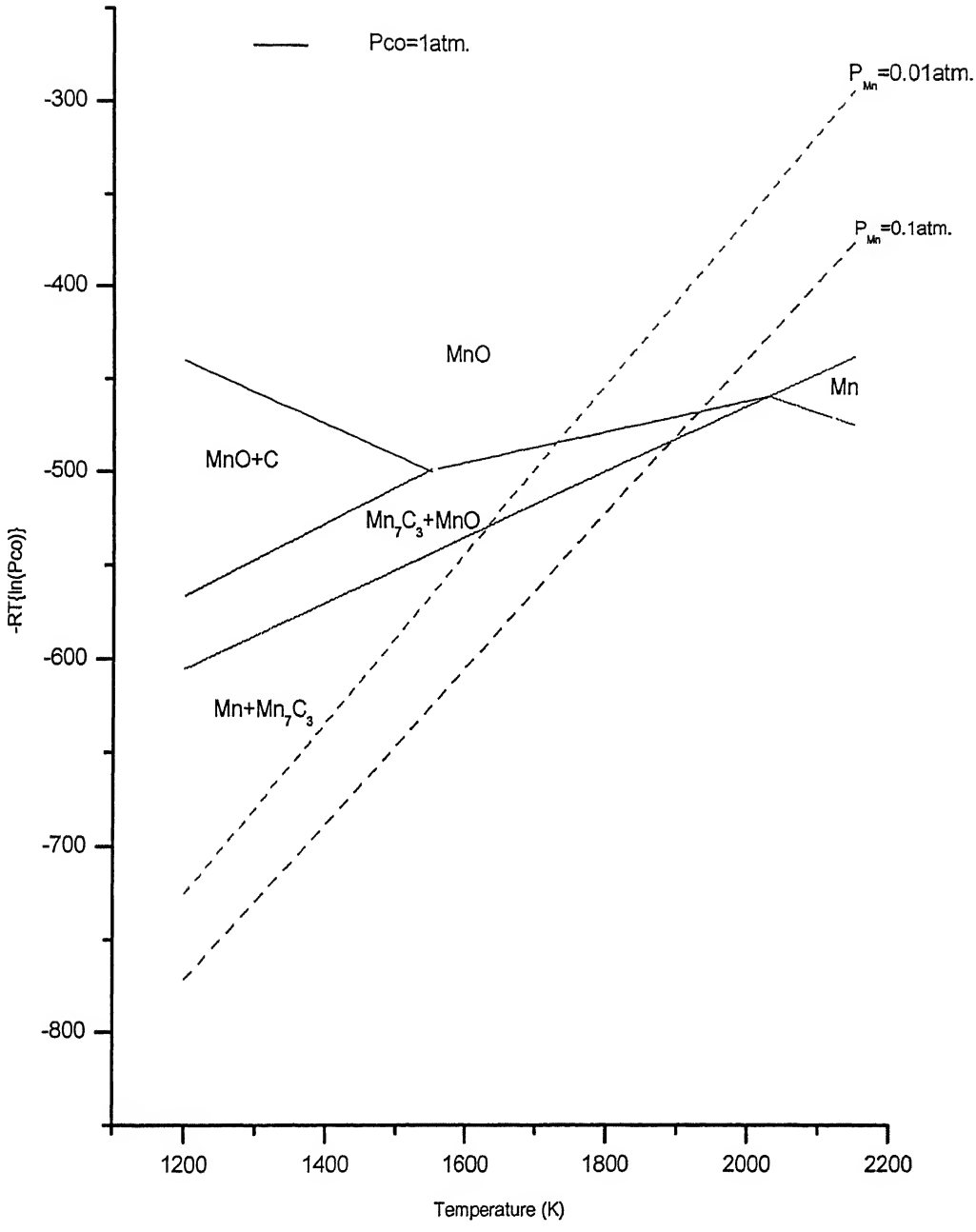

Fig.3.3: Pour baix diagram of Mn-O-C system.

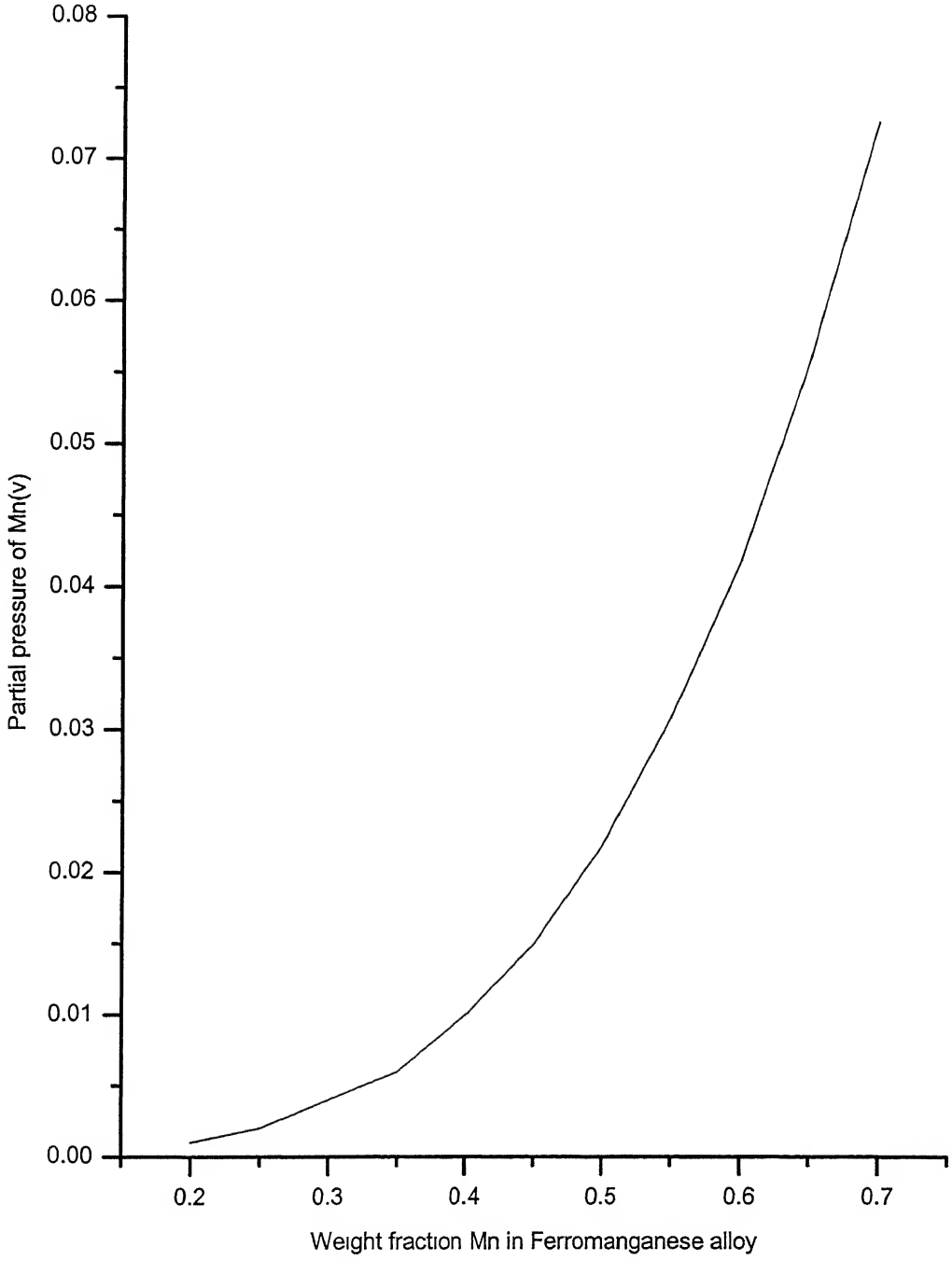

Fig.3.4: Computed Partial pressure of Mn (v) verses Weight fraction Mn in Fe-Mn alloy.

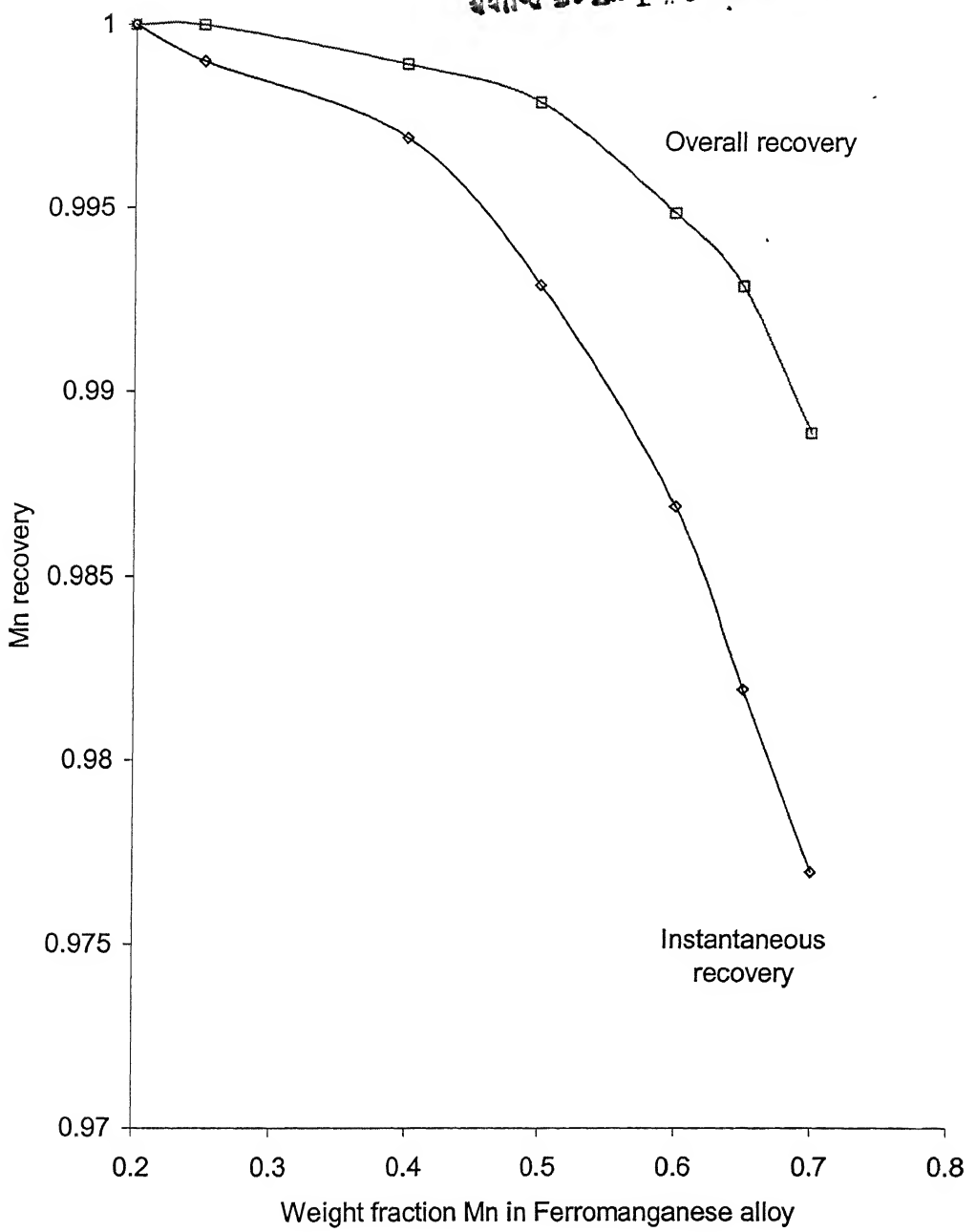

Fig.3.5: Instantaneous and Overall recovery of Mn verses weight fraction Mn in Fe-Mn alloy.

Chapter: 4

Results and Discussion

Results and Discussion:

Computed values of smelting temperature, silica, Mn_3O_4, energy, carbon and Mn_3O_4 consumption with and without recycling of SiO and with recirculation of Mn vapor through model equations of chapter (3) for both Ferrosilicon and Ferromanganese alloys are given in tables (4.1) to (4.6). These values are plotted against silicon or Manganese content of the alloy in Figs. (4.1) to (4.9) respectively.

Figs. 4.1 to 4.2 show that the smelting temperature vs. weight fraction Si or Mn content in Ferrosilicon or Ferromanganese alloy. Smelting temperature increases with increase in weight fraction Si or Mn content in Ferrosilicon or Ferromanganese alloy

Fig.4.3 shows Silica consumption vs. weight fraction of Si to produce 1 ton of Ferrosilicon with or without recirculation of SiO gas. Initially Silica consumption for both the cases approximately identical up to 35 pct Si in Ferrosilicon alloy. Because at lower at lower Silicon content in the alloy requires lower smelting temperature which results in lower production of SiO gas and hence loss of SiO will be very low for model 1 and 2. Above 35 pct Si in Ferrosilicon alloy Silica consumption increases for model 1 (without recirculation of SiO) because Si content increases with increase in smelting temperature which increases the production of SiO and hence more SiO_2 consumption.

Fig.4.4 shows the Carbon consumption rate vs. weight fraction Si in Ferrosilicon alloy with or without recirculation of SiO gas. Carbon consumption up to 35 pct Si in Ferrosilicon alloy is same because at lower Silicon content in the alloy requires lower smelting temperature, results in lower production of SiO hence Carbon required for reduction of SiO_2 for both models is approximately identical. Above 35 pct Si in Ferrosilicon alloy, Carbon consumption for model 1(without recirculation of SiO) is higher because at higher Silicon content in the alloy requires higher smelting temperature, results in higher production of SiO gas and loss of SiO and hence more Carbon is required for reduction of SiO_2 for model 1.

The energy consumption to produce one ton Ferrosilicon vs. weight fraction Si in Ferrosilicon alloy is shown in the Fig. 4.5, with or without recirculation of SiO gas. Energy consumption up to 35 pct Si in Ferrosilicon alloy is approximately identical, but above 35 pct Si energy consumption higher for model 1(without recirculation of SiO gas), because at lower silicon content of the alloy requires lower smelting temperature and results in lower

production of SiO gas hence losses of energy due to SiO gas is approximately identical for both cases. But with increase in Si content of the alloy requires higher smelting temperature and result in higher production of SiO gas hence losses of energy due to SiO gas is higher for model 1.

Fig. 4.6 shows the energy consumption to produce one ton Ferrosilicon vs. weight fraction Si in Ferrosilicon alloy with recirculation of SiO for different conditions. When Fe_2O_3 is used in the burden, energy consumption is highest for model 3 (direct reduction of Fe_2O_3) and lowest for models 5, because for model 3 Fe_2O_3 directly reduced by C, more CO will form than other models, more loss of calorific value due to CO and hence more loss of energy. Energy consumption is lowest for model 5 (pre reduced Fe_2O_3 and FeO reduced by C and CO). Here loss of CO is lowest because some CO is used for pre reduction of Fe_2O_3 to FeO in the burden and also a part of FeO to Fe.

Energy consumption is higher for model 5 than model 2 (Pure Fe is used) up to 44 pct Si in Ferrosilicon alloy, above 44 pct Si in alloy energy consumption is same for both models. For model 5, energy consumption to produce Ferrosilicon is function of sensible heat of Ferrosilicon alloy and slag, moles of CO and CO_2 produced, energy required for dissociation of Silica and Fe_2O_3. For model 2, energy consumption to produce Ferrosilicon is function of sensible heat of Ferrosilicon alloy and slag, sensible heat of CO produced, energy required for dissociation of Silica. Energy consumption is higher up to 44 pct Si, because sum of the energy consumption due to dissociation of Fe_2O_3 to Fe and loss of energy due to flue gases (CO and CO_2) is higher for model 5 than loss of energy due to loss of flue gas (CO) for model 2. Above 44 pct Si in Ferrosilicon alloy energy consumption for both models (2 & 5) is approximately identical, because losses of energy due to CO for model 2 is approximately identical sum of the energy due to dissociation of Fe_2O_3 to Fe and loss of energy due to CO and CO_2 for model 5.

Fig.4.7 shows the Carbon consumption (Kg) to produce on ton Ferrosilicon vs. weight fraction Si in Ferrosilicon alloy. Carbon consumption is highest for model 3 and lowest for model 5 when Fe_2O_3 is used in the burden, because in model 3 Fe_2O_3 directly reduced by C to Fe, no utilization of reducing potential of CO, but in case of model 5 Fe_2O_3 is pre reduced to FeO in the burden by CO and FeO also reduced by CO hence less C is required for reduction of Fe_2O_3. Carbon consumption for model 5 is higher than model 2 up

to 44 pct Si and same above 44 pct Si in Ferrosilicon alloy. Because up to 44 pct Si in alloy, a part of FeO directly reduced by C and above 44 pct Si in alloy, CO produced due to dissociation of SiO_2 by C is used for complete reduction of Fe_2O_3 to Fe.

Fig.4.8 shows the energy consumption vs. weight fraction Mn in Ferromanganese alloy. When Fe_2O_3 is used in the burden, energy consumption is highest for model 3 (direct reduction of Fe_2O_3) and lowest for model 1, because loss of energy due to flue gas (CO) for model 3 is higher than losses of energy due to loss of energy due to flue gases (CO and CO_2) for model 1. No utilization of CO for model 3 for reduction, loss of calorific value of CO is higher for model 3. When pure Fe is used in the burden, energy consumption is higher for model 5 than model 4, because for model 5 Mn_3O_4 is directly reduced by C and will for CO. Formation of CO from model 5 due to direct reduction of Mn_3O_4 is higher than model 1(pre reduction of Mn_3O_4 in the burden) due to direct reduction of MnO by C. Losses of energy due to flue gas for model 5 is higher than model 4.

At around 70 pct Mn in Ferromanganese alloy energy consumption is approximately identical for model 2 and 5 and for model 1 and 4. For model 2, energy consumption to produce Ferromanganese is function of sensible heat of Ferromanganese alloy and slag, moles of CO and CO_2 produced, energy required due to dissociation of Mn_3O_4 and Fe_2O_3 to Mn and Fe respectively. For model 5, energy consumption to produce Ferromanganese is function of sensible heat of Ferromanganese alloy and slag, Sensible heat of CO produced, energy required due to dissociation of Mn_3O_4 to Mn. For model 2, energy required for dissociation of Fe_2O_3 to Fe and loss of energy due to flue gases (CO & CO_2) is approximately identical than loss of energy due to flue gas (CO) for model 5. For model 1, energy consumption to produce Ferromanganese is function of sensible heat of Ferromanganese alloy and slag, moles of CO and CO_2 produced, energy required due to dissociation of Mn_3O_4 and Fe_2O_3 to Mn and Fe respectively. For model 4, energy consumption to produce Ferromanganese is function of sensible heat of Ferromanganese alloy and slag, moles of CO produced, energy required due to dissociation of Mn_3O_4 to Mn. For model 1, energy required for dissociation of Fe_2O_3 to Fe and loss of energy due to flue gases (CO & CO_2) is approximately identical than loss of energy due to flue gases (CO & CO_2) for model 4.

Fig. 4.9 shows the Carbon consumption rate vs. weight fraction Mn in Ferromanganese alloy. When Fe_2O_3 used in the burden, C consumption is highest for model 3 and lowest for model 1. Because for model 3, Fe_2O_3 and Mn_3O_4 directly reduced by C and CO produced, not used for reduction, more loss of calorific value due to CO, but in case of Model 1, Fe_2O_3 and Mn_3O_4 pre reduced in the burden to FeO and MnO and a part of FeO also reduced by CO. Carbon consumption for model 1 is higher than model 4 up to approximately 60 pct Mn in Ferromanganese alloy but above 60 pct Mn Carbon consumption is approximately same for both models.

Breakdown of energy calculations for Fe-50Si, Fe-80Si and Fe-5.6C-50Mn, Fe-5.6C-70Mn alloys for different conditions are included in Table (4.7) to (4.8). Energy required for Fe-50Si, Fe-80Si and Fe-5.6C-50Mn, Fe-5.6C-70Mn alloys for different conditions (Slag rate, Circuit loss, and Flue gas temperature) are given in table 4.9-4.10 and is plotted against slag rate, circuit loss and flue gas temperature in Figs. (4.9) to (4.13). Typical energy diagram are depicted in Fig. (4.14) to (4.33) to highlight the importance of different terms. Results show that as much as 47 pct and 39 pct of total energy via the electricity and the calorific value of carbon is consumed in obtaining the elemental silicon and Manganese. Around 31 pct and 30 pct of input energy is wasted as calorific value of carbon monoxide for Ferrosilicon and Ferromanganese respectively. Only 8 pct and 22 pct is of the energy is being accounted for by the sensible heat of the alloy.

Computed consumption of electricity in producing different grades of Ferro silicon alloys are compared with the actual operating data [21] in Table 4.11. Results show that agreement between model calculations and the plant data is better if silicon monoxide evolved at high temperature beneath the electrode is assumed being recycled to form silicon carbide and silica. Models, calculations reveal that recycling of silicon monoxide could be resulting in savings of more than 1908 KWh/t of Fe-75Si alloy. There could be a decrease of 47 to 65 KWh/t for Fe-50Si, 75 to 80KWh/t for Fe-80Si and 13 to 28 KWh/t for 50pct and 14-50 KWh/t for 70pct Ferromanganese alloy for every 100^0C decrease in the temperature of outgoing gas or gases depending upon the grade of the alloy produced due to incomplete recovery of heat. Heat capacity of gas is 0.4 to 0.6 times that of the solid burden. Pre heating of solid particles will be limited to around 800°C while gases cool down to near room temperature.

Every one kg of liquid slag produced would consume of additional 2000 KJ of energy and it could increase the energy demand by about 0.55 KWh. Typical slag rate may lie in the range of 20 to 50 kg per ton due to presence of ash in coke and impurities in quartz. Overall effect of slag on energy consumption will be marginal and need not be considered. Any simultaneous reduction of aluminum oxide at high temperature would affect the quality of alloy produced without changing much of the energy demand or carbon requirements. For this reason, quartz and reducing agents with minimal of impurities are used to produce high quality Ferro silicon alloys. Use of iron ore or mill scale instead of steel chips could increase the carbon and energy requirements of the process besides adding the impurities. Changes in electrical energy requirement due to change in parameters such as slag volume, heat losses and electrical losses are included in Table 4.12.

One factor that gives more uncertainty on the calculation of power consumption than any other parameter is the thermal efficiency of the furnace. It is very difficult to estimate losses due to resistance heating of electrode and transformer cables as well as heat losses due to conduction through furnace walls. Heat losses contribute as high as 1790-2102 KWh/t of Fe-50 Si alloy, 2864-3617 KWh/t of Fe-80 Si alloy and 542-955 KWh/t of Fe-50 Mn alloy, 624-1006 KWh/t of Fe-70 Mn alloy at assumed furnace efficiency of 70 percent. Steps to reduce electrical and heat losses will have marked effect on improvement in the unit performance and lowering the cost of the alloy.

Significant reduction in carbon and electrical energy consumption rates could be affected if the carbon deposition reaction were to take place in the furnace:

$$2\,CO\,(g) = CO_2\,(g) + C \qquad P_{CO2} / P_{CO}^2 = e^{(-21+20650/T)} \qquad (4.1)$$

This reaction is thermodynamically favored at low temperatures but for all practical purposes, reaction is sluggish. This is born out from the date on the top gas analysis of most of the iron blast furnaces and direct reduction units in the world. For example, flue gases tend to leave the furnace shaft at around 200^0C with CO/CO_2 ratio of around 1 while the equilibrium ratio is less than 0.0001 as per equation (4.1). Carbon deposition reaction has, therefore, been ignored in the present study.

Table 4.1

Computed Smelting temperature, SiO_2, Fe/Fe_2O_3 required to produce one ton different graded Ferrosilicon for different models

Weight fraction Silicon in alloy	Smelting temperature (^0K)	SiO_2 required (Kg/ton Ferrosilicon),when no recirculation of SiO	SiO_2 required (Kg/ton Ferrosilicon),when recirculation of SiO	Fe required (Kg/ton Ferrosilicon) ,when pure Fe used	Fe_2O_3 required (Kg/ton Ferrosilicon),when Fe_2O_3 used
0.20	1803	428.8	428.6	800	1142.9
0.25	1823	536.2	535.7	750	1071.4
0.30	1927	646.1	642.9	700	1000.0
0.35	1971	761.8	750.0	650	928.6
0.40	1996	883.2	857.1	600	857.1
0.45	2018	1014.7	964.3	550	785.1
0.50	2025	1153.0	1071.4	500	714.3
0.55	2032	1296.9	1178.6	450	642.9
0.60	2038	1449.2	1285.7	400	571.4
0.65	2044	1612.1	1392.9	350	500.0
0.70	2050	1789.2	1500.0	300	428.6
0.75	2055	1987.0	1607.1	250	357.1
0.80	2061	2214.2	1714.3	200	285.7

Table 4.2

Computed Energy required to produce one ton different graded Ferrosilicon for different models

Wt. Fraction Si	Energy required (KWh/ton Ferrosilicon)				
	Using pure Fe, without recirculation of SiO	Using pure Fe,With recirculation of SiO	Fe_2O_3 without pre-reduction, with recirculation of SiO	Fe_2O_3 with pre-reduction, with recirculation of SiO	Fe_2O_3 with pre-reduction, FeO reduced by CO and C. with recirculation of SiO
0.20	2331.2	2329.9	3986.2	3466.6	2893.6
0.25	2922.2	2933.3	4486.1	3999.0	3378.2
0.30	3562.1	3560.7	5010.0	4555.3	3886.7
0.35	4214.8	4168.8	5514.6	5092.4	4376.0
0.40	4889.5	4770.8	6013.1	5623.4	4859.1
0.45	5614.9	5372.0	6510.7	6153.5	5385.1
0.50	6368.6	5971.0	7006.4	6681.6	5983.1
0.55	7152.9	6564.4	7496.1	7203.8	6575.1
0.60	7976.6	7160.4	7988.5	7728.7	7169.9
0.65	8853.5	7756.3	8481.0	8253.6	7764.6
0.70	9803.3	8352.3	8973.4	8778.6	8359.4
0.75	10856.6	8948.0	9465.6	9303.2	8953.9
0.80	12058.3	9548.8	9962.8	9832.9	9553.5

Table 4.3

Computed Carbon required to produce one ton different graded Ferrosilicon for different model

Weight Fraction Si.	**Carbon required (Kg/ton Ferrosilicon alloy)**				
	Using pure Fe, without recirculation of SiO	Using pure Fe,With recirculation of SiO	Fe_2O_3 without pre-reduction, with recirculation of SiO	Fe_2O_3 with pre-reduction, with recirculation of SiO	Fe_2O_3 with pre-reduction, FeO reduced by CO and C. with recirculation of SiO
0.20	171.4	171.4	428.6	342.9	261.3
0.25	214.4	214.3	455.4	375.0	284.7
0.30	257.7	257.1	482.1	407.1	308.2
0.35	302.3	300.0	508.9	439.3	331.6
0.40	348.0	342.9	535.7	471.4	355.1
0.45	395.8	385.7	562.5	503.6	385.7
0.50	444.9	428.6	589.3	535.7	428.6
0.55	495.1	471.4	616.1	567.9	471.4
0.60	547.0	514.3	642.9	600.0	514.3
0.65	601.0	557.1	669.6	632.1	557.1
0.70	657.8	600.0	696.4	664.3	600.0
0.75	718.8	642.9	723.2	696.4	642.9
0.80	785.7	685.7	750.0	728.6	685.7

Table 4.4

Computed smelting temperature, Mn_3O_4, Fe or Fe_2O_3 required to produce one ton different graded Ferromanganese.

Weight fraction Mn	Smelting temperature (^{0}K)	Fe_2O_3required (Kg/ton alloy)	Fe required (kg/ton alloy) if Fe is used as charge	Mn_3O_4 required (Kg/ton alloy)if no loss of Mn vapor
0.20	1589.2	862.8	604	277.6
0.25	1643.9	791.4	554	347.0
0.30	1691.5	720.0	504	416.4
0.35	1734.0	648.6	454	485.8
0.40	1772.6	577.1	404	555.2
0.45	1808.0	505.7	354	624.5
0.50	1841.0	434.3	304	693.9
0.55	1871.8	362.8	254	763.3
0.60	1900.9	291.4	204	832.7
0.65	1928.4	220.0	154	902.1
0.70	1954.7	148.6	104	971.5

Table 4.5

Energy required to produce one ton different graded Ferromanganese for different models

Weight Fraction Mn in Ferromanganese alloy	Energy required (KWh/ton Ferromanganese alloy)				
	Pre reduced Fe and Mn ore, FeO reduced by CO and C	Pre reduced Fe and Mn ore, FeO reduced by C	No pre-reduction of Fe and Mn ore, directly reduced by C	Pure Fe and pre-reduced Mn ore (Mn_3O_4)	Pure Fe and no pre-reduction of Mn ore (Mn_3O_4)
0.20	1609.0	1927.2	2999.5	866.0	954.5
0.25	1654.7	1973.2	3025.9	983.3	1094.0
0.30	1701.2	2020.0	3053.0	1101.5	1234.2
0.35	1748.5	2067.6	3080.9	1220.4	1375.3
0.40	1796.5	2115.9	3109.4	1340.0	1517.0
0.45	1845.2	2164.9	3138.5	1460.3	1659.5
0.50	1898.8	2218.8	3172.3	1585.6	1806.8
0.55	1952.1	2272.4	3205.4	1710.5	1953.9
0.60	2004.8	2325.5	3237.7	1834.8	2100.3
0.65	2057.1	2378.0	3269.0	1958.7	2246.4
0.70	2112.0	2430.2	3299.2	2082.1	2391.9

Table 4.6

Computed Carbon required to produce one ton different graded Ferromanganese for different models

Weight Fraction Mn in Ferromanganese alloy	**Carbon required (Kg/ton Ferromanganese alloy)**				
	Pre reduced Fe and Mn ore, FeO reduced by CO and C	Pre reduced Fe and Mn ore, FeO reduced by C	No pre-reduction of Fe and Mn ore, directly reduced by C	Pure Fe and pre-reduced Mn ore (Mn_3O_4)	Pure Fe and no pre-reduction of Mn ore (Mn_3O_4)
0.20	206.8	259.1	353.3	99.6	114.2
0.25	206.9	259.3	351.8	110.5	128.7
0.30	207.1	259.5	350.3	121.5	143.3
0.35	207.2	259.6	348.9	132.4	157.8
0.40	207.4	259.8	347.6	143.3	172.4
0.45	207.5	260.0	346.3	154.2	186.9
0.50	207.6	260.2	345.2	165.1	201.5
0.55	207.8	260.4	344.2	176.0	216.0
0.60	207.9	260.6	343.4	186.9	230.5
0.65	208.1	260.8	342.9	197.8	245.1
0.70	208.7	261.0	342.8	208.7	259.6

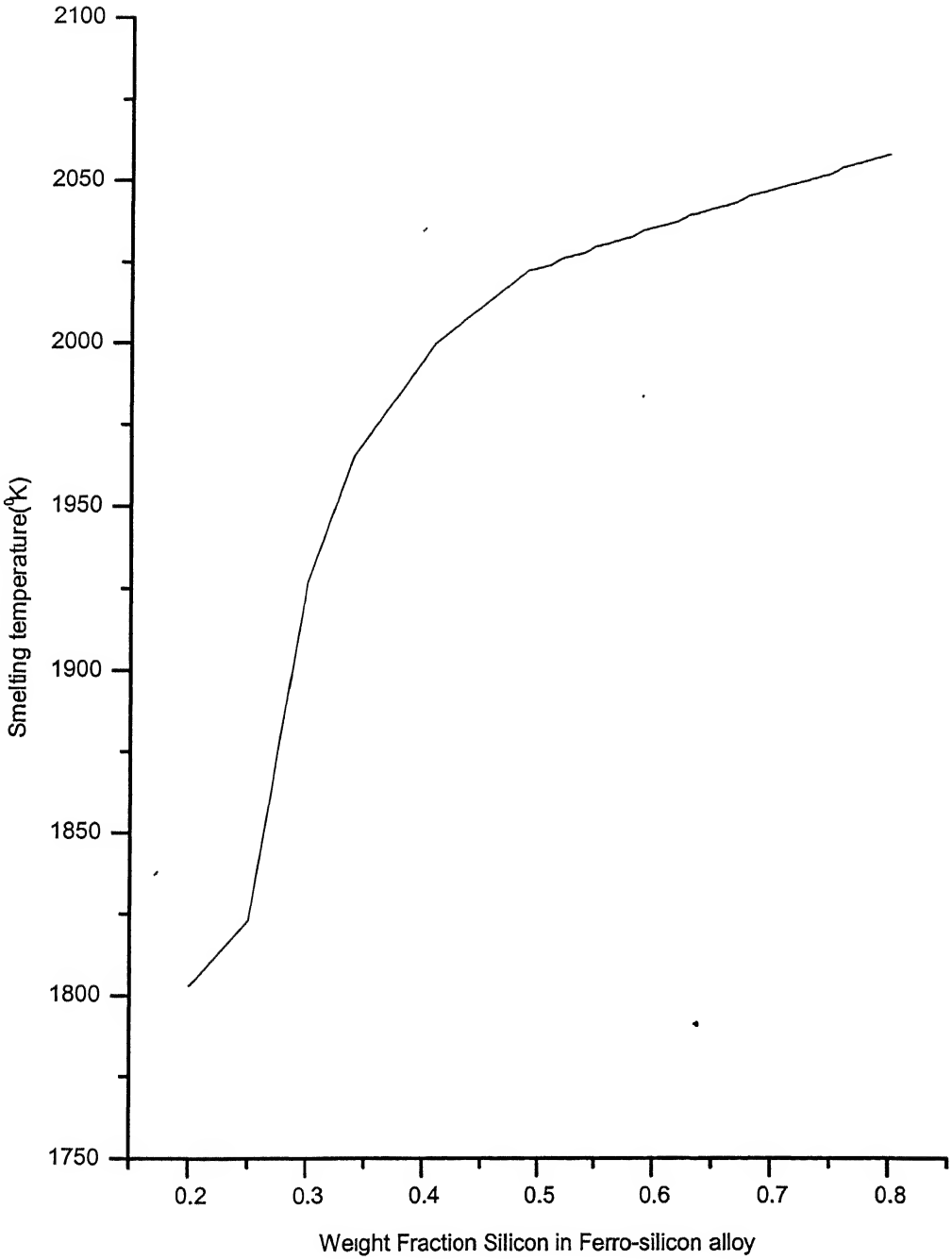

Fig.4.1: Computed smelting temperature versus Silicon content in Fe-Si alloy

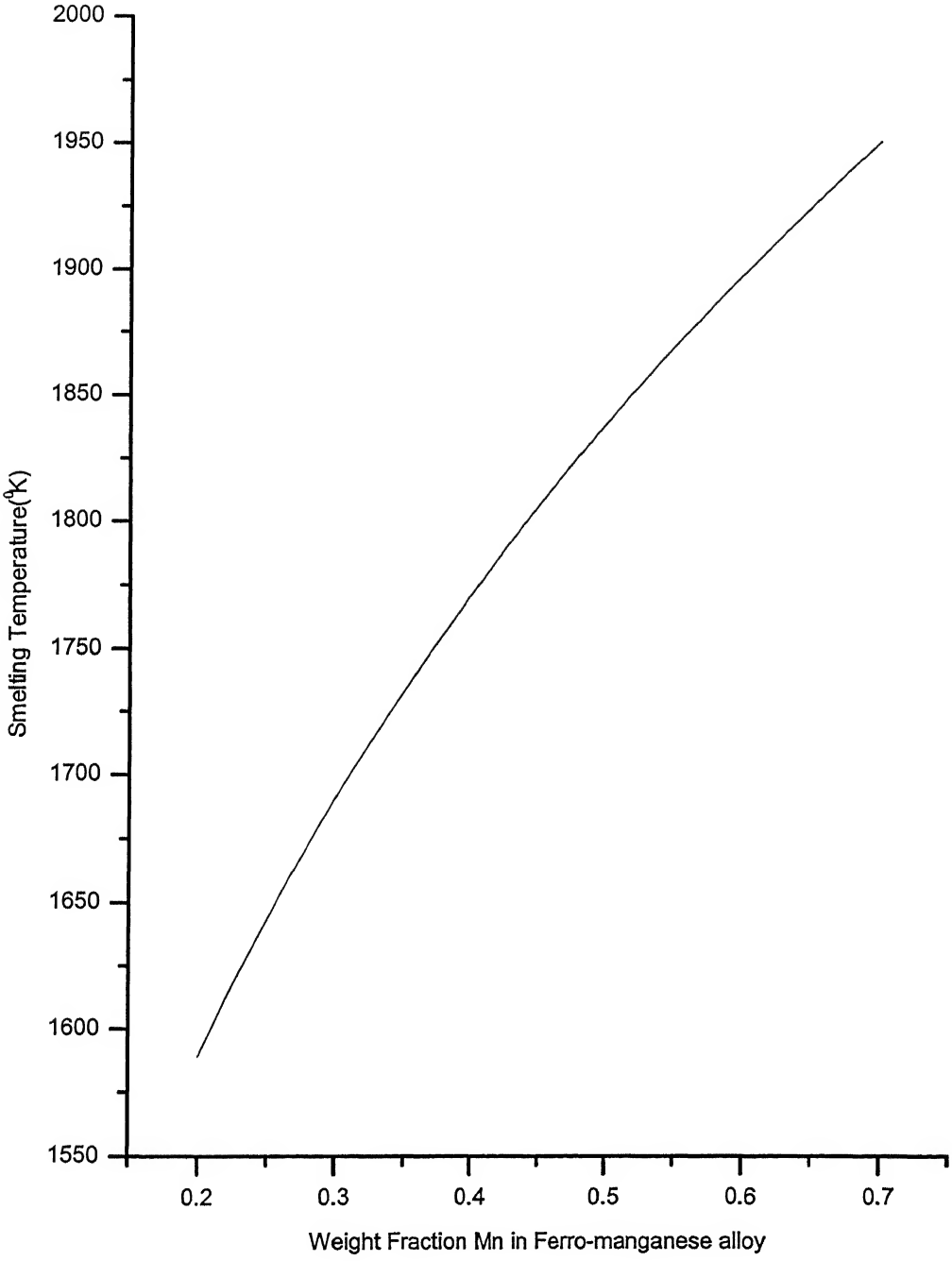

Fig.4.2: Computed smelting temperature verses Weight fraction Mn in Fe-Mn alloy

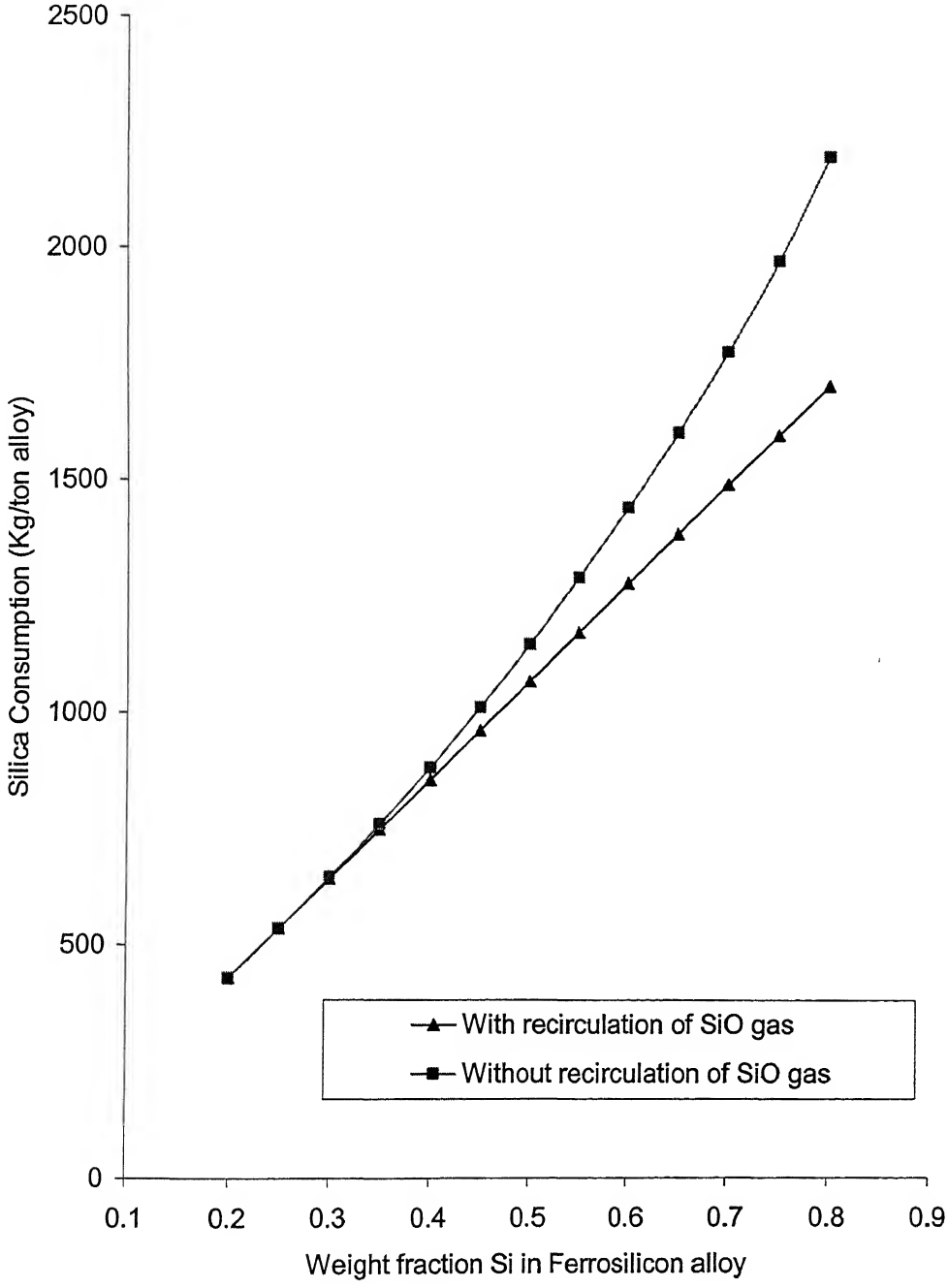

Fig.4.3: Silica consumption verses weight fraction Si in Fe-Si alloy (by using pure Fe), with or without recirculation of SiO.

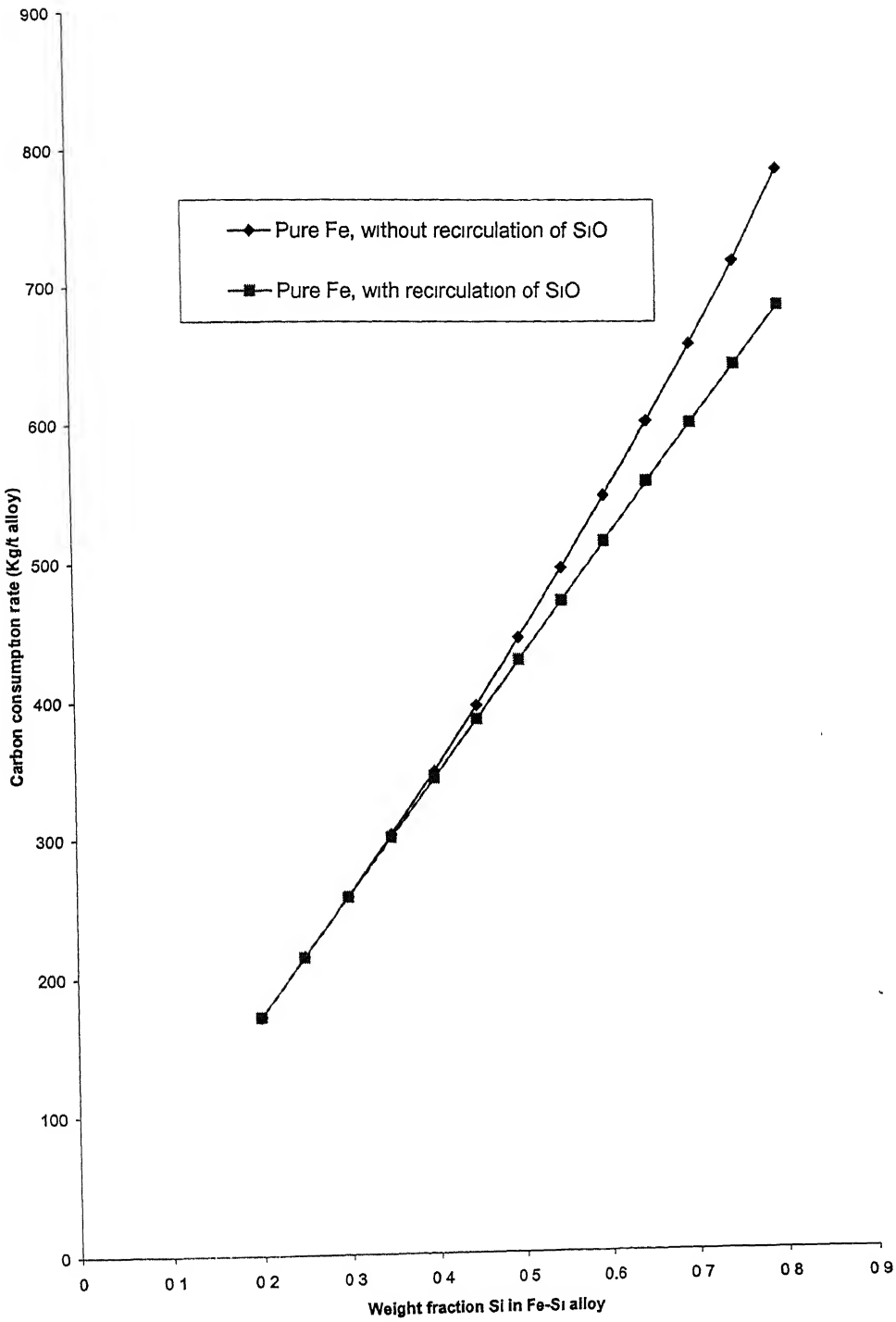

Fig.4.4: Carbon consumption rate verses Si content in Fe-Si alloy (by using pure Fe), with or without recirculation of SiO

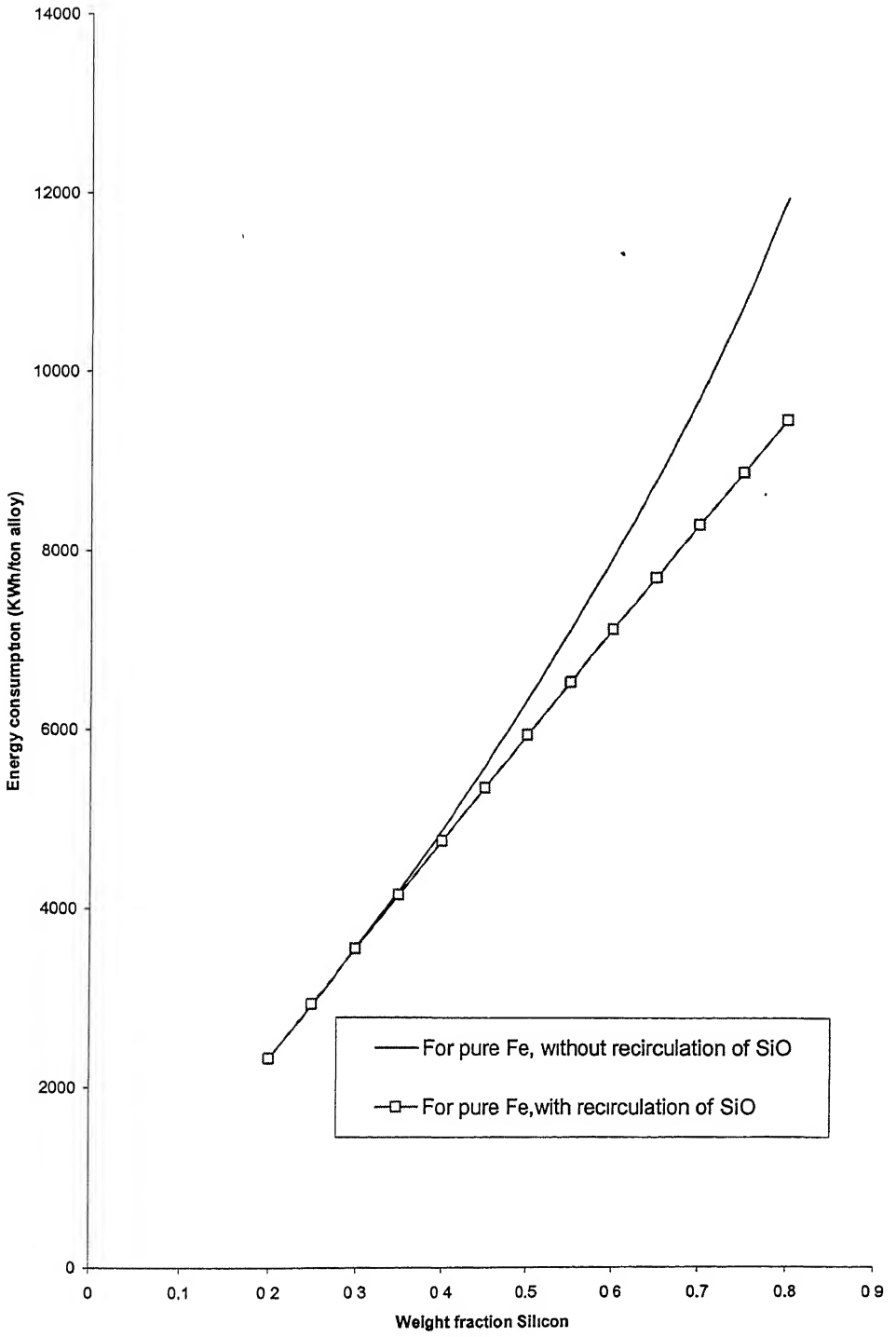

Fig.4.5: Electrical energy consumption verses Silicon content of Fe-Si alloy with or without recirculation of SiO.

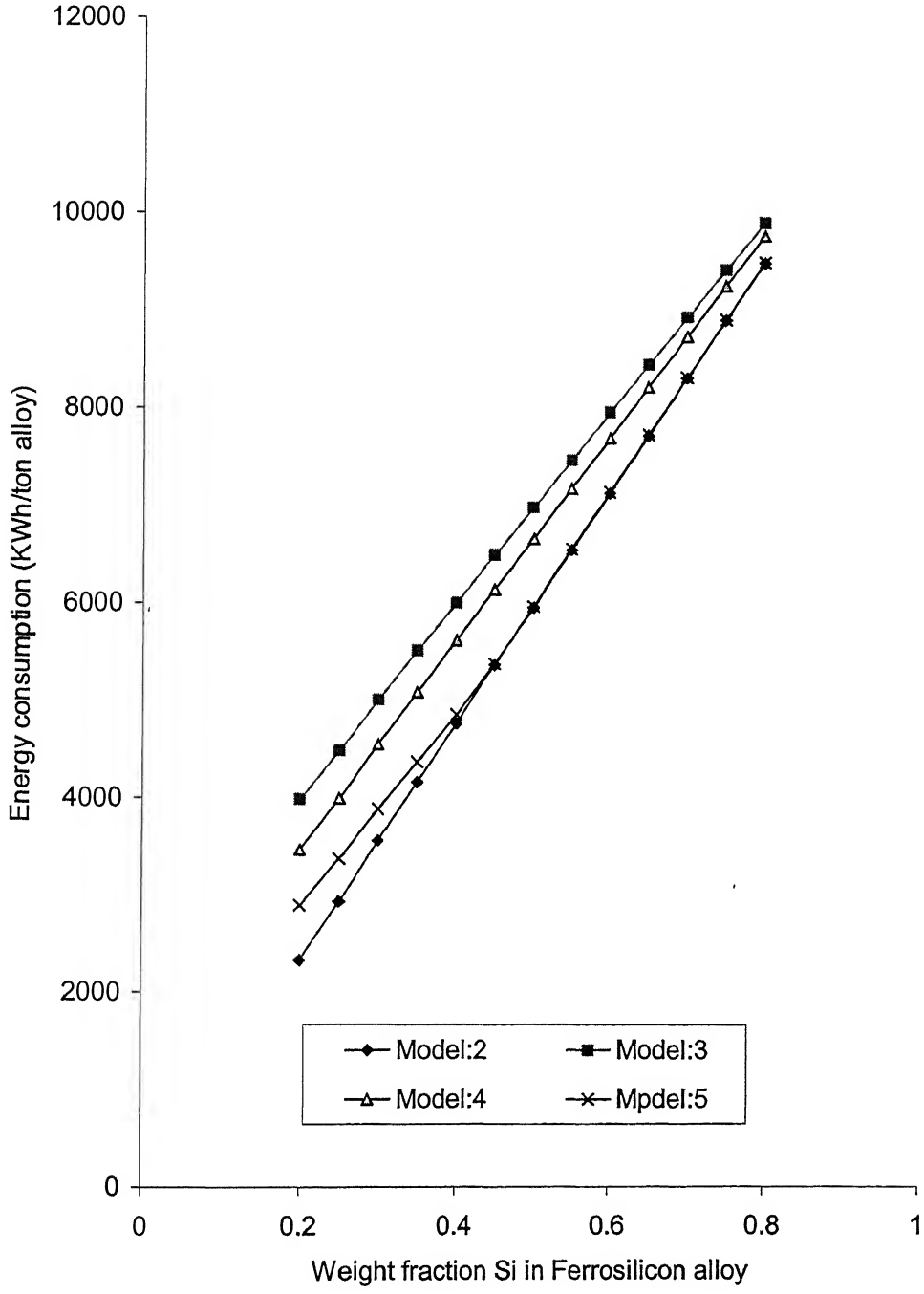

Fig.4.6: Computed Electrical energy consumption verse weight fraction Si in alloy for different models, with recirculation of SiO

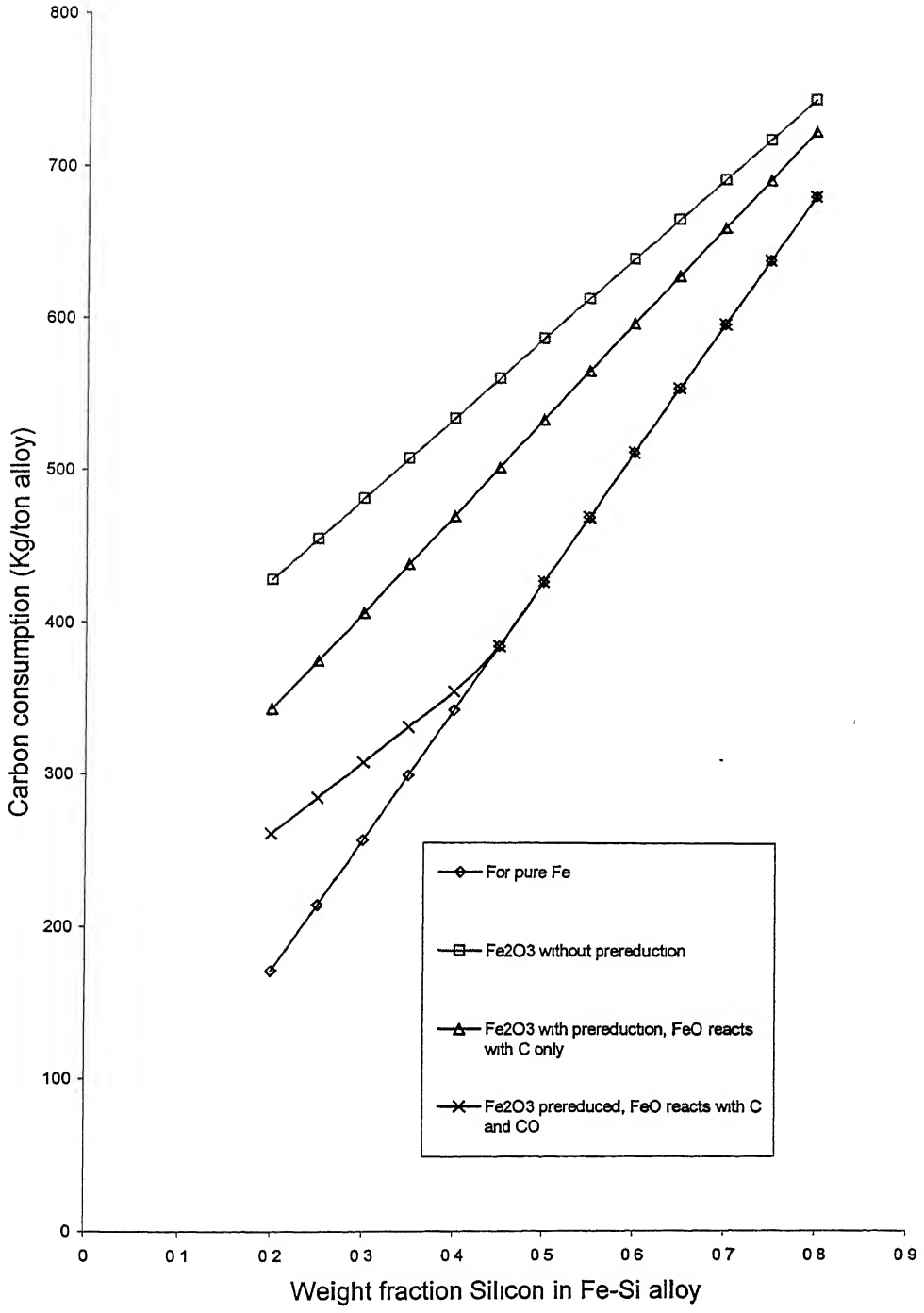

Fig.4.7: Carbon consumption rate verses Si content in Fe-Si alloy, with recirculation of SiO

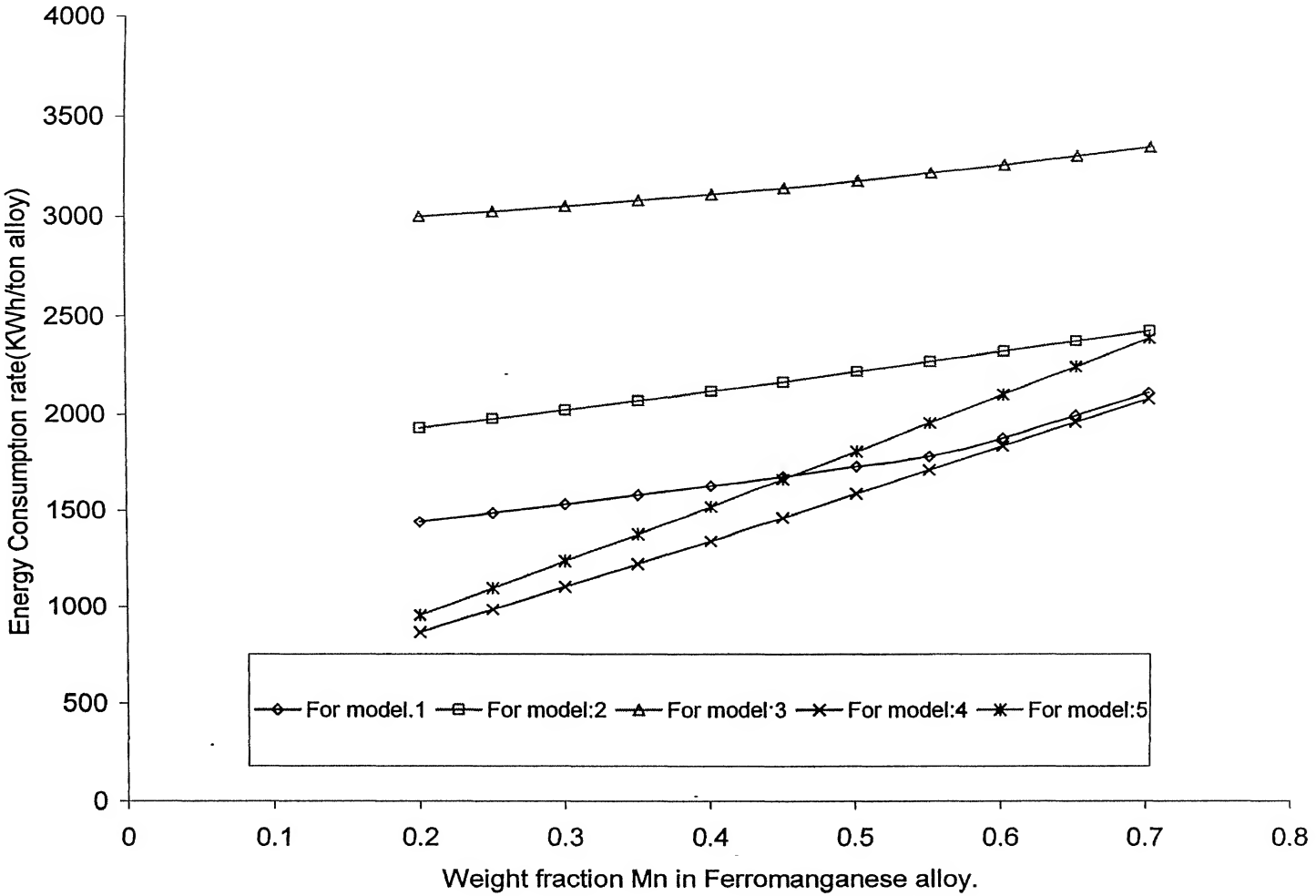

Fig.4.8: Computed Electrical energy consumption verse weight fraction Mn in Ferromanganese alloy for different models

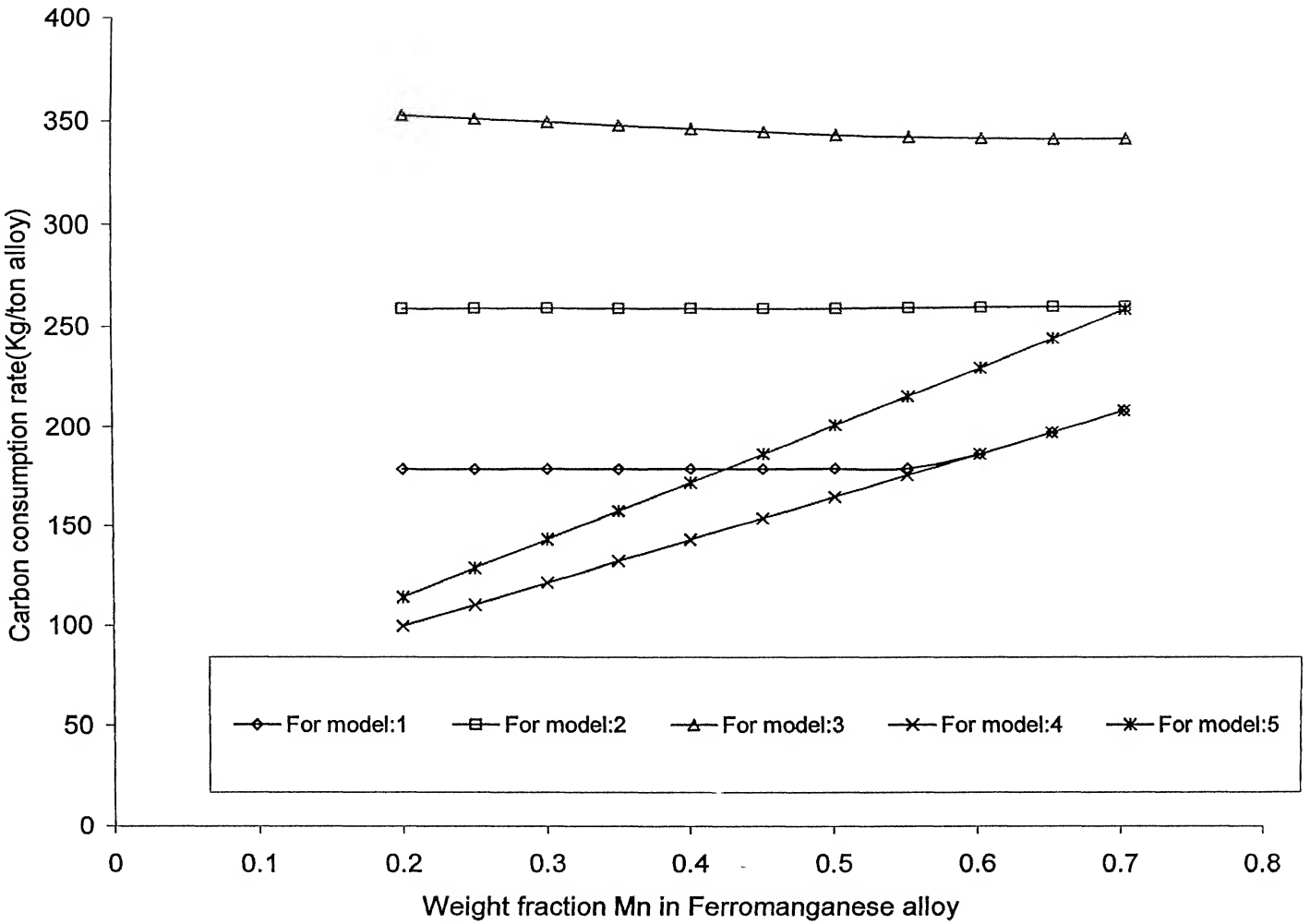

Fig.4.9: Computed Carbon consumption verse weight fraction Mn in Ferromanganese alloy for different models.

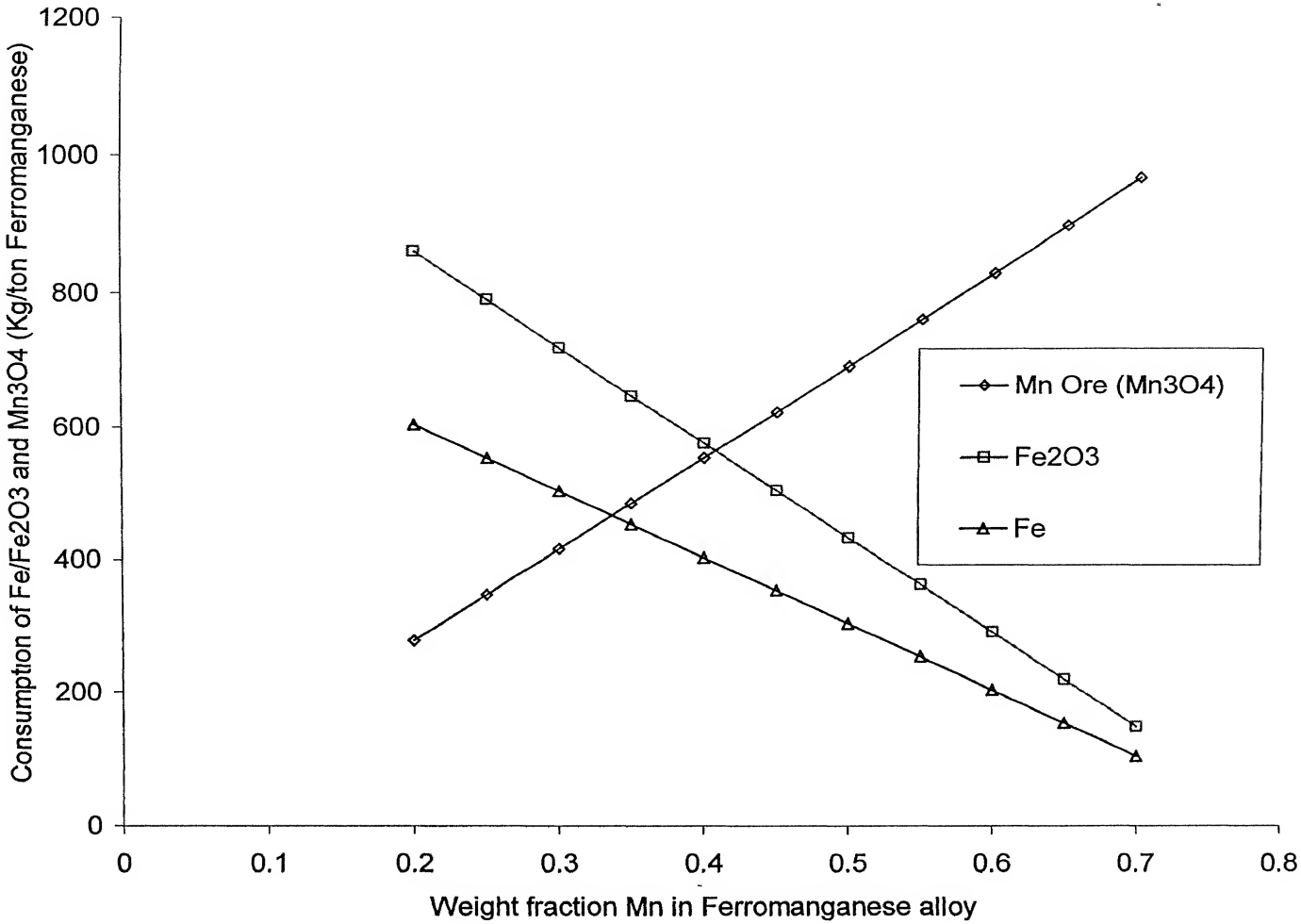

Fig.4.10: Computed Mn_3O_4 consumption verses weight fraction Mn in Ferromanganese alloy

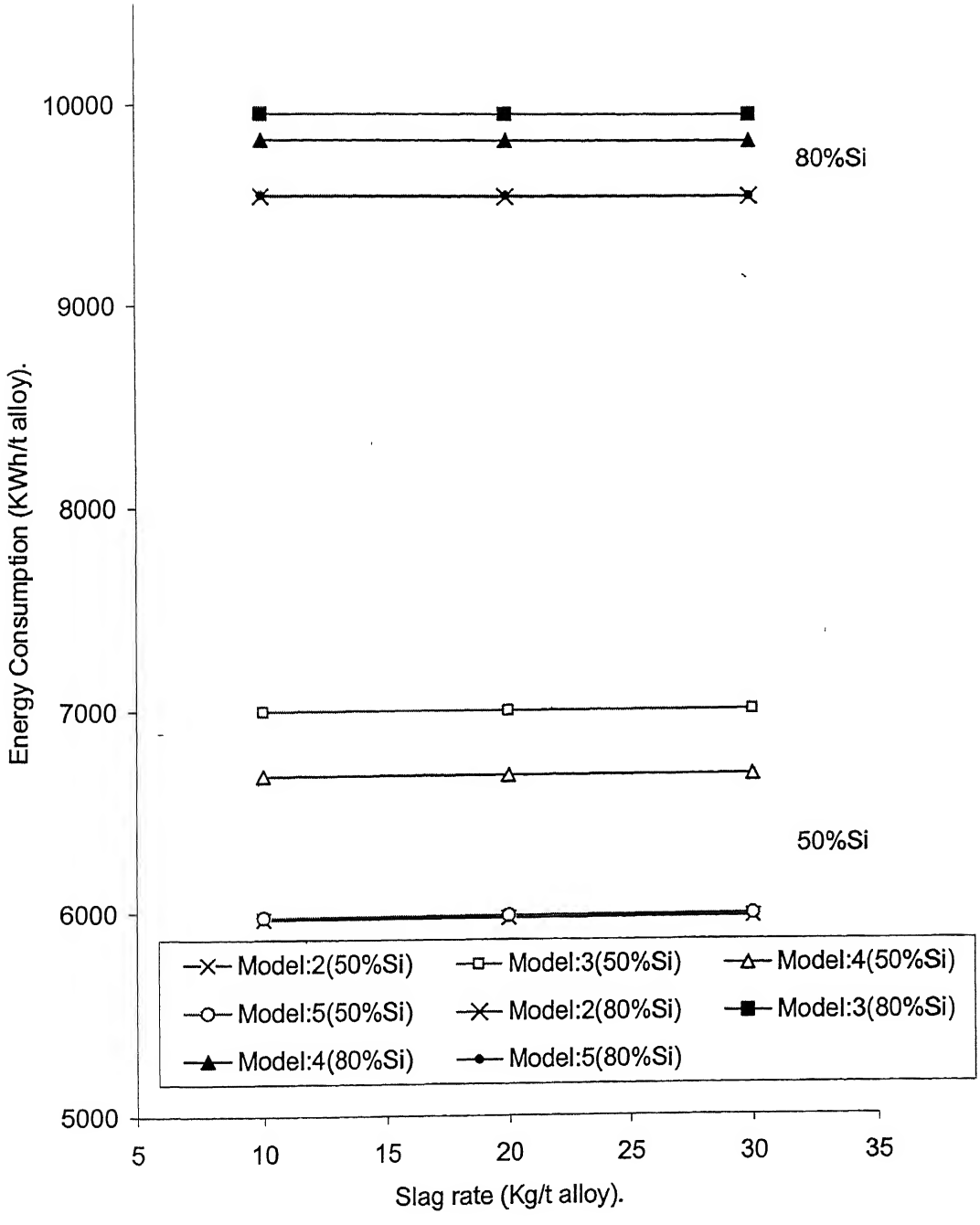

Fig.4.11: Effect of Slag rate on Electrical energy consumption for 50% and 80% Si in alloy

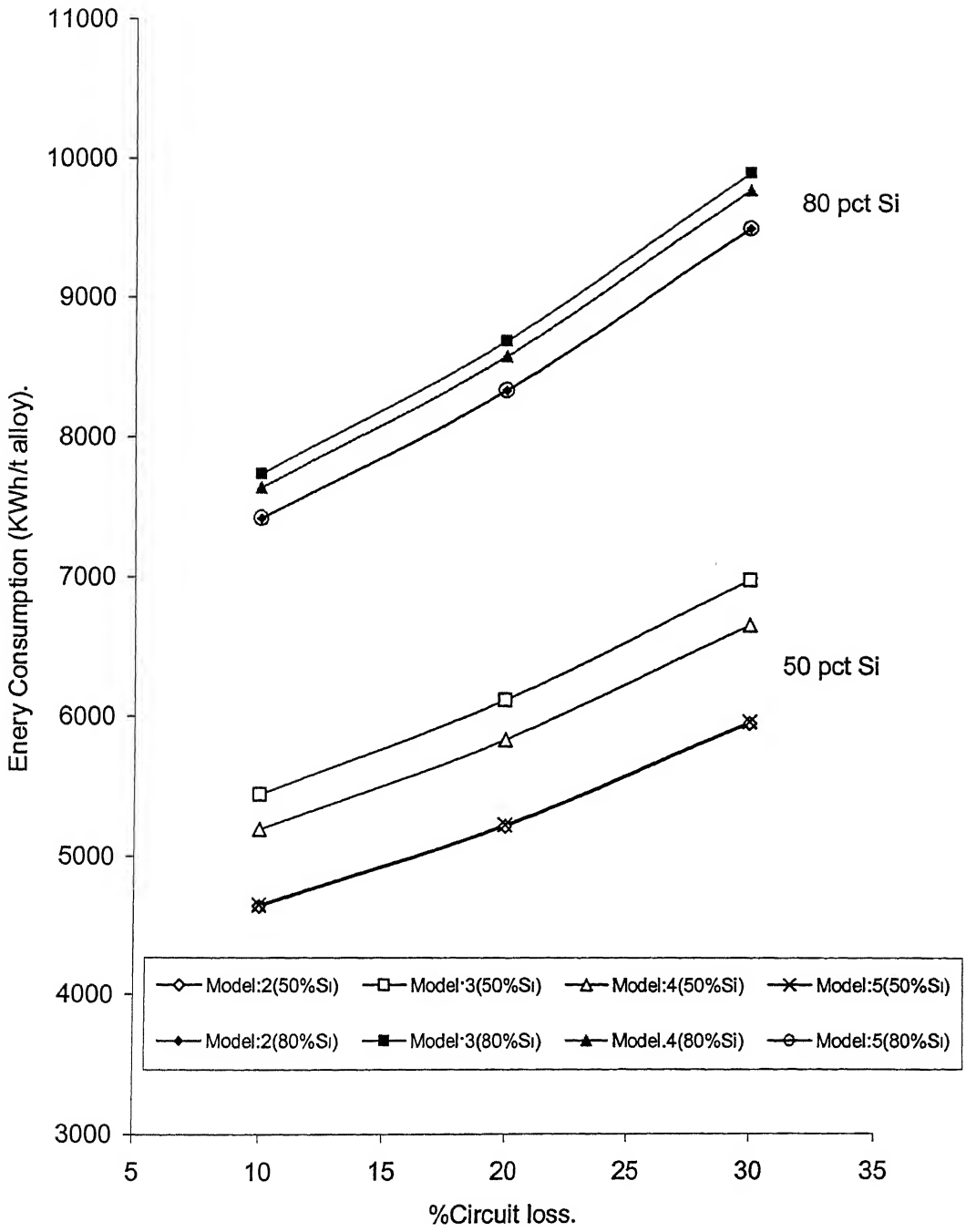

Fig.4.12: Effect of pct Circuit loss on Electrical energy consumption for 50 and 80% Si in Ferrosilicon alloy

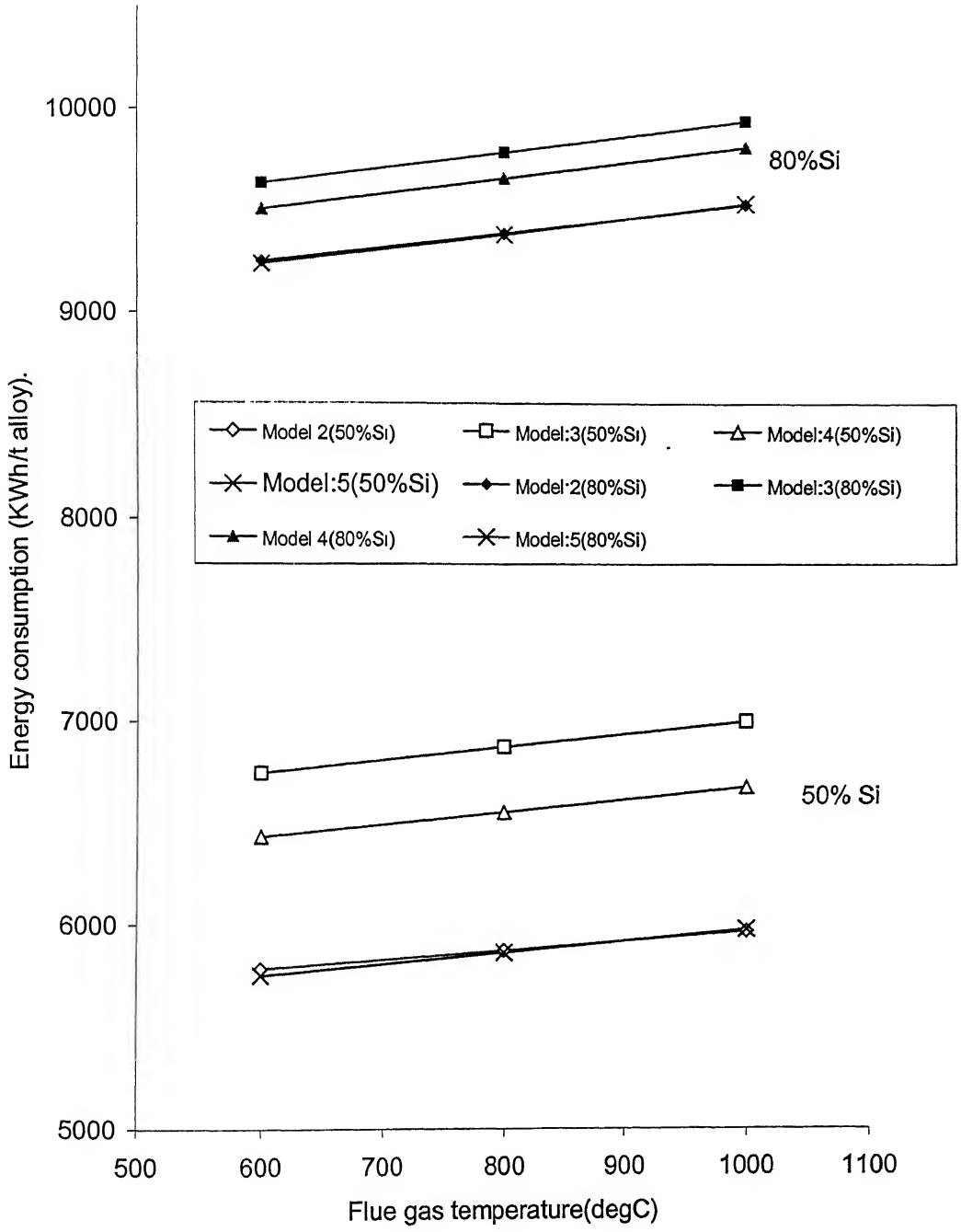

Fig.4.13: Effect of flue gas temperature on Electrical energy consumption for 50% and 80% Si in Ferrosilicon alloy.

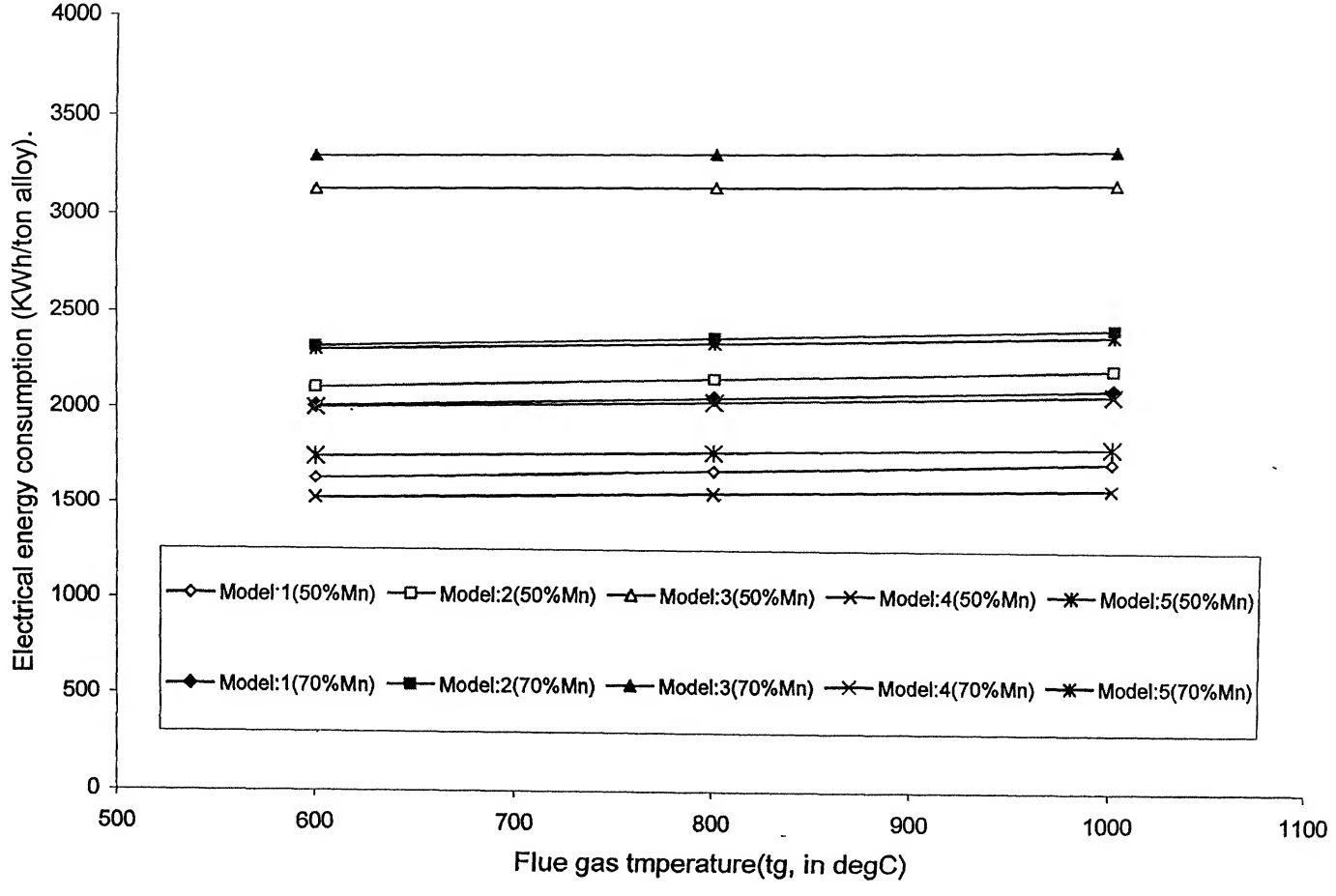

Fig.4.14: Effect of Flue gas temperature temperature on Electrical energy consumption for 50% and 70% Mn in Ferromanganese.

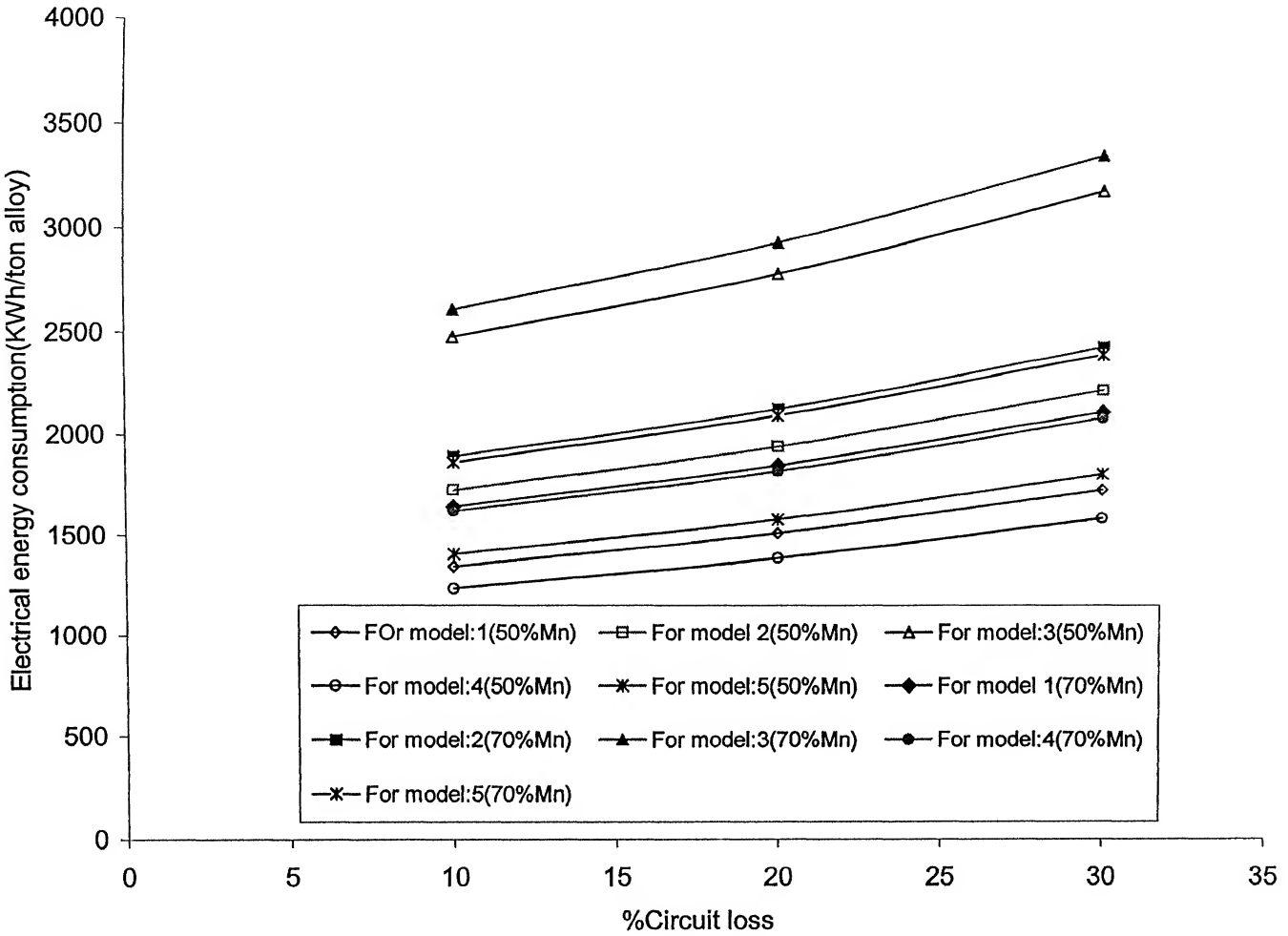

Fig.4.15: Effect of %Circuit loss on Electrical energy consumption for 50% and 70% Mn in Ferromanganese alloy

Table 4.7
Details of energy balance in smeltıng of Ferrosılıcon alloys for different conditions: base 1000Kg alloy

Item	Energy rate (KWh/1000 Kg alloy)									
	Using pure Fe, without recirculation of SiO		Using pure Fe,With recırculation of SiO		Fe_2O_3 without prereduction, with recirculation of SıO		Fe2O3 with prereduction, with recirculation of SiO		Fe2O3 with prereductıon, FeO reduced by CO and C	
	50% Si	80% Sı	50% Si	80% Si	50% Si	80% Si	50% Si	80% Si	50% Sı	80% Sı
Heat demand										
Dıssociation of SiO_2	4822.2	9267.6	4495.7	7183.1	4495.7	7183.1	4495.7	7183.1	4495.7	7183.1
Dıssocıation of Fe_2O_3	0	0	0	0	1029.3	411.7	1029.3	411.7	1029.3	411.7
Formation of CO	-1139.2	-2011.2	-1096.2	-1753.3	-1507.7	-1919.1	-1234.4	-1808.6	-627.4	-1584.4
Formation of CO_2	0	0	0	0	0	0	-491.9	-196.7	-1519.4	-601.2
Formation of SiO	-37.7	-223.8	0	0	0	0	0	0	0	0
Net heat of reaction	3645.3	7032.6	3399.5	5429.8	4017.3	5675.7	3798.7	5589.5	3378.2	5409.2
Sensible heat of FeSi	479.9	764	479.9	764	479.9	764	479.9	764	479.9	764
Sensible heat of CO	324.85	561.2	306.1	489.8	420.9	535.7	344.4	505.1	187.3	442.2
Sensible heat of CO_2	0	0	0	0	0	0	63.0	25.2	195.7	78.3
Sensible heat of SiO	13.55	78.68	0	0	0	0	0	0	0	0
Circuit loss (30%)	1910.59	3617.5	1791.4	2863.2	2101.9	2987.4	2003.6	2948.5	1794.9	2864.6
Total	6374.2	12054	5977	9546.8	7020	9962.8	6689.6	9832.2	6036	9558.3

Contd....

Item	Energy rate (KWh/1000 Kg alloy)									
	Using pure Fe, without recirculation of SiO		Using pure Fe,With recirculation of SiO		Fe_2O_3 without prereduction, with recirculation of SiO		Fe2O3 with prereduction, with recirculation of SiO		Fe2O3 with prereduction, FeO reduced by CO and C	
	50% Si	80% Si	50% Si	80% Si	50% Si	80% Si	50% Si	80% Si	50% Si	80% Si
Heat supply										
Electrical energy	6368.63	12058.34	5971.0	9548.8	7006.4	9962.8	6681.6	9832.9	5983.1	9553.5
Calorific value of C	4052.21	7156.87	3903.8	6246.1	5367.8	6831.7	4879.8	6636.5	3903.8	6246.1
Chemical heat Fe	1021.1	408.44	1021.1	408.44	0	0	0	0	0	0
Total	11442	19623.68	10896	16203.3	12374.2	16794.5	11561.4	16469.4	9886.9	15799.6
Heat utilization										
Calorific value of CO	2897.37	5146	2807.2	4492.5	3859.9	4913.6	3159.1	4632.8	1717.6	4056.6
Calorific value of SiO	304.35	1868	0	0	0	0	0	0	0	0
Chemical heat of "Si" in alloy	4484.93	7175.89	4484.9	7175.9	4484.9	7175.9	4484.9	7175.9	4484.9	7175.9
Chemical heat of Fe	1021.1	408.44	1021.1	408.44	1021.1	408.44	1021.1	408.44	1021.1	408.44
Sensible heat of Fe-Si	479.9	764	479.9	767.5	479.9	767.5	479.9	767.5	479.9	767.5
Sensible heat of Slag	5.56	5.56	5.56	5.56	5.56	5.56	5.56	5.56	5.56	5.56
Sensible heat of CO	324.85	561.2	306.1	489.8	420.9	535.7	344.4	505.1	187.3	442.2
Sensible heat of CO_2	0	0	0	0	0	0	63.0	25.2	195.7	78.3
Sensible heat of SiO	13.55	76.68	0	0	0	0	0	0	0	0
Circuit loss	1910.59	3617.5	1791.4	2863.2	2101.9	2987.4	2003.6	2948.5	1794.9	2864.6
Total	11442.2	19623.3	10896.2	16203	12374.2	16794.1	11561.56	16469	9886.9	15799.1

Table 4.8
Details of energy balance in smelting of Ferromanganese alloys for different conditions: base 1000Kg alloy

Item	Energy rate (KWh/1000 Kg alloy)									
	Prereduced Fe and Mn ore, FeO reduced by CO and C		Prereduced Fe and Mn ore, FeO reduced by C		No preduction of Fe and Mn ore, directly reduced by C		Pure Fe and prereduced Mn ore (Mn_3O_4)		Pure Fe and no prereduction of Mn ore (Mn_3O_4)	
	50% Mn	70% Mn	50% Mn	70% Mn	50% Mn	70% Mn	50% Mn	70% Mn	50% Mn	70% Mn
Heat demand										
Dissociation of Mn_3O_4	1155.48	1540.64	1155.48	1540.64	1155.48	1540.64	1155.48	1540.64	1155.48	1540.64
Dissociation of Fe_2O_3	914.9	457.45	914 9	457.45	914.9	457.45	0	0	0	0
Formation of CO	-30 7	-399.2	-307.06	-337.76	-736.94	-736.94	-184.23	-245.65	-368.47	-522.0
Formation of CO_2	-1243.91	-1178.33	-764.05	-701.75	0	0	-662.40	-926.92	0	0
Net heat of reaction	795.77	420.56	999.27	958.58	*1318.5*	1187.8	308.85	368.07	787.01	1018.64
Sensible heat of Ferromanganese	315.0	345.1	315.0	345.1	315.0	345.1	315.0	345.1	315.0	345.1
Sensible heat of CO	10.8	16.7	85.9	91.4	206.5	204.9	51.9	72.7	103.9	145.4
Sensible heat of CO_2	160.6	152.1	98.7	96.6	0	0	42.8	59.9	0	0
Sensible heat of Mn vapor	0	0	0	0	0.98	5.21	0	0	0	0
Circuit loss (30%)	569.7	633.6	665.7	729.1	955.1	1006.3	475.1	624.6	542.1	717.6
Total	1855.87	1568.06	2164.57	1530.58	2811.02	2675.9	1193.65	1470.37	1748.01	2226.74

Contd....

Item	Energy rate (KWh/1000 Kg alloy)									
	Prereduced Fe and Mn ore, FeO reduced by CO and C		Prereduced Fe and Mn ore, FeO reduced by C		No preduction of Fe and Mn ore, directly reduced by C		Pure Fe and prereduced Mn ore (Mn_3O_4)		Pure Fe and no prereduction of Mn ore (Mn_3O_4)	
	50% Mn	70% Mn	50% Mn	70% Mn	50% Mn	70% Mn	50% Mn	70% Mn	50% Mn	70% Mn
Heat supply										
Electrical energy	1898.8	2112.0	2218.8	2430.2	3172.3	3354.2	1585.6	2082.1	1806.8	2391.9
Calorific value of C	1891.4	1901.3	2370.4	2377.5	2829.76	2793.3	1503.8	1901.3	1835.0	2365.0
Chemical heat Fe	0	0	0	0	0	0	906.73	498.3	906.73	498.3
Total	3790.2	4013.3	4589.2	4807.7	6002.1	6147.5	3996.1	4481.7	4548.5	5255.2
Heat utilization										
Calorific value of CO	99.1	153.2	788.0	838.2	1894.0	1878.8	476.4	666.9	952.7	1333.8
Calorific value of Carbon in alloy	510.1	510.1	510.1	510.1	510.1	510.1	510.1	510.1	510.1	510.1
Chemical heat of "Mn" in alloy	1167.15	1634.01	1167.15	1634.01	1167.15	1634.01	1167.15	1634.01	1167.15	1634.01
Chemical heat of Fe in alloy	906.73	498.3	906.73	498.3	906.73	498.3	906.73	498.3	906.73	498.3
Sensible heat of Ferromanganese	315.0	345.1	315.0	345.1	315.0	345.1	315.0	345.1	315.0	345.1
Sensible heat of Slag	46.3	64.8	46.3	64.8	46.3	64.8	46.3	64.8	46.3	64.8
Sensible heat of CO	12.8	18.9	88.9	91.4	207.5	210.1	53.9	74.7	108.4	151.4
Sensible heat of CO_2	162.6	154.1	101.2	96.6	0	0	45.3	62.9	0	0
Circuit loss	569.7	633.6	665.7	729.1	955.1	1006.3	475.1	624.6	542.1	717.6
Total	3789.5	4012.1	4589.1	4807.6	6001.8	6147.52	3995.98	4481.4	4548.3	5255.11

Table: 4.9

Effect of operating parameters on Electrical energy to produce one ton Ferrosilicon for different models.

Condition	Energy required to produce 1000Kg Fe-Si alloys for different conditions									
	Using pure Fe, without recirculation of SiO		Using pure Fe,With recirculation of SiO		Fe_2O_3 without prereduction, with recirculation of SiO		Fe2O3 with prereduction, with recirculation of SiO		Fe2O3 with prereduction, FeO reduced by CO and C	
	Effect of flue gas temperature (^{0}C) on energy required (KWh/1000Kg alloy), when circuit loss 30% and slag rate 10Kg/t									
	50%Si	80%Si	50%Si	80%Si	50%Si	80%Si	50%Si	80%Si	50%Si	80%Si
1000	6368.6	12058.3	5971.2	9548.8	7006.4	9962.8	6681.6	9832.9	5983.1	9553.5
900	6317.6	11959.7	5920.9	9468.3	6938.3	9875.3	6615.8	9746.2	5921.2	9468.4
800	6267.1	11862.3	5874.1	9393.5	6874.1	9793.5	6553.7	9665.3	5863.2	9389.1
	Effect of circuit loss on energy required, when flue gas temperature 1000^{0}C and slag rate 10Kg/t									
30	6368.6	12058.3	5971.2	9548.8	7006.4	9962.8	6681.6	9832.9	5983.1	9553.5
20	5572.5	10551.1	5222.2	8351.0	6128.0	8713.3	5843.8	8599.7	5232.6	8355.2
10	4953.4	9378.7	4641.9	7423.1	5447.1	7745.2	5194.5	7644.1	4651.2	7426.8
	Effect of slag rate on energy required, when flue gas temperature 1000^{0}C and circuit loss 30%									
30	6381.8	12074.8	5984.1	9559.9	7019.3	9974.0	6694.5	9844.1	5996.0	9564.6
20	6373.6	12061.7	5976.1	9551.9	7011.3	9966.0	6686.6	9836.1	5988.0	9556.7
10	6368.6	12058.3	5971.2	9548.8	7006.4	9962.8	6681.6	9832.9	5983.1	9553.5

Table: 4.10

Effect of operating parameters on Electrical energy to produce one ton Ferromanganese alloy for different models.

Condition	Energy required to produce 1000Kg Ferromanganese alloys for different conditions									
	Prereduced Fe and Mn ore, FeO reduced by CO and C		Prereduced Fe and Mn ore, FeO reduced by C		No preduction of Fe and Mn ore, directly reduced by C		Pure Fe and prereduced Mn ore (Mn_3O_4)		Pure Fe and no prereduction of Mn ore (Mn_3O_4)	
	Effect of flue gas temperature (^{0}C) on energy required (KWh/1000Kg alloy), when circuit loss 30% and slag rate 10Kg/t									
	50% Mn	70% Mn	50% Mn	70% Mn	50% Mn	70% Mn	50% Mn	70% Mn	50% Mn	70% Mn
1000	1898.8	2113.3	2218.8	2430.2	3173.7	3299.2	1585.6	2082.1	1806.8	2391.9
900	1872.5	2073.0	2190.4	2401.1	3160.3	3292.5	1570.9	2061.7	1790.7	2369.4
800	1846.6	2032.7	2162.3	2374.4	3147.2	3278.5	1556.5	2041.5	1774.8	2347.1
	Effect of circuit loss on energy required, when flue gas temperature 1000^{0}C and slag rate 10Kg/t									
30	1898.8	2113.3	2218.8	2430.2	3173.7	3299.2	1585.6	2082.1	1806.8	2391.9
20	1661.5	1849.0	1941.5	2126.4	2777.0	2893.4	1387.4	1821.9	1581.0	2093.0
10	1476.9	1640.0	1725.8	1890.1	2468.4	2571.9	1233.2	1619.4	1405.3	1860.4

Table: 4.11
Operating and calculated energy consumption rates (KWh/ton Ferrosilicon alloy)

	Fe-45Si	**Fe-65Si**	**Fe-75Si**
Operating data for Submerged arc furnace[21]	4360	7640	8400
Computed value without recycling of SiO and heat recovery	5615	8853	10856
Computed value with recycling of SiO and heat recovery	5372	7756	8948

Table: 4.12 Step change in electricity consumption rates for changes in operating parameters

Operating parameters	Unit change	Change in electricity consumption (KWh/ 1000Kg alloy)				
		Using pure Fe, without recirculation of SiO	Using pure Fe,With recirculation of SiO	Fe_2O_3 without prereduction, with recirculation of SiO	Fe_2O_3 with prereduction, with recirculation of SiO	Fe_2O_3 with prereduction, FeO reduced by CO and C
Slag rate						
Fe-50%Si	+10Kg	+5	+4.9	+4.9	+5	+4.9
Fe-80%Si	+10Kg	+3.3	+3.1	+3.2	+3.2	+3.1
Temperature of flue gas						
Fe-50%Si	-100^0K	-51.0	-50.1	-68.1	-61.9	-58.9
Fe-80%Si	-100^0K	-98.6	-75.7	-82.8	-82.0	-80.4
Thermal efficiency of furnace						
Fe-50%Si	+10%	-796.1	-746	-875.4	-834.9	-746.5
Fe-80%Si	+10%	-1507.2	-1193	-1244.8	-1228.5	-1193.6

Operating parameter	Unit change	Change in electricity consumption (KWh/ 1000Kg alloy)				
		Pre reduced Fe and Mn ore, FeO reduced by CO and C	Pre reduced Fe and Mn ore, FeO reduced by C	No pre-reduction of Fe and Mn ore, directly reduced by C	Pure Fe and pre-reduced Mn ore (Mn_3O_4)	Pure Fe and no pre-reduction of Mn ore (Mn_3O_4)
Temperature of flue gas						
Fe-50Mn	-100^0K	+26.3	+28.4	+13.4	+14.7	+16.1
Fe-70Mn	-100^0K	+50.3	+29.1	+14.2	+20.4	+22.5
Thermal efficiency of furnace						
Fe-50Mn	+10%	-237.3	-277.3	-396.7	-198.2	-225.8
Fe-70Mn	+10%	-264.3	-303.8	-413.3	-260.2	-298.9

Input energy: (KWh/ton Ferrosilicon alloy)

1: Electrical energy (12058.34) **2**: Calorific value of carbon (7156.87) **3**: Chemical heat of iron (408.44)

Output energy: (KWh/ton Ferrosilicon alloy)

4: Loss of energy due to SiO (1944.68) **5**: Circuit loss (3617.5) **6**: Sensible heat of slag and gas (566.76)

7: Calorific value of CO (5146) **8**: Sensible heat of alloy (764) **9**: Chemical heat of iron (408.44)

10: Chemical heat of silicon (7175.89)

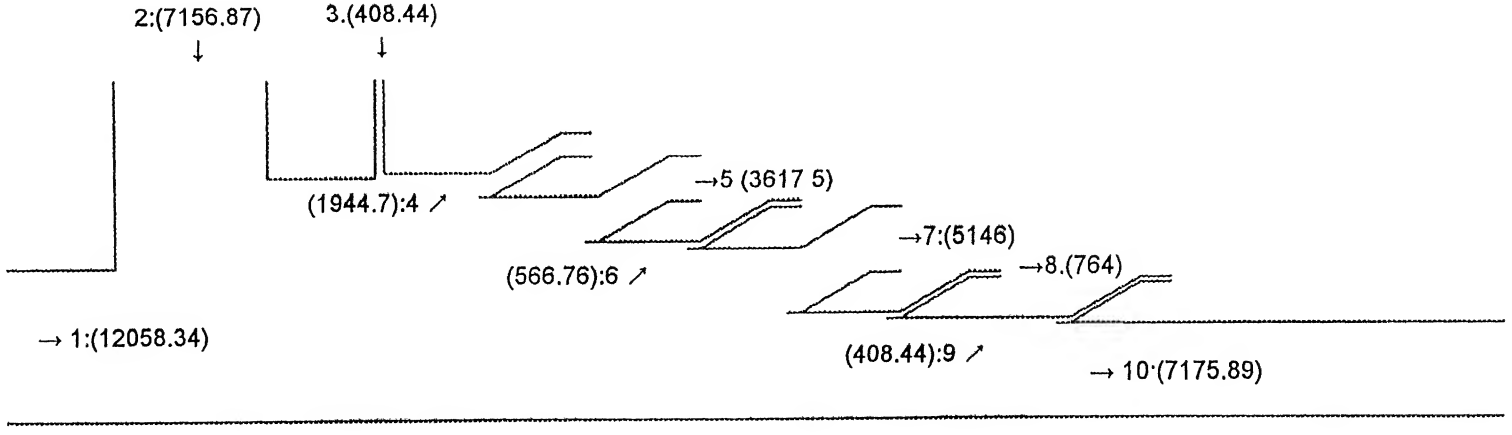

Fig. 5.14: Representative energy diagram(**Model:1**) for smelting of Fe-80Si alloy without recirculation of SiO.

Fig.5.15 Representative energy diagram (**Model:2**)for smelting of Fe-80Si alloy with recirculation of SiO

Input energy: (KWh/ton Ferrosilicon alloy)

1: Electrical energy (9548.8) **2**: Calorific value of carbon (6246.1) **3**: Chemical heat of iron (408.44)

Output energy: (KWh/ton Ferrosilicon alloy)

4: Recirculation of energy due to SiO (1944.68) **5**: Circuit loss (2863.2) **6**: Sensible heat of slag and gas (495.36)

7: Calorific value of CO (4492.5) **8**: Sensible heat of alloy (767.5) **9**: Chemical heat of iron (408.44)

10: Chemical heat of silicon (7175.9)

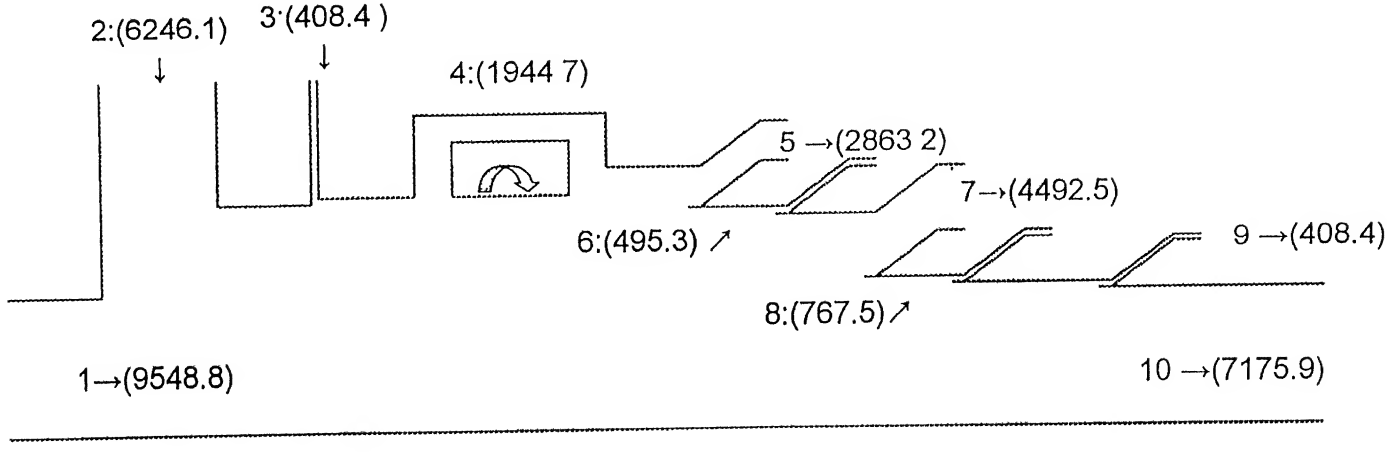

Input energy: (KWh/ton Ferrosilicon alloy)

1: Electrical energy (9962.8) 2: Calorific value of carbon (6831 7)

Output energy: (KWh/ton Ferrosilicon alloy)

3: Recirculation of energy due to SiO (1944.68) 4: Circuit loss (2987.4) 5: Sensible heat of slag and gas (541.26)

6: Calorific value of CO (4913.6) 7: Sensible heat of alloy (767 5) 8: Chemical heat of iron (408.44)

9: Chemical heat of silicon (7175.9)

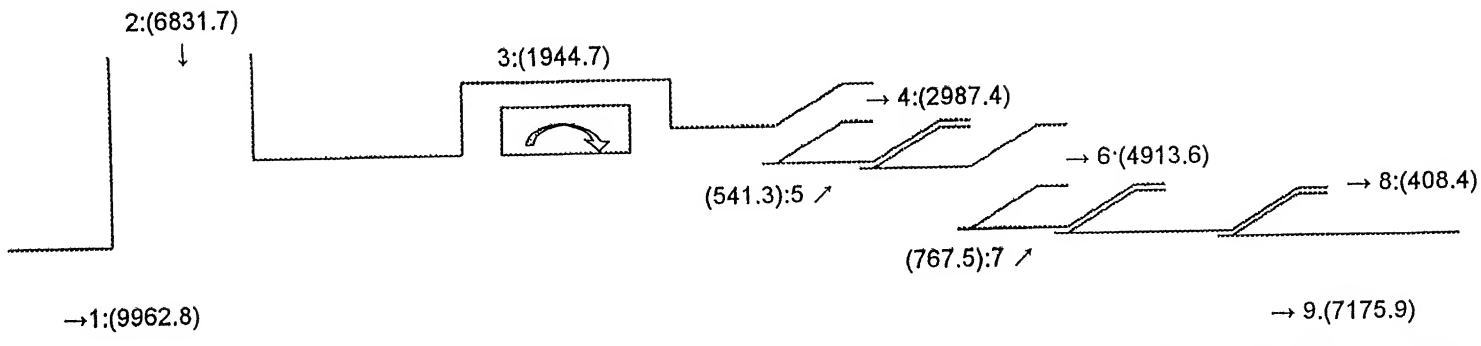

Fig. 5.16 Representative energy diagram(**Model:3**) for smelting of Fe-80Si alloy with recirculation of SiO

Input energy: (KWh/ton Ferrosilicon alloy)

1: Electrical energy (9832.9) 2: Calorific value of carbon (6636.5)

Output energy: (KWh/ton Ferrosilicon alloy)

3: Recirculation of energy due to SiO (1944.68) 4: Circuit loss (2948.5) 5: Sensible heat of slag and gas (535.84)

6: Calorific value of CO (4632.8) 7: Sensible heat of alloy (767.5) 8: Chemical heat of iron (408.44)

9: Chemical heat of silicon (7175.9)

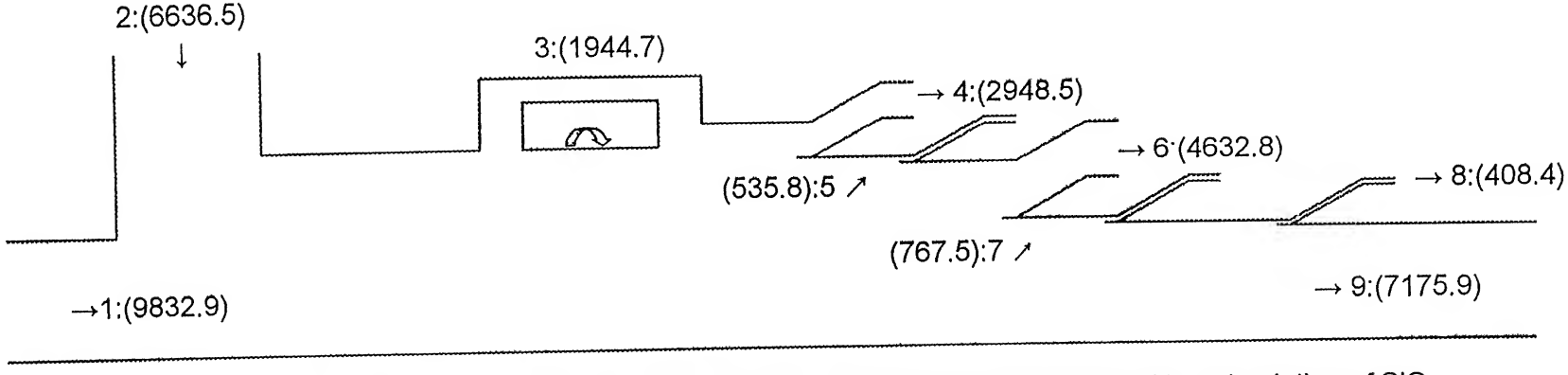

Fig. 5.17 Representative energy diagram (**Model:4**) for smelting of Fe-80Si alloy with recirculation of SiO

Input energy: (KWh/ton Ferrosilicon alloy)

1: Electrical energy (9553.5) 2: Calorific value of carbon (6246.1)

Output energy: (KWh/ton Ferrosilicon alloy)

3: Recirculation of energy due to SiO (1944.68) 4: Circuit loss (2864.6) 5: Sensible heat of slag and gas (526.06)

6: Calorific value of CO (4056.6) 7: Sensible heat of alloy (767.5) 8: Chemical heat of iron (408.44)

9: Chemical heat of silicon (7175.9)

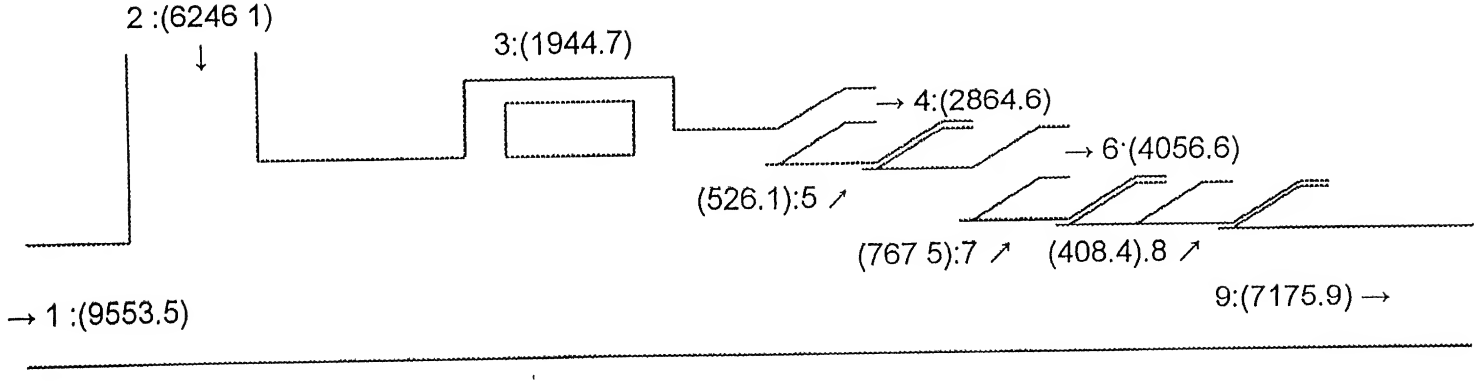

Fig.5.18 Representative energy (**Model:5**) diagram for smelting of Fe-80Si alloy with recirculation of SiO

Fig.5.19 Representative energy diagram (**Model:1**) for smelting of Fe-70Mn alloy

Input energy: (KWh/ton Ferromanganese alloy)

1: Electrical energy (2112) 2: Calorific value of carbon (1901.3)

Output energy: KWh/ton

3: Circuit loss (633.6) 4: Sensible heat of slag and gas (221.7) 5: Calorific value of CO (153.2)

6: Sensible heat of alloy (345.1) 7:Chemical heat of Carbon in alloy (510.1) 8: Chemical heat of iron (498.3)

9: Chemical heat of manganese (1634.01)

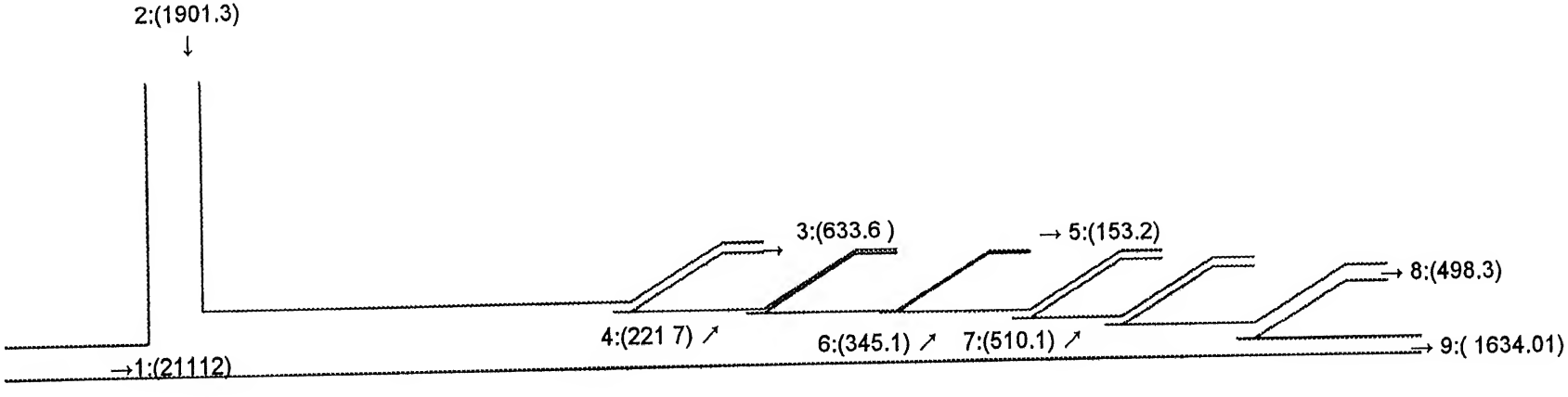

Input energy: KWh/ton

1: Electrical energy (2430.2) 2: Calorific value of carbon (2377.5)

Output energy: (KWh/ton Ferrosilicon alloy)

3: Circuit loss (729.1) 4: Sensible heat of slag and gas (252.8) 5: Calorific value of CO (838.2)

6: Sensible heat of alloy (345.1) 7: Chemical heat of Carbon in alloy (510.1) 7: Chemical heat of iron (498.3)

9: Chemical heat of manganese (1634.01)

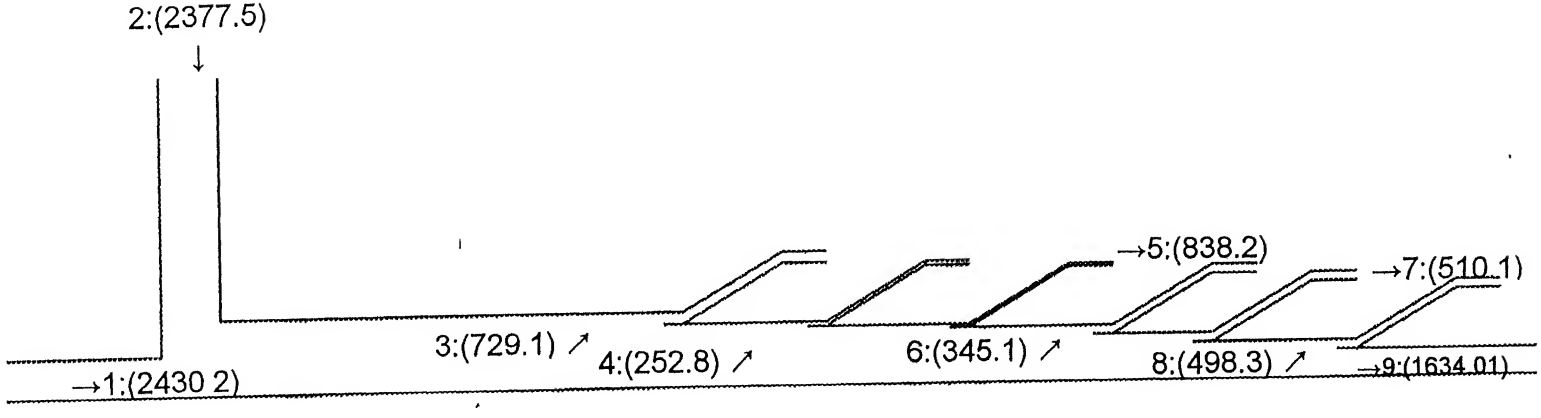

Fig.5.20 Representative energy diagram (**Model:2**) for smelting of Fe-70Mn alloy

Input energy: KWh/ton

1: Electrical energy (3354.2) 2: Calorific value of carbon (2793.3)

Output energy: (KWh/ton Ferrosilicon alloy)

3: Circuit loss (1006.3) 4: Sensible heat of slag and gas (274.9) 5: Calorific value of CO (1878.8)

6: Sensible heat of alloy (345.1) 7: Chemical heat of Carbon in alloy (510.1) 8: Chemical heat of iron (498.3)

9: Chemical heat of manganese (1634.01)

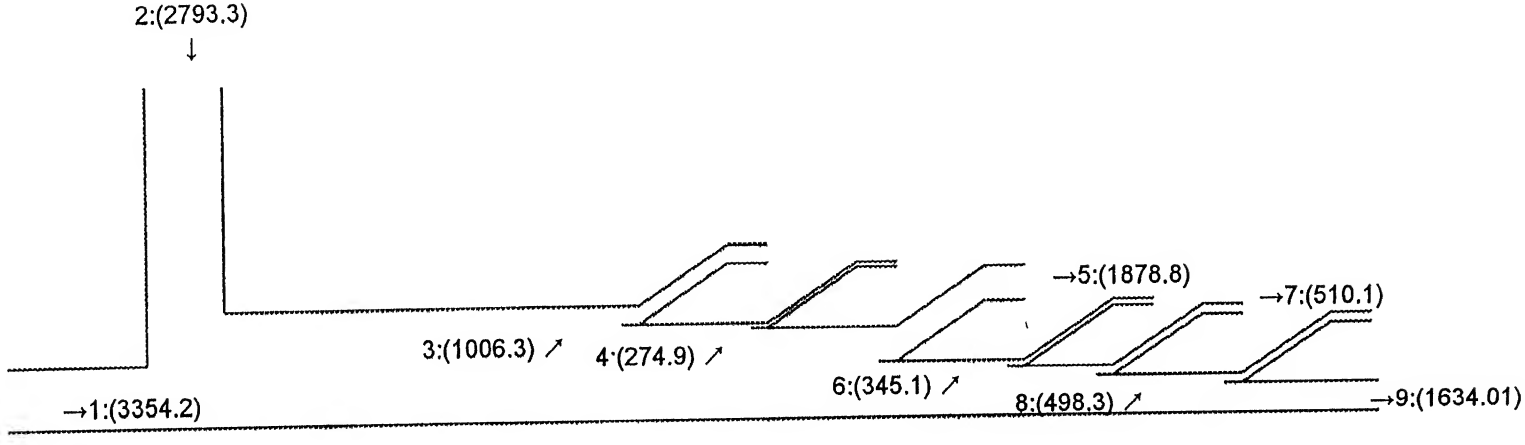

Fig.5.21 Representative energy diagram(**Model:3**) for smelting of Fe-70Mn alloy.

Input energy: KWh/ton

1: Electrical energy (3354.2) 2: Calorific value of carbon (2793.3)

Output energy: (KWh/ton Ferrosilicon alloy)

3: Circuit loss (1006.3) 4: Sensible heat of slag and gas (274.9) 5: Calorific value of CO (1878.8)

6: Sensible heat of alloy (345.1) 7: Chemical heat of Carbon in alloy (510.1) 8: Chemical heat of iron (498.3)

9: Chemical heat of manganese (1634.01)

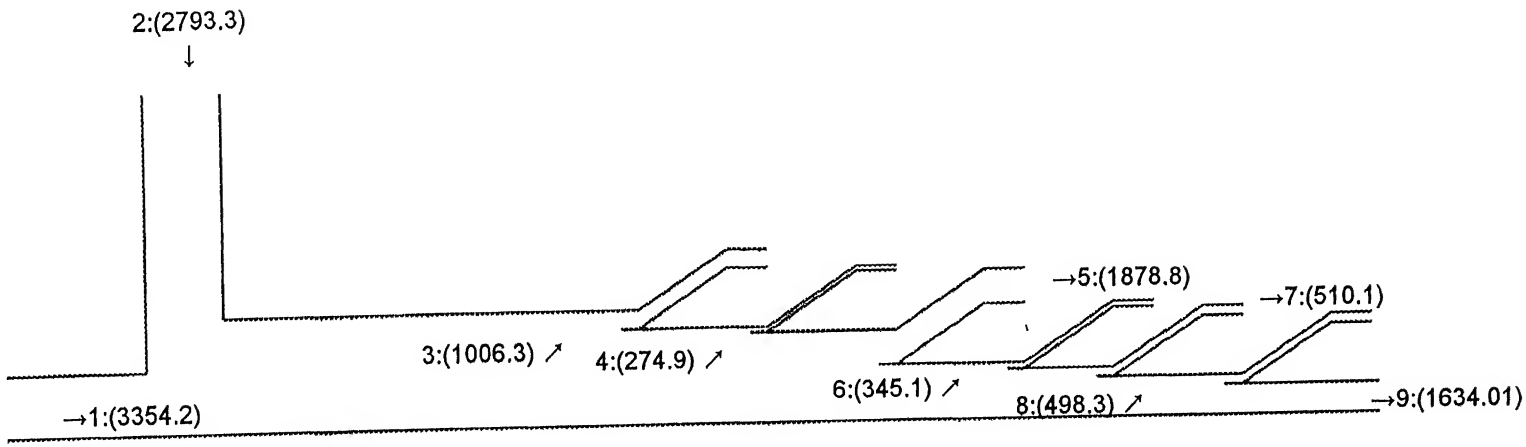

Fig.5.21 Representative energy diagram(**Model:3**) for smelting of Fe-70Mn alloy.

Chapter: 5

Summary and Conclusions

Summary and Conclusions

(1) Model equations based on thermodynamic considerations are developed to calculate the temperature to which the materials must be heated to obtain a certain grade of the alloys.

(2) In presence of carbon, silica and Mn_3O_4 are transformed to silicon carbide and Mn_7C_3 at 1537^0C and Mn_3O_4 transformed to Mn_7C_3 at 1273^0C with little evolution of silicon monoxide and Mn vapor.

(3) Silicon carbide will be in equilibrium with the liquid alloy containing around 22 wt. pct silicon. Solubility of carbon in the Fe-Si alloy is practically nil above 22 wt. pct Silicon. Manganese carbide will be in equilibrium with the liquid alloy containing around 15.5 wt. pct manganese. Solubility of carbon in the Ferromanganese alloy increases with smelting temperature as well as Manganese content of the alloy.

(4) Further increase in silicon or Manganese content of the alloy occurs due to reaction between silica and silicon carbide for Fe-Si at temperature above 1535^0C and reaction between Mn_3O_4 and Mn_7C_3 for Ferromanganese at temperature above 1742^0C.

(5) Heat and mass balances based on available thermal data of species are carried out to determine the carbon and energy consumption rates for different grades of the alloys.

(6) Results of model calculations tend to agree with the plant data if recycling of silicon monoxide within the furnace is taken into consideration.

(7) Electrical and heat losses may be around 1670 KWh for producing one ton of Fe-50Si alloy, 2670 KWh per ton of Fe-80Si alloy, and around 750 KWh per ton of Fe-50Mn alloy, 1006 KWh per ton of Fe-70Mn alloy..

(8) Among all the models, cost of production to produce Ferro silicon or Ferromanganese alloy will be low for model 5 for Ferrosilicon and model 1 for Ferromanganese alloy.

References

1. Michal D. Fenton, "U.S.Geological Survey Mineral yearbook" 2000, p.28.5-10
2. A.Riss, Y.Khodorosky, "Production of Ferroalloys",V.2, Foreign language publishing house, Moscow(1979)
3. J.Chipman, J.C.Fulton, N.Gokcen and G.R.Caskey: Acta Metallurgica, 1954, Vol.2, p.439.
4. J. Chipman, R.M.Gott, Arfred, L.W.Small, R.B.Wilson, D.M.Thomson, Trans. Amer. Soc.Metals 1952, Vol.44, p.1212.
5. Y.H.Chou: Doctorate thisis, Dept. of Mctallurgy, Carnegie Institute of Technology, Pittsburg, pern, 1947,p.89
6. E.T.Turkdogan, P.Grieveson, and J.F.Bister: Trans. Met. Soc. AIME, 1963, Vol.227, p.1258.
7. J.Chipman and R. baschwitz: Trans. Met. Soc.AIME, 1963.Vol.227,p.473.
8. N.A.Goken and J. Chipman: Trans. AIME,!(52, Vol195,p.171 and 1953, Vol197, p.1017.
9. D.A.R.Key and J.Taylor, Transation of Faraday Soc.1960,Vol.56,p.1372
10. Richardson, Jeffers and Withers, J.I.S.I,1950,Vol.166,p.213
11 F. J. Schottman, "Ferroalloys", Mineral Yearbook, Volume 1:Metals and Minerals, Bureau of Mines, Department of The Interior, Washington, DC, 1980.
12. Willams T, lanford, Jr. Norman L, Samways. Robert F,Craven, Horal E. Mcgannon, "Making, Shaping and treating of Steels", United state Steel, Tenth edition, p.371-377, 388-391.
13. E.W.Filer and L.S.Darken; JOM,1952,194,253
14. J.C. Fulton and J. Chipman; JOM, 1954,196,1136.
15. J.R. Rawaling and J. Elliot; Trans AIME,1965, 233,1539
16. M. Aghizuka, M. Tokuda and M. Ohtani; Trans ISIJ 12,1972,383
17. N. Tschiya, M.Tokuda and M. Ohtani Met Trans. B (1976) 315
18. E.T. Turkdogan, G.J.W. Kor and R.J. Fruehen IMSM (1980) 268

19. R.J. Pomfret and P. Grieveson; Canadian Metallurgical review 22(3) (1983) 287

20. N.K. Batra and P. Bhaduri IMSM 17 (1990) 389

21. F.P. Edneral " Electrometallurgy of Steel and Ferro-alloys V2,MIR publishers

Programme for Modeling of Ferro-Silicon alloy

For Model: 1

```
ınclude<math.h>
ınclude<stdıo.h>
include<conıo.h>
ınclude<dos.h>
ıt T,t,z;
oat asi,x,Pco,Psio,P,R,F,tg=1273.0,CL=0.70;
oat Gco,Gsıc,Gsio2,Gsio,G3,G4,mHsio,Nco,Nsıo,Nsıo2,sio2_ip_per_tonne_alloy;
oat a_op,sı_op,si_op1,dsi_op,sdsi_op,sio2_ip,q;
oat or,nsıo,nco,wc,wa,nsio2,hsıo2=(-216100),hsio=(-23200),hco=(-26420);
----------HEAT CONTENT OF AT DIFFERENT TEMPERATURES (K)----------
                Hfe_1(298 to 1042), Hfe_2(1042 to 1184),Hfe_3(1184 to 1665),
                    Hfe_4(1665 to 1810),Hfe(1810 to t) ,Hfe_1(298-1685)
-----------------------------------------------------------------------------------------------------------------
oat Hfe_1=(3.04*(1042.0-298)+(.00758/2)*(1042^2-298^2)-60000.0*(1/1042.0-1/298.0));
oat Hfe_2=11.13*(1184.0-1042.0);
oat Hfe_3=(5.8*(1665.0-1184.0)+(.00198/2)*(1665.0*1665.0-1184.0*1184.0));
oat Hfe_4=(6.74*(1810.0-1665.0)+(.0016/2)*(1810.0*1810.0-1665.0*1665.0));
oat Hsi_1=(5.7*(1685.0-298.0)+(.0007/2)*(1685.0^2-298^2)+(104000*(1/1685.0-1/298.0)));
oat Hfe_5,Hf=(326.0+215.0+165.0),Ht=3670.0,Hf_si=12100.0,total,wt_c_per_tonne_alloy;
oat HFE=(Hfe_1+Hfe_2+Hfe_3+Hfe_4+Hf+Ht),Wslag=10.0,Hslag,sensiheat_sio,chemheat_sio;
oat Hsio2,Hsio,Hco,Hfe,Hsi,Hfesi,sensiheat_fesi,hr,hrımj,thr,kwhpt;
oat cv_c,hco2=(94050),sensiheat_co,chemheat_co,heatcontent_sio2,sensiheat_slag,cls,chemheat_fe;
oat hfe2o3=(-196800.0),nfe2o3,Hfe2o3,chemheat_si,chemheat_Fe;
oıd main()

oid ft(float);
oid test(float asi);
lrscr();
=0.20;
dsi_op=(x-0.01)/(1.0-x+0.01);
hile(x<=0.8)

(x<=0.30)
si=exp((0.2274*(x*100.0))-8.4906);
lse
```

```
{
if(x<=0.42)
asi=exp((0.0556*(x*100.0))-3.145);
else
asi=exp((0.0158*(x*100.0))-1.3832);
}
T=1700;
while(T<=2500)
{
ft(T);
Pco=sqrt(exp((-G3)/(1.98*T))*asi*asi*asi);
Psio=sqrt(exp((-G4)/(1.98*T))*asi);
P=(Psio)+(Pco);
if(P>=1.000)
{
F=((Psio)/(Pco));
R=(3-F)/(3+F);
t=T;
break;
}
T++;
}
a_op=1/(1-x);
si_op=x/(1-x);
si_op1=(x-0.01)/(1-(x-0.01));
dsi_op=si_op-si_op1;
sdsi_op+=((dsi_op)/R);
sio2_ip=(sdsi_op)*(60.0/28.0);
sio2_ip_per_tonne_alloy=sio2_ip*1000.0;
nsio2=(sio2_ip)/60.0;
or=(si_op)/((sdsi_op));
nsio=nsio2*(1.0-or);
nco=((1.0+or)*(nsio2));
wc=12.0*(nco);
Nsio2=nsio2*(1.0-x);
Nsio=nsio*(1.0-x);
Nco=nco*(1.0-x);
```

```
wt_c_per_tonne_alloy=(wc/a_op)*1000 0;
Hco=Nco*(hco+6.79*(tg-298)+(.00098/2)*(tg*tg-298*298)-(11000.0/-1)*((1.0/tg)-(1.0/298)));
Hsio=Nsio*(hsio+7.7*(tg-298)+(.00074/2)*(tg*tg-298*298)-(70000.0/-1)*((1.0/tg)-(1.0/298)));
Hsio2=(Nsio2*hsio2);
if(t>=1810.0)
{
Hfe_5=((9.77*(t-1810.0))+((.0004/2)*(t*t-1810.0*1810.0)));
}
else
Hfe_5=0.0;
Hfe=((1.0-x)/56.0)*(HFE+Hfe_5);
Hsi=(x/28.0)*(6.1*(t-1685.0)+Hsi_1+Hf_si);
Hfesi=-19200*((1-x)/56.0);
Hslag=(Wslag*2000*1000)/(1000000);
hr=((Hsi+Hfe+Hfesi+(-Hsio2+Hco+Hsio))*(4.184)+Hslag)/CL;
kwhpt=(hr/3.6);
cls=kwhpt*0.30;
cv_c=(hco2*(wa/12.0)*4.184/1000)/3.6;

sensiheat_co=(Nco*( 6.79*(tg-298)+( 00098 2)*(tg^2-298^2)-(11000.0/-1)*((1.0/tg)-(1.0/298))))*(4.184/3.6);
sensiheat_fesi=((Hfe+Hsi+Hfesi)*4.184)/3.6;
sensiheat_slag=Hslag/3.6;

sensiheat_sio=Nsio*((7.7*(tg-298)+(.00074/2)*(tg*tg-298*298)-(70000.0/-1)*((1.0/tg)-(1.0/298))))*(4.184/3.6);
chemheat_co=(Nco*(hco2-hco)*4.184)/3.6;
chemheat_sio=(hsio2-hsio)*Nsio*(4.184/3.6);
chemheat_si=(hsio2*x/28.0)*(4.184/3.6);
nfe2o3=(1/112.0);
Hfe2o3=(nfe2o3*hfe2o3)*(1.0-x);
chemheat_Fe=(Hfe2o3)*(4.184/3.6);
//printf("\n%.2f  %d  %.1f  %.1f %.1f",x,t,sio2_ip_per_tonne_alloy,wt_c_per_tonne_alloy,kwhpt);
//printf("\n%.2f..%d...%.3f",x,t,sio2_ip,);
//printf("\n%.2f...%.3f",x,kwhpt);
//printf("\n%.2f...%.2f...%.2f ...%.2f....%.2f",x,sensiheat_fesi,sensiheat_slag,sensiheat_co,sensiheat_sio);
//printf("\n%.2f...%.2f...%.2f....%.2f....%.2f...%.2f",x,chemheat_co,chemheat_sio,chemheat_si,chemheat_Fe,cls);
//printf("\n%.2f....%.3f...%.3f",x,kwhpt,cv_c);
```

```
//printf("\n%.2f....%.1f...%.1f...%.1f...%.1f.... %.1f...% 1f....%.1f",x,mHco,mHslag,mHfesi,mHsio,hls_co,mHsio2,cl
s);
//printf("\n%.2f....%..3f...%.3f...%.3f...%.3f ....%.3f...%.3f....%.3f...%.3f",x,mHco,mHslag,mHfesi,mHsio,hls_co,Hsi
o2,Hfe,cls);
x+=0.01;
getch();
}
}
void ft(float T)
{
Gco=(-26700.00-(20.95*T));
Gsic=(-25100.0+(7.91*T));
Gsio2=(-227700.0+(48.7*T));
Gsio=(-36150.0-(11.51*T));
G3=((2.0*Gco)-Gsio2-(2.0*Gsic));
G4=(2.0*Gsio-Gsio2);
}
```

For Model: 2, 3, 4 and 5 (Modeling of Ferrosilicon)

```
#include<math.h>
#include<stdio.h>
#ınclude<conio.h>
#include<dos.h>
float C = (hco+6.79*(tg-298)+(.00098/2)*(tg*tg-298*298)-(11000.0/-1)*((1.0/tg)-(1.0/298)));
float  h3= Hsi+Hfe+Hfesi, y = (.00098/2), j = (1685.0-298.0), m = 4.184/1000, k1= (0.95*56 );
float T,t,asi,x,Pco,Psıo,P,F,tg=(273.0+1000),R,CL=0.9,Wslag=20.0;
float Gco,Gsic,Gsio2,Gsio,Gfe2o3,Gfeo,Gco2,G3,G4,G5,nc, m= 4.184/1000, n1= (hco2-hco);
float a_op,sio2_ip,q,K,f,te=1200.0,hsıo=(-23200);
float nsio2,hsio2=(-216000),hco=(-26420),hco2=(-94050),hfe2o3=-196800,Hfe2o3;
```

HEAT CONTENT OF "Fe" AT DIFFERENT TEMPERATURES (K)

Hfe_1(298 to 1042), Hfe_2(1042 to 1184), Hfe_3(1184 to 1665),
Hfe_4(1665 to 1810), Hfe(1810 to t) ,

```
float Hfe_1= (3.04*(1042.0-298)+(.00758/2)*(1042.0^2-298.0^2) -60000.0*(1/1042.0-1/298.0));
float Hfe_2 =11.13*(1184.0-1042.0);
float Hfe_3 = (5.8*(1665.0-1184.0)+(.00198/2)*(1665.0^2-1184.0^2));
float Hfe_4 = (6.74*(1810.0-1665.0)+(.0016/2)*(1810.0^2-1665.0^2));
float Hsi_1= (5.7*j + (.0007/2)*(1685.0^2-298.0^2)+(104000*(1/1685.0-1/298.0)));
float Hfe_5, Hf = (326.0+215.0+165.0), Ht = 3670.0, Hf_si = 12100.0;
float c_cv,c_cv_1,c_cv_2,c_cv_3,mHco_1,mHco_2,mHco2_2,mHco,mHco_3,mHco2_3;
float hls_co,hls_co_1,hls_co_2,hls_co_3,mHfesi,mHfe2o3,mHsio2;
float cls,cls_1,cls_2,cls_3,mHslag;
float sı_op,si_op1,dsi_op,sdsi_op,or,nsıo,Hsio,mHsio,H_recir,wt_sio2_pertonne_alloy;
float HFE=(Hfe_1+Hfe_2+Hfe_3+Hfe_4+Hf+Ht),Fe2o3_ip_tonne_alloy;
float Fe2o3_ip,nFe2o3,Hslag,hslag,
float nco,nco_1,nco_2,nco_3,wc,wc_1,wc_2,wc_3,nco2_2,nco2_3;
float Hsio2,Hco_1,Hco_2,Hco2_2,Hco,Hco_3,Hco2_3,Hfe,Hsi,Hfesi,hr,hr_1,hr_2,hr_3,
float kwhpt,kwhpt_1,kwhpt_2,kwhpt_3;

void maın()
{
```

```
void ft(float);
void test(float asi);
clrscr();
x=0.20;
sdsi_op=(x-0.01)/(1.0-x+0.01);
while(x<=0.8)
{
if(x<=0.30)
asi=exp((0.2274*(x*100.0))-8.4906);
else
{
if(x<=0.42)
asi=exp((0.0556*(x*100.0))-3.145);
else
asi=exp((0.0158*(x*100.0))-1.3832);
}
T=1700.0;
while(T<=2500)
{
ft(T);
Pco=sqrt(exp((-G3)/(1.987*T))/(asi*asi*asi));
Psio=sqrt(exp((-G4)/(1.987*T))*asi);
P=(Psio)+(Pco);
if(P>=1.000)
{
F=((Psio)/(Pco));
R=(3-F)/(3+F);
t=T;
break;
}
T++;
}
si_op=x/(1-x);
si_op1=(x-0.01)/(1-(x-0.01));
```

```
dsi_op=si_op-si_op1;
sdsi_op+=((dsi_op)/R);
or=(si_op)/((sdsi_op));
sio2_ip=x*(60.0/28.0);
wt_sio2_pertonne_alloy=sio2_ip*1000.0;
nsio2=(sio2_ip)/60.0;
nsio=nsio2*(1.0-or);
Hsio=nsio*(hsio + 7.7*b + (.00074/2)*C - (70000.0/-1)*d);
Fe2o3_ip=(1.0-x)*(56.0*2+16.0*3)/(56.0*2);
Fe2o3_ip_tonne_alloy=Fe2o3_ip*1000.0;
```

----------***For pure Fe*** ----------

```
nco=nsio2*2.0;
wc=12.0*(nco)*1000;
```

----------***For Fe_2O_3 without pre-reduction*** ----------

```
nFe2o3=(1-x)/(56.0*2);
nco_1=2*nsio2+3*nFe2o3;
wc_1=12.0*nco_1*1000.0;
```

----------***For Fe_2O_3 with pre-reduction*** ----------

```
nco2_2=nFe2o3;
nco_2=2.0*nsio2+nFe2o3;
wc_2=12.0*(nco_2+nco2_2)*1000.0;
```

----------***For pre-reduced Fe_2O_3 and FeO***----------

```
G5=5.8*te-5450.0;
K=exp(-G5/(1.987*te));
f= (1.0/(1+2*K))*((1+K)-(3.8*K*x)/(1-x));
if(f>=0.0)
{
nc=2*nsio2+f*(1.0-x)/ k1;
nco2_3=(1.0-f)*(1.0-x)/(k1)+(1.0/2)*(1-x)/56.0;
nco_3=nc-nco2_3;
}
else
{
f=0.0;
```

```
nc=2*nsio2+f*(1.0-x)/ k1;
nco2_3=(1.0-f)*(1.0-x)/(k1)+(1.0/2)*(1-x)/56.0;
nco_3=nc-nco2_3;
}
wc_3 =12.0*(nco_3+nco2_3)*1000;
Hco=nco*C;
Hco_1 = nco_1*C;
Hco_2 = nco_2*C;
Hco_3 = nco_3*C;
Hco2_2 = nco2_2*(hco2 + (10.57*b) + (0.0021/2)*C -(206000/-1)*d);
Hco2_3 = nco2_3*(hco2 + (10.57*b) + (0.0021/2)*C - (206000/-1)*d);
Hsio2 = (nsio2*hsio2);
---------- Heat recirculation due to SiO ----------
H_recir =nsio*(Hsio2-Hsio)*4.184/3.6;
---

Hfe2o3=nFe2o3*hfe2o3;
if(t>=1810.0)
{
Hfe_5=((9.77*(t-1810.0))+((.0004/2)*(t*t-1810.0*1810.0)));
} else
Hfe_5=0.0;
Hfe=((1.0-x)/56.0)*(HFE+Hfe_5);
Hsi=(x/28.0)*(6.1*(t-1685.0)+Hsi_1+Hf_si);
Hfesi= -19200*((1-x)/56.0);
Hslag=(Wslag*2000*1000)/(1000000);  /*in MJ  */
----------Calculation of calorific values of carbon in kwh/ton alloy ----------
c_cv=(hco2*(wc/12.0)*m)/3.6;
c_cv_1=(hco2*(wc_1/12.0)*m)/3.6;
c_cv_2=(hco2*(wc_2/12.0)*m)/3.6;
c_cv_3=(hco2*(wc_3/12.0)*m)/3.6;
---------- Sensible heat of CO & CO2 in kwh/ton alloy ----------

mHco=((Hco-hco*nco)*4.184)/3.6;
mHco_1=((Hco_1-hco*nco_1)*4.184)/3.6;
```

```
mHco_2=((Hco_2-hco*nco_2)*4.184)/3 6,
mHco_3=((Hco_3-hco*nco_3)*4.184)/3.6;
mHco2_2=((Hco2_2-hco2*nco2_2)*4.184)/3.6;
mHco2_3=((Hco2_3-hco2*nco2_3)*4.184)/3.6;
----------Heat loss by CO----------
hls_co=(nco*n1*4.184)/3.6;
hls_co_1=(nco_1*n1*4.184)/3.6;
hls_co_2=(nco_2*n1*4.184)/3.6;
hls_co_3=(nco_3*n1*4.184)/3.6;
----------Sensible heat----------
mHfesi=( h3*4.184 )/3.6;
mHfe2o3=(Hfe2o3*4.184)/3.6;
mHsio2=(Hsio2*4.184)/3.6;
mHslag Hslag/3.6.
mHsio=(Hsio*4.184)/3.6;
---------------------------------------------------------------------------------------------
hr=((( h3 +(-Hsio2+Hco))*(4.184)+Hslag)/CL);
hr_1=(((h3 +(-Hsio2+Hco_1-Hfe2o3))*(4.184)+Hslag)/CL);
hr_2=(((h3 +(-Hsio2+Hco_2+Hco2_2-Hfe2o3))*(4.184)+Hslag)/CL);
hr_3=(((h3 +(-Hsio2+Hco_3+Hco2_3-Hfe2o3))*(4.184)+Hslag)/CL);
---------- Electrical Energy(KWh/ ton)----------
kwhpt=(hr/3.6);
kwhpt_1=(hr_1/3.6);
kwhpt_2=(hr_2/3.6);
kwhpt_3=(hr_3/3.6);
---------- Electrical energy loss (KWh / ton alloy)----------
 cls=kwhpt*0.30;
cls_1=kwhpt_1*0.30;
cls_2=kwhpt_2*0.30;
cls_3=kwhpt_3*0.30;
---------------------------------------------------------------------------------------------
printf("\n%.2f  %.1f  %.1f  %.1f  %.1f",x,kwhpt,kwhpt_1,kwhpt_2,kwhpt_3);
printf("\n%.2f  %.1f  %.1f  %.1f  %.1f",x,wc,wc_1,wc_2,wc_3);
printf("\n%.2f..%.1f..%.1f..%.1f...%.1f",x,c_cv,c_cv_1,c_cv_2,c_cv_3);
```

```
printf("\n%.2f..%.1f..%.1f..%.1f...%.1f",x,mHco,mHco_1,mHco_2,mHco_3);
printf("\n%.2f...%.1f....%.1f.....%.1f....%.1f",x,hls_co,hls_co_1,hls_co_2,hls_co_3);
printf("\n%.2f..%.1f..%.1f",x,mHco2_2,mHco2_3);
printf("\n%.2f....%.1f...%.1f",x,mHslag,mHsio2);
printf("\n%.2f..%.1f..%.1f",x,mHfesi,mHfe2o3);
printf("\n%.2f....%.1f...%.1f...%.1f....%.1f",x,cls,cls_1,cls_2,cls_3);
x+=0.01;
getch();
}
}
void ft(float T)
{
Gco = (-26700.00-(20.95*T));
Gsic = (-25100.0+(7.91*T));
Gsio2 = (-227700.0+(48.7*T));
Gsio = (-36150.0-(11.51*T));
G3 = ((2.0*Gco)-Gsio2-(2.0*Gsic));
G4 = (2.0*Gsio-Gsio2);
}
```

Programme for Modeling of Ferro-Manganese alloy for different condition

```
#include<math.h>
#include<stdio.h>
#include<conio.h>
#include<dos.h>
float x,T,t,pco,pmn,p,G1,Gmn,Gco,Gmno,amn,y,pctloss_mn,z;
float a_C,wtf_Mn,Gmn7c3,G2,a,q,C_reqd;
float wt_mn3o4,n_mn3o4,wtfe2o3_mn_ore,wtfe_mn_ore,wtfe2o3;
float nfe2o3,nco,nco2,Hco2,Hco,total_wt_fe2o3;
float chemheat_co,sensiheat_co,Hmn3o4,c_femn;
float Hfe_5,Hfe,Hmn,sensiheat_Fe_C_Mn,Hfe2o3,sensiheat_c,wt_fe;
float pct_al2o3sio2_mn_ore=12.0,tg=1000+273.0,hco2=(-94050.0),hco=(-26420.0);
float hfe2o3=(-196800.0),hmn3o4=(-331400.0),pct_mn_ore=44.0, pct_fe_ore=14.0;
float CL=0.70,te=1200.0;
float Hfe_1=(3.04*(1042.0-298)+(.00758/2)*(1042.0*1042.0-298.0*298.0) - 60000.0*(1/1042.0-
1/298.0));
float Hfe_2=11.13*(1184.0-1042.0);
float Hfe_3=(5.8*(1665.0-1184.0)+(.00198/2)* (1665.0*1665.0-1184.0*1184.0));
float Hfe_4=(6.74*(1810.0-1665.0)+(.0016/2)* (1810.0*1810.0-1665.0*1665.0));
float hmn_1=5.7*(1000-298)+(0.00338/2)*(1000*1000-298*298)- (-37000/1.0)*(1/1000-1/298);
float hmn_2=8.33*(1374-1000)+(0.00066/2)*(1374*1374-1000*1000);
float hmn_3=10.7*(1410-1374),hmn_4=11.3*(1517-1410),hmn_5,  hr_pht_mn=(535.0+545+430);
float wt_slag,Hslag,hr,kwhpt,s,nfe;
float amt_mn_alloy,amt_c_alloy,amt_fe_alloy,moles_mn_alloy, moles_mn3o4,wt_fe_mn3o4;
float moles_fe_mn3o4,moles_c_alloy,moles_fe_alloy,loss_mn;
float G5,k,f,nc,Hf_c,wt_mn3o4_per_tonne,wt_fe2o3_per_tonne,     moles_mn_loss,heat_loss_mn_vap;
float nc_2,nco2_2,nco_2,C_reqd_2,moles_fe2o3_alloy,Hco2_2,Hco_2, hr_2,kwhpt_2;
float nc_3,nco_3,C_reqd_3,Hco_3,hr_3,kwhpt_3;
float moles_mn3o4_3,wt_mn3o4_3,wt_mn3o4_per_tonne_3,Hmn3o4_3;

void main()
{
clrscr();
x=0.20;
```

```
while(x<=0.70)
{
amn=x;
z=log(amn);
T=211550.0/(101.14-1.987*10.0*z);
t=T;
y=exp(-(53857.143-23.04762*T)/(1.987*T));
pmn=amn*y;
pco=1.0-pmn;
pctloss_mn=(.3*pmn/pco)*100.0;
loss_mn=(pctloss_mn/100.0)*x;
moles_mn_loss=loss_mn/55.0;
amt_mn_alloy=x;
amt_c_alloy=0.056;
amt_fe_alloy=(1-x-0.056);

moles_mn_alloy=x/55.0;
moles_c_alloy=0.056/12;
moles_fe_alloy=(1-x-0.056)/56;
moles_fe2o3_alloy=(1/2.0)*moles_fe_alloy;
moles_mn3o4=(x/55.0)*(1.0/3);

wt_mn3o4=moles_mn3o4*(55.0*3+16.0*4);
wt_mn3o4_per_tonne=1000.0*wt_mn3o4;

moles_fe_mn3o4=(x/56.0)*(pct_fe_ore/pct_mn_ore);
wt_fe2o3_per_tonne=1000.0*(1/2.0)*(moles_fe_alloy-moles_fe_mn3o4)*(56*2+16*3.0);

/* FeO+CO=Fe+CO2 */
G5=5.8*te-5450.0;
k=exp(G5/(1.987*te));

f= ((k+1)*(amt_fe_alloy)-56.0*(moles_mn_alloy))/((k+2)* (amt_fe_alloy));
```

```
if(f>=0.0)
{
nc=(moles_mn_alloy)+f*(1-x-0.056)/56.0;
nco2=(1-f)*(amt_fe_alloy)/(56.0);
nco=nc-nco2;
}
else
{
f=0.0;
nc=(moles_mn_alloy)+f*(1-x-0.056)/56.0;
nco2=(1-f)*(amt_fe_alloy)/(56.0);
nco=nc-nco2;
}
C_reqd=(12.0*(nc)+0.056)*1000;
Hco2=nco2*(hco2+(10.57*(tg-298))+(0.0021/2)*(tg*tg-298*298) -(206000/-1)*(1/tg-1/298));
Hco=nco*(hco+6.79*(tg-298)+(.00098/2)*(tg*tg-298*298)-(11000.0/-1)*((1.0/tg)-(1.0/298)));
Hmn3o4=moles_mn3o4*hmn3o4;
if(t>=1810.0)
{
Hfe_5=((9.77*(t-1810.0))+((.0004/2)*(t*t-1810.0*1810.0)));
} else
Hfe_5=0.0;
Hfe=moles_fe_alloy*(Hfe_1+Hfe_2+Hfe_3+Hfe_4+Hfe_5);
if(t>=1517.0)
{
hmn_5=11.0*(t-1517.0);
} else
hmn_5=0.0;
Hmn=(moles_mn_alloy)*(hmn_1+hmn_2+hmn_3+hmn_4+hmn_5+hr_pht_mn);
heat_loss_mn_vap=(moles_mn_loss)*(hmn_1+hmn_2+hmn_3+hmn_4+hmn_5+hr_pht_mn);
sensiheat_c=(4.03*(t-298)+(1.14/2000)*(t*t-298*298)+(2.04/100000) *((1.0/t)-(1.0-298)))*(0.56/12)
/*100kg mn3o4=14kg slag*/
wt_slag=((pct_al2o3sio2_mn_ore)/100.0)*wt_mn3o4;
/*sesible heat of slag= 2000kj   /kg alloy*/
```

```
Hslag=(wt_slag*1000*2000)/1000.0;
Hfe2o3=hfe2o3*(1/2.0)*moles_fe_alloy;
/* total heat reqd per tonne of alloy */
hr=(((Hmn+Hfe+sensıheat_c+(-Hmn3o4+Hco+Hco2-Hfe2o3))*(4.2)+Hslag)/CL);
kwhpt=(hr/3.6);
----------CASE:2 no Mn vapour loss & no gas reduction of FeO----------
nc_2=(moles_fe_alloy+moles_mn_alloy);
nco2_2=(moles_mn3o4+moles_fe2o3_alloy);
nco_2=(nc_2-nco2_2);
C_reqd_2=(12.0*(nc_2)+0.056)*1000;
Hco2_2=nco2_2*(hco2+(10.57*(tg-298))+(0.0021/2)*(tg*tg-298*298)-(206000/-1)*(1/tg-1/298));
Hco_2=nco_2*(hco+6.79*(tg-298)+[illegible]-298*298)-(11000.0/-1)*((1.0/tg)-(1.0/298)));
Hmn3o4=moles_mn3o4*hmn3o4;
hr_2=(((Hmn+Hfe+sensiheat_c+(-Hmn3o4+Hco_2+Hco2_2-Hfe2o3))*(4.2)+Hslag)/CL);
kwhpt_2=(hr_2/3.6);

----------CASE:3 No prereduction of Fe2O3 & Mn3O4; CO & no Mn vapor loss----------
moles_mn3o4_3=((x+loss_mn)/55.0)*(1.0/3);
wt_mn3o4_3=moles_mn3o4_3*(55.0*3+16.0*4);
wt_mn3o4_per_tonne_3=1000.0*wt_mn3o4_3;
nc_3=3.0*(1/2.0)*moles_fe_alloy+4.0*moles_mn3o4_3;
nco_3=nc_3;
C_reqd_3=(12.0*(nc_3)+0.056)*1000;
Hco_3=nco_3*(hco+6.79*(tg-298)+(.00098/2)*(tg*tg-298*298)-(11000.0/-1)*((1.0/tg)-(1.0/298)));
Hmn3o4_3=moles_mn3o4*hmn3o4;
hr_3=(((Hmn+Hfe+sensiheat_c+(-Hmn3o4_3+Hco_2-Hfe2o3))*(4.2)+Hslag)/CL);
kwhpt_3=(hr_3/3.6);

----------MODEL: 4 and 5 , No Fe2O3 in the burden, pure Fe is used----------
float nc_4a,nco2_4a,nco_4a,C_reqd_4a,Hco2_4a,Hco_4a,hr_4a,kwhpt_4a;
float nc_4b,nco2_4b,nco_4b,C_reqd_4b,Hco_4b,hr_4b,kwhpt_4b;
/*  Mn3O4+CO= 3MnO+CO2  & MnO+ C=Mn+CO*/
nc_4a=(moles_mn_alloy);
nco2_4a=moles_mn3o4;
```

```
nco_4a=(nc_4a-nco2_4a);
C_reqd_4a=(12.0*(nc_4a)+0.056)*1000;

Hco2_4a=nco2_4a*(hco2+(10.57*(tg-298))+(0.0021/2)*(tg*tg-298*298)-(206000/-1)*(1/tg-1/298));
Hco_4a=nco_4a*(hco+6.79*(tg-298)+(.00098/2)*(tg*tg-298*298)-(11000.0/-1)*((1.0/tg)-(1.0/298)));
Hmn3o4=moles_mn3o4*hmn3o4;
hr_4a=(((Hmn+Hfe+sensiheat_c+(-Hmn3o4+Hco_4a+Hco2_4a))*(4.2)+Hslag)/CL);
kwhpt_4a=(hr_4a/3.6);
nc_4b=(3/4.0)*moles_mn_alloy;
nco_4b=(nc_4b);
C_reqd_4b=(12.0*(nc_4b)+0.056)*1000;
Hco_4b=nco_4b*(hco+6.79*(tg-298)+(.00098/2)*(tg*tg-298*298)-(11000.0/-1)*((1.0/tg)-(1.0/298)));
Hmn3o4=moles_mn3o4*hmn3o4;
hr_4b=(((Hmn+Hfe+sensiheat_c+(-Hmn3o4+Hco_4b))*(4.2)+Hslag)/CL);
kwhpt_4b=(hr_4b/3.6);
printf("\n%.2f...%.1f....%.1f...%.1f...%.1f....%.1f",x,kwhpt,kwhpt_2,kwhpt_3,kwhpt_4a,kwhpt_4b);
x+=.01;
getch();
}
}
```